VOLUME LXXV NUMBER 3

MAY 5 - 193

THE ASTROPHYSICAL JOURNAL

AN INTERNATIONAL REVIEW OF SPECTROSCOPY AND ASTRONOMICAL PHYSICS

Edited by

GEORGE E. HALE
Mount Wilson Observatory of the Carnegie Institution of Washington

EDWIN B. FROST
Yerkes Observatory of the University of Chicago

HENRY G. GALE
Ryerson Physical Laboratory of the University of Chicago

APRIL 1932

ON THE INTERPRETATION OF THE EMISSION LINES IN STARS OF EARLY SPECTRAL CLASS - - - - - - - - - - - - *O. Struve and P. Swings* 161

MEASUREMENTS OF ULTRA-VIOLET SOLAR RADIATION - - - *Edison Pettit* 185

SOME RESULTS FROM A STUDY OF THE ATOMIC LINES IN THE SUN-SPOT SPECTRUM - - - - - - - - - - - - - - *Charlotte E. Moore* 222

REVIEWS

Revision of Rowland's Preliminary Table of Solar Spectrum Wave-Lengths with an Extension to the Present Limit of the Infra-Red, C. E. St. John, C. E. Moore, L. M. Ware, E. F. Adams, H. D. Babcock (P. C. Keenan), 274; *Photo-electric Cells and Their Applications*, John S. Anderson (ed.) (C. T. Elvey), 274; *Johannes Kepler Festschrift, Teil I*, Dr. Karl Stöckl (F.), 275.

THE UNIVERSITY OF CHICAGO PRESS
CHICAGO, ILLINOIS, U.S.A.

April 1932 Vol. LXXV, No. 3

THE ASTROPHYSICAL JOURNAL

AN INTERNATIONAL REVIEW OF SPECTROSCOPY AND ASTRONOMICAL PHYSICS

Edited by

GEORGE E. HALE
Mount Wilson Observatory of the Carnegie Institution of Washington

EDWIN B. FROST
Yerkes Observatory of the University of Chicago

HENRY G. GALE
Ryerson Physical Laboratory of the University of Chicago

WITH THE COLLABORATION OF

WALTER S. ADAMS, Mount Wilson Observatory
JOSEPH S. AMES, Johns Hopkins University
ARISTARCH BELOPOLSKY, Observatoire de Pulkovo
WILLIAM W. CAMPBELL, Lick Observatory
HENRY CREW, Northwestern University
CHARLES FABRY, Université de Paris
ALFRED FOWLER, Imperial College, London
†CHARLES S. HASTINGS, Yale University
HEINRICH KAYSER, Universität Bonn
ROBERT A. MILLIKAN, Institute of Technology, Pasadena
HUGH F. NEWALL, Cambridge University
FRIEDRICH PASCHEN, Reichsanstalt, Charlottenburg
HENRY N. RUSSELL, Princeton University
FRANK SCHLESINGER, Yale Observatory
SIR ARTHUR SCHUSTER, Twyford
FREDERICK H. SEARES, Mount Wilson Observatory
HARLOW SHAPLEY, Harvard College Observatory

† Died January 30, 1932.

The Astrophysical Journal is published by the University of Chicago at the University of Chicago Press, 5750 Ellis Avenue, Chicago, Illinois, during each month except February and August. ¶ The subscription price is $6.00 a year; the price of single copies is 75 cents. Orders for service of less than a half-year will be charged at the single-copy rate. ¶ Postage is prepaid by the publishers on all orders from the United States, Porto Rico, Hawaiian Islands, Philippine Islands, Guam, and the Samoan Islands. ¶ Postage is charged extra as follows: for Canada and Newfoundland, 50 cents on annual subscriptions (total $6.50); on single copies, 5 cents (total 80 cents); for all other countries in the Postal Union, 90 cents on annual subscriptions (total $6.90), on single copies, 9 cents (total 84 cents). ¶ Patrons are requested to make all remittances payable to The University of Chicago Press, in postal or express money orders or bank drafts.

The following are authorized agents:

For the British Empire, except North America, India, and Australasia: The Cambridge University Press, Fetter Lane, London, E.C. 4. Prices of yearly subscriptions and of single copies may be had on application.

For Japan: The Maruzen Company, Ltd., Tokyo.

For China: The Commercial Press, Ltd., Paoshan Road, Shanghai. Yearly subscriptions, $6.00; single copies, 75 cents, or their equivalents in Chinese money. Postage extra, on yearly subscriptions 90 cents, on single copies 9 cents.

Claims for missing numbers should be made within the month following the regular month of publication. The publishers expect to supply missing numbers free only when losses have been sustained in transit, and when the reserve stock will permit.

Business correspondence should be addressed to The University of Chicago Press, Chicago, Illinois.

Communications for the editors and manuscripts should be addressed to the Editors of THE ASTROPHYSICAL JOURNAL, Yerkes Observatory, Williams Bay, Wisconsin.

The cable address is "Observatory, Williamsbay, Wisconsin."

The articles in this journal are indexed in the *International Index to Periodicals*, New York, N.Y.

Applications for permission to quote from this journal should be addressed to The University of Chicago Press, and will be freely granted.

Entered as second-class matter, January 17, 1895, at the Post-Office at Chicago, Ill., under the act of March 5, 1879.
Acceptance for mailing at special rate of postage provided for in Section 1103, Act of October 3, 1917, authorized on July 15, 1918.

PRINTED IN THE U.S.A.

THE ASTROPHYSICAL JOURNAL

AN INTERNATIONAL REVIEW OF SPECTROSCOPY AND ASTRONOMICAL PHYSICS

VOLUME LXXV APRIL 1932 NUMBER 3

ON THE INTERPRETATION OF THE EMISSION LINES IN STARS OF EARLY SPECTRAL CLASS

By O. STRUVE and P. SWINGS[1]

ABSTRACT

The emission-line spectra.—The presence of bright *Fe* II in the spectra of Be stars suggests that lines of other elements requiring similar conditions of excitation may also be present. A search in the spectra of several stars yielded definite evidence of the presence of *Mg* II and *Si* II; *Sc* II, *Cr* II, and *Ni* II are probably present; forbidden *Fe* II is uncertain. No lines belonging to *Ti* II could be identified, with certainty. The width of the bright line *Mg* II 4481 greatly exceeds those of the emission lines of *H*, and in one star the lines of *Fe* II are definitely wider than those of *H*. Attributing the origin of the bright lines to a rotating shell of gas, and neglecting support by radiation pressure, we find that the effective distance of *Mg* II from the center is about seven times the radius of the star, while that of *H* is ten times the radius of the star. A rough computation of the density of the shell gives 2.5×10^{-13} gr/cm^3. The bright lines of *Mg* II and of *Si* II are always weak. *He* I and *Ti* II are rarely seen in emission.

Classification of bright-line spectra.—The published data on Be and Oe stars were collected and arranged according to the Harvard spectral class as derived from the absorption lines. The character of the emission lines shows a definite progression with spectral class. The degrees of effective excitation of the bright and dark lines are not very different in the Oe's but they differ by more than one spectral class in the Be's. There is relatively little dispersion within any given spectral subdivision. This would indicate, on the rotational hypothesis, that the product of the density of the shell and the dilution factor is approximately constant within a given subdivision, but that it varies as a function of spectral type.

A new Be star.—Data are given for the Be star 60 Cygni (α 20^{h}57^m.7 δ +45°46′), which has variable hydrogen lines.

Variations in the spectra of Be stars.—Variations in the hydrogen lines of 31 Pegasi (α 22^{h}16^m.6 δ +11°42′) are described. The Be star 31 *o* Aquarii (α 21^{h}58^m.1 δ −2°38′) is found to have broad and hazy absorption lines of *He* I and *Mg* II, and sharp and narrow lines of *Fe* II. The latter are probably variable. This star is similar to the Be star ϵ

[1] I wish to express my gratitude to the C. R. B. Educational Foundation for assigning to me an advanced fellowship which has made possible my stay in the United States. I should also like to express my heartiest thanks to Director Edwin B. Frost and Professor G. Van Biesbroeck for their hospitality and help.—P. S.

Capricorni; and the suggestion is advanced that the hazy lines are broadened by rotation, while the narrow lines originate through absorption in the same rotating gaseous shell which is believed to give rise to the bright hydrogen lines and to their narrow central absorptions.

The spectrum of 17 Leporis.—This spectrum seems to be related to spectra of the P Cygni type: 17 Leporis has bright $H\beta$ in the normal position, accompanied by a strong absorption line on its violet side. Preliminary measurements of one plate give: *Mg* II +14 km/sec., *Fe* II and *Ti* II −64 km/sec., *H* −93 km/sec.

The rotational hypothesis of the origin of bright lines.—A summary is given in support of the hypothesis that the bright lines originate in a rotating shell or ring of gas, and that the dispersion in line widths is mainly due to the effect of inclination.

Objections to the rotational hypothesis are discussed and found not to be of a sufficiently serious nature to outweigh the positive evidence. The rotational hypothesis is adopted as the one which fits the observed facts better than any other theory thus far proposed.

I. EMISSION-LINE SPECTRA

Various investigators[1] have pointed out that the presence of bright lines of *Fe* II in stellar spectra classified as B0, B1, B2, B3, or B5 constitutes an interesting astrophysical problem. The absorption lines of ionized iron observable in the ordinary photographic region of the spectrum reach maximum intensity in or near class F0; they are strong in many A stars (e.g., α Cygni), but are faint in B8 and B9 (e.g., β Orionis) and are last seen in certain stars classified at Harvard as B3 (e.g., ι Herculis).[2] On the other hand, the emission lines of ionized iron seem to be most frequent in class B3e, but they have also been observed in several stars of classes B2e, B1e, and even B0e.[3] It seems obvious that in these "normal Be stars," as they have been called by Paul W. Merrill,[4] the state of effective excitation corresponding to the bright lines is much lower than that corresponding to the absorption lines. A tentative explanation of this interesting phenomenon has recently been given in a paper by Struve and Schwede.[5]

We shall assume here that the bright lines originate in an outer gaseous shell or ring which is sufficiently far removed from the photosphere of the star to permit large deviations from thermodynamic equilibrium. Under such conditions the usual equations defining the state of ionization of the medium are not applicable, and

[1] B. P. Gerasimovič, private communication; O. Struve and H. F. Schwede, *Physical Review*, **38**, 1203, 1931; C. H. Payne, *Harvard Observatory Circular*, No. 364, 1931.

[2] O. Struve, *Astrophysical Journal*, **74**, 225, 1931.

[3] P. W. Merrill, *ibid.*, **65**, 290, 1927; Table II.

[4] *Ibid.*

[5] *Op. cit.*, p. 1204.

we must follow the treatment of A. S. Eddington[1] and S. Rosseland,[2] i.e., the ionization of a medium of temperature T and density ρ will be the same as that of a gas in thermodynamic equilibrium of the same temperature and of density $\rho\delta$, where δ is the dilution factor

$$\delta = \frac{4r^2}{R^2},$$

r is the distance of the gas from the center of the star, and R is the radius of the star.

The rotational hypothesis of the origin of bright lines[3] attributes the broadening of the emission lines to the rotation of a gaseous shell or ring around the star. The actual measurements refer, of course, to the component of the velocity in the line of sight. It is therefore reasonable to assume that the greatest measured line-widths refer to cases in which the axis of rotation is perpendicular to the line of sight. A total width of about 6 A for $H\beta$ has been observed in several stars.[4] The corresponding velocity of rotation would be approximately 200 km/sec. Assuming that the particles of the shell move freely under the attraction of a star of class Bo, having a mass ten times that of the sun, and a radius five times that of the sun, we find for the dilution factor (neglecting radiation pressure):

$$\delta = 400 .$$

In view of the uncertainty of the masses and diameters of the stars, this value merely indicates the order of magnitude concerned.[5]

In a former paper the suggestion was advanced[6] that the bright lines are caused by recombination of free electrons with positive ions. If this is correct, we should have a maximum concentration of Fe^{++} ions in the medium in order to observe strong emission lines of *Fe* II. The first two ionization potentials of iron are 7.8 and 16.5 volts. The

[1] A. S. Eddington, *The Internal Constitution of the Stars* (German ed.), p. 478, 1928.

[2] S. Rosseland, *Astrophysik auf atomtheoretischer Grundlage*, p. 232, 1931.

[3] Struve, *Astrophysical Journal*, **73**, 94, 1931.

[4] R. H. Curtiss, *Publications of the Observatory, University of Michigan*, **3**, 9, 1923.

[5] This revises the earlier value of δ given in *Physical Review*, **38**, 1204, 1931.

[6] Struve and Schwede, *Physical Review*, **38**, 1195, 1931.

excitation potentials for the upper states of the lines of *Fe* II which are usually observed are about 5.5 volts above the ground level of the singly-ionized atom. The usual ionization equations indicate a maximum concentration of Fe^{++} in the late B's. It is therefore permissible to assume, in a rough computation, that the state of ionization of the nebulous shell is approximately the same as that of the reversing layer of the star. In other words, $\rho_0 \approx \rho\delta$, where ρ_0 is the density of the reversing layer. Assuming

$$\rho_0 \approx 10^{-10} \text{ gr/cm.}^3 \ (p = 10^{-4} \text{ atm.} ; \ T = 20{,}000^\circ) ,$$

we find

$$\rho \approx 2.5 \times 10^{-13} \text{ gr/cm.}^3 .$$

This density is not unreasonable, as it is similar to that of the solar chromosphere.[1] A more serious difficulty arises from the fact that in a nebula of this density the temperature may not be equal to that of the photosphere.[2] Whether or not the proximity of the nebula to a B star insures the equality of these temperatures cannot be definitely stated.

The maximum concentration of Fe^{++} atoms in the spectral sequence depends, primarily, upon the value of the second ionization potential of iron, 16.5 volts. It is reasonable to expect that among the bright lines other elements having similar ionization potentials will be present. The following have been selected as being sufficiently abundant in the crust of the earth: *H* (13.5), *N* I (13.7), *O* I (13.6), *Mg* II (15.0), *Al* II (18.2), *Si* II (16.2), *Sc* II (12.8), *Ti* II (13.6), *Cr* II (16.6), *Fe* II (16.5), and *Ni* II (18.2).

N I has not been observed in Be stars. (The strongest laboratory lines are[3] 4109.98 [12], 4151.46 [12], and 4358.27 [10].) Two forbidden lines of *O* I ($\lambda\lambda$ 6300 and 6363) were observed by Merrill[4] in H.D. 50138 of spectral class B8ev. Bright *Al* II has not been seen in normal Be stars, but Merrill[5] thought that it was probably present

[1] Rosseland, *Astrophysik*, p. 188, 1931.

[2] Eddington, *op. cit.*, p. 477.

[3] O. S. Duffendack and R. A. Wolfe, *Physical Review*, **34**, 409, 1929.

[4] *Astrophysical Journal*, **73**, 348, 1931.

[5] *Ibid.*, **69**, 330, 1929.

UNIV. OF WIOH.

PLATE X

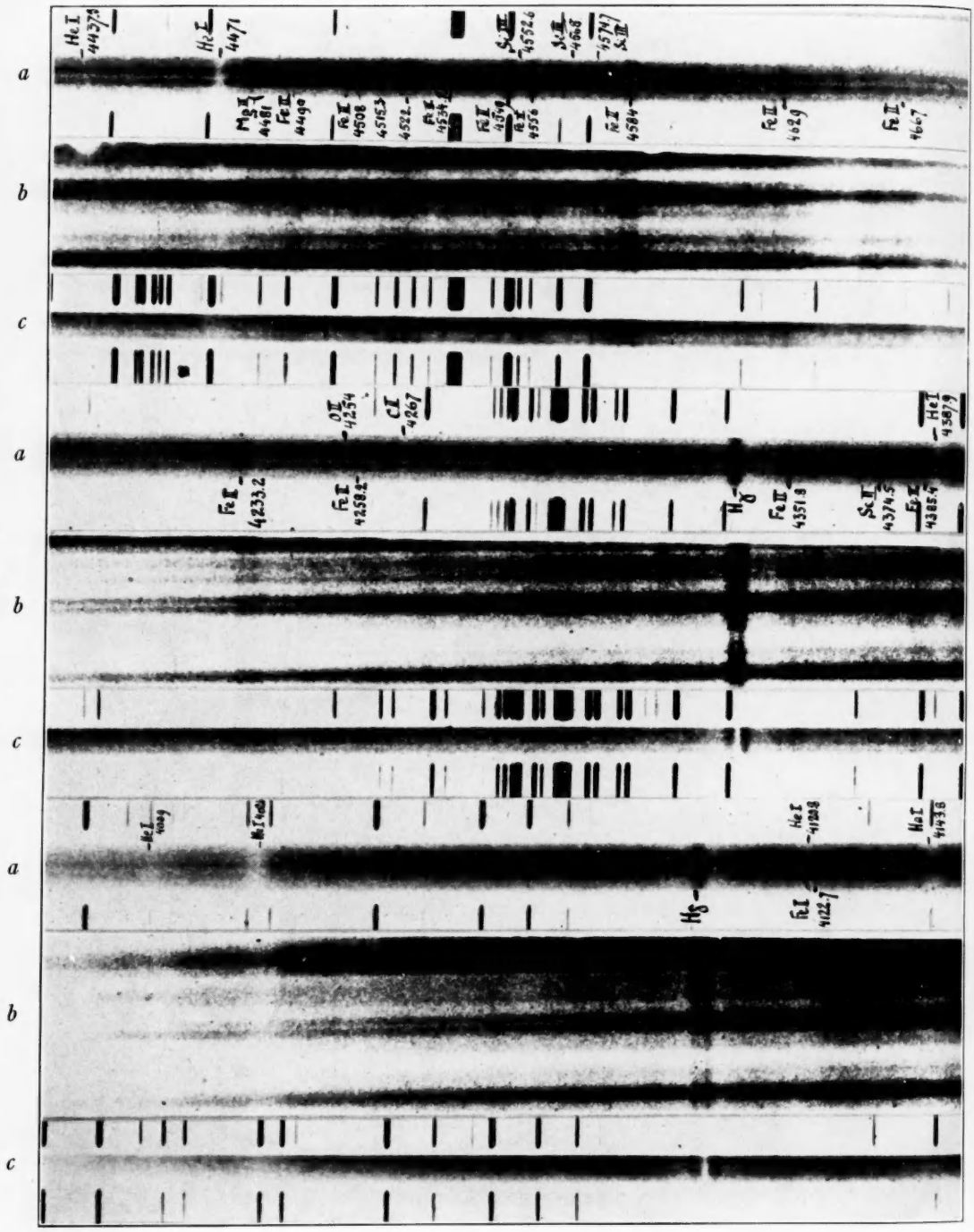

a) χ Ophiuchi; *b*) γ Cassiopeiae; *c*) φ Persei

in B.D.+11°4673, of the P Cygni type. Some new evidence concerning *Mg* II, *Si* II, *Sc* II, *Cr* II, and *Ni* II in normal Be's is given in Table I.

The observations used in this work were made with the single-prism Bruce spectrograph attached to the 40-inch refractor. Eastman Process emulsion was used for most of the spectrograms.

The presence of *Mg* II and *Si* II is certain; *Sc* II, *Cr* II, and *Ni* II are probable; while Merrill's forbidden lines of *Fe* II are uncertain; *Ti* II was not observed by us with certainty.

The comparatively low excitation of the emission lines in normal Be stars is thus amply confirmed. It resembles that of an average A star of high luminosity, with the following differences: (*a*) *Ti* II is absent; (*b*) *Mg* II and *Si* II are relatively faint. These peculiarities may perhaps be due to a scarcity of those particular elements in the nebulous shell. It should also be noted that one or two peculiar stars of class A are known, in which *Mg* II and *Si* II are nearly absent in absorption; 17 Leporis is a striking example.[1]

Table II contains a list of the absorption lines seen on our plates. From these we find that the spectral classes assigned in the *Henry Draper Catalogue* are approximately correct.

Table III is a summary of the line widths measured on our plates. The tabulated values represent the distances between the steepest points of the outer edges of the emission components. They are directly comparable with those of R. H. Curtiss.[2] In agreement with his results, the widths of the iron lines are strongly correlated with those of hydrogen.

However, in any given star the lines of different elements do not necessarily have the same widths. This is shown in Plate X, where *Mg* II is much wider than *H* or *Fe* II.

The general correlation between the widths of hydrogen and iron lines is so well established that there can be no reasonable doubt that the widening is due to Doppler effect. We are inclined to explain the differing line widths observed in individual stars as an effect of distance: Thus in χ Ophiuchi *Mg* II would be closer to the star than *H*. Since the widths are directly proportional to the rotational

[1] Struve, *ibid.*, **72**, 343, 1930.

[2] R. H. Curtiss, *op. cit.*, p. 1

TABLE I

Bright Lines

Laboratory					χ Ophiuchi			γ Cassiopeiae			11 Camelopardalis		φ Persei	Remarks
λ	Element	Intensity	Notation	Total Excitation	λ	Int.	Width	λ	Int.	Width	Int.	Width	Int.	
3970.1	*H*	.....	$H\epsilon$	13.3	69.2	2	.....	70.0	5	.....	2	.....	1	
4067.1	*Ni* II	.....	$a^2G_5 - a^2F_4$	7.6+12.1	.....	.....	.....	66.9	3	.....	.....	.....	.....	1
4101.7	*H*	.....	$H\delta$	13.2	01.6	15	2.3	01.7	20	3.9	15	1.6	15	
4122.7	*Fe* II	.....	$b^4P'_3 - a^4F_3$	7.8+ 5.6	23.1	2	.....	23.0	2	.....	.....	.....	1	
4128.0	*Si* II	.....	$2^2D_2 - 3^2F$	8.1+12.7	.....	.....	.....	29.2	3	.....	.....	.....	.....	2
4130.0	*Si* II	.....	$2^2D_1 - 3^2F$	8.1+12.7	.....	.....	.....							
4173.5	*Fe* II	5	$b^4P'_3 - a^4D'_3$	7.8+ 5.5	73.4	3	.....	72.0	2	.....	2	.....	2	
4178.9	*Fe* II	8	$b^4P'_3 - a^4F_4$	7.8+ 5.5	78.6	3	.....	78.1	3	.....	2	.....	2	
?	?	.....	?	.....	.....	.....	.....	05.8	2	.....	.....	.....	.....	
4233.2	*Fe* II	10	$b^4P'_3 - a^4D'_4$	7.8+ 5.5	33.3	7	4.1	33.2	10	3.9	5	.....	5	
4244.0	[*Fe* II]	.....	$a^4F'_5 - a^4G_6$	7.8+ 3.1	.....	.....	.....	46.0	2	.....	.....	.....	.....	3
4244.9	[*Fe* II]	.....	$a^4F'_4 - a^4G_4$	7.8+ 3.2	.....	.....	.....							
4258.2	*Fe* II	.....	$b^4P'_2 - a^4F_2$	7.8+ 5.6	57.9	1	.....	58.0	2	.....	.....	.....	1	
4273.3	*Fe* II	1	$b^4P'_2 - a^4D_1$	7.8+ 5.6	73.0	1	.....	73.0	3	.....	.....	.....	1	
?	?	.....	?	.....	.....	.....	.....	81.2	2	.....	.....	.....	.....	
4287.4	[*Fe* II]	.....	$a^6D_5 - a^6S_3$	7.8+ 2.9	.....	.....	.....	89.0	1	.....	.....	.....	.....	4
4296.6	*Fe* II	3	$b^4P'_2 - a^4F_3$	7.8+ 5.6	96.3	2	.....	97.0	3	.....	1	.....	.....	
4303.2	*Fe* II	4	$b^4P'_2 - a^4D'_2$	7.8+ 5.6	02.9	1	.....	03.1	3	.....	.....	.....	.....	
4314.1	*Sc* II	10	$b^3F_4 - a^3D'_3$	6.7+ 3.5	.....	.....	.....	14.0	1	.....	.....	.....	.....	
?	?	.....	?	.....	.....	.....	.....	31.9	1	.....	.....	.....	.....	
4340.5	*H*	.....	$H\gamma$	13.0	39.5 41.0	50	2.6	40.5	50	.....	50	1.1	50	
4351.8	*Fe* II	10	$b^4P'_2 - a^4D'_3$	7.8+ 5.5	51.5	4	.....	51.6	6	.....	2	2.1	3	
4358.4	[*Fe* II]	.....	$a^4F'_2 - a^4G_3$	7.8+ 3.2	.....	.....	.....	59.7	1	.....	.....	.....	.....	5
4359.3	[*Fe* II]	.....	$a^6D_4 - a^6S_3$	7.8+ 3.2	.....	.....	.....							
4374.5	*Sc* II	10	$a^3F_4 - b^3F'_4$	6.7+ 3.4	75.2	2	.....	74.0	2	.....	.....	.....	.....	6
4385.4	*Fe* II	5	$b^4P'_1 - a^4D'_1$	7.8+ 5.6	85.7	2	.....	85.0	8	.....	1	.....	3	

4413.8	[*Fe* II]	.....	$a^6D_3 - a^6S_3$	7.8+ 2.9	.....	.....	.....	13.0	0	.....	.....	.....	.....	
4416.8	*Fe* II	8	$b^4P'_1 - a^4D'_2$	7.8+ 5.6	16.5	1	.....	17.0	1	.....	1	.....	.....	
4481.13	*Mg* II	.....	$3^2D_2 - 4^2F'_3$	7.6+11.6	81.2	3	5.7	81.0	3	6.6	.....	.....	.....	7
4481.33	*Mg* II	.....	$3^2D_3 - 4^2F'_3$	7.6+11.6										
4489.2	*Fe* II	10	$b^4F'_4 - a^4F_3$	7.8+ 5.6	90.5	3	.....	90.8	5	.....	2	.....	2	
4491.4	*Fe* II	8	$b^4F'_2 - a^4F_2$	7.8+ 5.6										
4508.3	*Fe* II	15	$b^4F'_2 - a^4D'_1$	7.8+ 5.6	08.1	4	.....	08.0	1	.....	3	.....	2	
4515.3	*Fe* II	15	$b^4F'_3 - a^4F_3$	7.8+ 5.6	14.8	5	.....	16.0	3	.....	3	.....	2	
4522.6	*Fe* II	10	$b^4F'_3 - a^4D'_2$	7.8+ 5.5	21.6	6	.....	22.4	5	.....	4	.....	5	
4534.2	*Fe* II	.....	$b^4F'_2 - a^4F_3$	7.8+ 5.6	35.3	4	.....	33.6	2	.....	3	.....	2	
4541.5	*Fe* II	.....	$b^4F'_2 - a^4D'_2$	7.8+ 5.6	42.0	2	.....	41.0	1	.....	1	.....	1	
4549.5	*Fe* II	20	$b^4F'_4 - a^4D'_3$	7.8+ 5.5	49.4	10	4.2	48.9	4	.....	6	.....	5	
4555.9	*Fe* II	15	$b^4F'_4 - a^4F_4$	7.8+ 5.5	55.6	7	4.0	56.7	4	.....	4	.....	3	
4558.7	*Cr* II	10	$b^4F'_{3,5} - a^4D'_4$	6.7+ 6.8	.....	.....	.....	59.0	3	.....	.....	.....	.....	
4576.3	*Fe* II	10	$b^4F'_3 - a^4D'_3$	7.8+ 5.5	76.0	2	.....	.....	.....	.....	1	.....	1	
4583.8	*Fe* II	30	$b^4F'_5 - a^4D'_4$	7.8+ 5.5	83.7	10	4.15	83.6	10	5.1	6	1.7	6	
?	?	.....	?	.....	93.3	2	.....	.....	.....	.....	.....	.....	.....	
4618.8	*Cr* II	10	$b^4F_3 - a^4D'_2$	6.7+ 6.7	.....	.....	.....	19.0	3	.....	.....	.....	.....	
4629.3	*Fe* II	20	$b^4F'_5 - a^4F_5$	7.8+ 5.5	28.3	2	.....	28.8	3	.....	1	.....	3	
?	?	.....	?	.....	.....	.....	.....	35.9	2	.....	.....	.....	.....	
?	?	.....	?	.....	45.6	4	.....	.....	.....	.....	.....	.....	.....	
4657.0	*Fe* II	.....	$a^6S_3 - a^4D'_3$	7.8+ 5.5	.....	.....	.....	56.6	3	.....	.....	.....	.....	
4666.7	*Fe* II	.....	$b^4F'_4 - a^4F_5$	7.8+ 5.5	65.2	2	.....	67.4	3	.....	1	.....	1	
4731.5	?*Fe* II	1	$a^6S - a^4D'_4$	7.8+ 5.5	.....	.....	.....	31.5	2	.....	.....	.....	.....	
4861.3	*H*	.....	*Hβ*	12.7	61.2	100	3.0	61.3	100	.....	100	.....	100	

REMARKS.—The intensities of *Fe* II have been taken from Russell and Merrill; those of *Cr* II and *Sc* II, from Kayser. In the notations we have added 1/2 to the inner quantum number j, in cases of even multiplicities. The wave-lengths of χ Ophiuchi have been corrected for the radial velocity as determined from the absorption lines. The bright lines observed by us in φ Persei agree with the results of W. J. S. Lockyer (*Monthly Notices of the Royal Astronomical Society*, **85**, 580, 1925). Forbidden iron lines are designated [*Fe* II]. 1. The presence of *Ni* II is probable in view of the similarity of the potentials of ionization and excitation with those of *Mg* II. 2. In B.D.+11°4673 and in Z Andromedae, these lines are very weak. 3. Uncertain. May be *Ni* II (4244.8) or *Sc* II (4246.8). 4. May be a blend of several lines. 5. Uncertain. May be *Ni* II 4362 ($a^2G_5 - a^4F_4$). 6. Uncertain identification. 7. Given by Curtiss as an absorption line in γ Cassiopeiae. The excitation potentials refer to the upper states.

TABLE II

ABSORPTION LINES

LABORATORY					χ OPHIUCHI		γ CASSIOPEIAE		11 CAMELOPARDALIS
λ	El.	Int.	Notation	Total Energy of the Lower Term	λ	Int.	λ	Int.	Int.
3964.7	*He* I	4	$2^1S_0 - 4^1P_1$	20.5	.....		65.0	1	
3995.0	*N* II	10	$1^1P'_1 - 1^1P_1$	14.5+18.5	.....		95.5	4	
4009.3	*He* I	1	$2^1P_1 - 7^1D_2$	21.1	09.1	3	09.2	8	2
4026.2	*He* I	5	$2^3P_{2,1} - 5^3D_{3,2,1}$	20.8	26.2	10	26.8	10	6
4042.0	*N* II	3	?	14.5+?	.....		42.6	2	
4060.6	*O* II	1	?	13.5+?	.....		60.0	2	
4061.0	*O* II	1		13.5+?	.....				
4069.9	*O* II	9	$3^4D_2 - 3^4F_2$	13.5+24.4	.....		71.1	3	
4072.2	*O* II	8	$3^4D_1 - 3^4F_2$	13.5+24.4					
4088.9	*Si* IV	10	$2^2S_1 - 3^2P_2$	8.1+16.3+31.6+23.5	.....		88.8	3	
4116.0	*Si* IV	8	$2^2S_1 - 3^2P_1$	8.1+16.3+31.6+23.5	.....		16.0	1	
4120.8	*He* I	3	$2^3P_{2,1} - 5^3S_1$	20.8	20.6	4	20.5	6	3
4132.8	*O* II	6	$3^4P_1 - 3^4P'_2$	13.5+24.8	.....		33.0	4	
4143.8	*He* I	2	$2^1P_1 - 6^1D_2$	21.1	43.7	5	44.1	6	3
4153.3	*O* II	6	$3^4P_2 - 3^4P'_3$	13.5+25.7	53.7	2			
4169.0	*He* I	1	$2^1P_1 - 6^1S_0$	21.1	69.3	1	.....		1
4254.0	*O* II	8	$a^2G_{5,4} - a^2H_{6,5}$	13.5+31.3	54.2	2			
4267.0	*C* II	...	$3^2D_3 - 4^2F_{4,3}$	11.3+17.9	66.8	3	.....		1
4267.3	*C* II	...	$3^2D_2 - 4^2F_{4,3}$	11.3+17.9					
4366.9	*O* II	7	$3^4P_3 - 3^4P'_2$	13.5+23	67.0	1			
4387.9	*He* I	3	$2^1P_1 - 5^1D_2$	21.1	87.8	5	88.0	4	3
4437.5	*He* I	1	$2^1P_1 - 5^1S_0$	21.1	36.8	2	37.6	1	
4447.0	*N* II	10	$2^1D'_2 - 1^1D_2$	14.5+20.3	.....		48.0	1	
4448.2	*O* II	6	$a^2F_4 - b^2F'_4$	13.5+27.4					
4471.5	*He* I	6	$2^3P_{2,1} - 4^3D_{3,2,1}$	20.8	71.3	10	71.1	3	6
4481.2	*Mg* II	...	$3^2D_{2,3} - 4^2F'_3$	7.6+11.6	.....		.....		2
4552.6	*Si* III	10	$2^2S_1 - 3^2P_2$	10.3+16.3+19.5	52.2	4	uncertain		2
4567.9	*Si* III	9	$2^2S_1 - 3^2P_1$	10.3+16.3+19.5	67.9	3	.....		1
4574.7	*Si* III	7	$2^2S_1 - 3^2P_0$	10.3+16.3+19.5	75.1	1	.....		1
4630.5	*N* II	10	$1^3P'_2 - 2^3P_2$	14.5+18.5	.....		30.0	1	
4638.9	*O* II	6	$3^4P_1 - 3^4D_2$	13.5+21.7	.....		40.2	3	
4641.8	*O* II	9	$3^4P_2 - 3^4D_3$	13.5+21.7					
4643.1	*N* II	5	$1^3P'_2 - 2^3P_1$	14.5+18.5	.....		44.0	1	
4650.8	*O* II	6	$3^4P_1 - 3^4D_1$	13.5+21.7	.....		50.7	4	
4673.7	*O* II	3	$3^4P_2 - 3^4D_1$	13.5+21.7	.....		74.3	2	
4685.8	*He* II	...	$3^2D_3 - 4^2F_4$	24.5+48.1	.....		86.0	2	
4713.14	*He* I	3	$2^3P_{2,1} - 4^3S_1$	20.8	.....		13.0	2	
4713.37	*He* I	3	$2^3P_0 - 4^3S_1$	20.8					

velocities and since the latter are inversely proportional to the square roots of the distances:

$$V^2 = \frac{k^2 M}{r},$$

we infer that for χ Ophiuchi

$$\frac{r(Mg\ \text{II})}{r(H)}=\sqrt{\frac{2\cdot7}{5\cdot7}}=0.69\ .$$

This interpretation is supported by the fact that in χ Ophiuchi and in γ Cassiopeiae the central depression of *Mg* II 4481 is much more conspicuous than in the lines of *H* or of *Fe* II. This is probably due to the fact that the ratio: Size of star/size of nebula, is greater for *Mg* II than for *H* and that, consequently, absorption in front of the star and obstruction of the nebula back of it are relatively more conspicuous in *Mg* II than in *H*.

TABLE III

SUMMARY OF LINE WIDTHS

Star	*Hβ*	*Hγ*	*Hδ*	*Fe* II	*Mg* II
11 Camelopardalis	.....	1.1 A	1.6 A	1.9 A	.....
7 χ Ophiuchi	3 A	2.6	2.3	4.1	5.7 A
γ Cassiopeiae	.....	.....	3.9	4.5	6.6

The effect described above seems to be a counterpart of the well-known observation that the images of planetary nebulae photographed in the lines of different elements are not always the same.

The widths of the bright lines of *Si* II could not be measured because of blending, but apparently they resemble the iron lines.

Interesting differences have been observed in the shapes of the lines of φ Persei The hydrogen lines consist of two bright components with a deep central absorption. Between the emission components and the deep absorption line there seems to be a narrow region (or step) where the intensity is similar to that immediately outside the emission. The lines of *Fe* II, while also double, show no trace of central absorption: the residual intensity in the center is nearly the same as that of the continuous spectrum. Apparently *Fe* II does not appreciably absorb the light of the photosphere.

There are some differences between our estimated intensities for χ Ophiuchi and those obtained in the laboratory. Thus, according

to Russell[1] and to Merrill,[2] *Fe* II 4508 ($b^4F'_2-a^4D'_1$) is stronger than *Fe* II 4523 ($b^4F'_3-a^4D'_2$), while the opposite is true in the star. Since these lines are close together, it is not possible to attribute this to the photographic emulsion or to the superposition of the continuous spectrum. The question of blends has not been investigated. The intensities of the absorption lines are normal.

II. CLASSIFICATION OF BRIGHT-LINE SPECTRA

If the bright lines in Be stars originate in a distinct shell not connected with the reversing layer of a star, it will be desirable to devise a classification for the emission spectra which is independent of that of the absorption lines. There is no theoretical reason for a one-to-one correspondence of the two spectra. The spectrum of the reversing layer is defined by its temperature (T) and density (ρ_0); that of the gaseous shell depends upon this same temperature (T), upon the density of the shell (ρ) and upon the dilution factor (δ). There is no a priori reason to suppose that the product $\rho\delta$ stands in any definite relation to ρ_0. In an isothermal nebula $\rho \propto r^{-2}$ at great distances from the center,[3] and $\rho\delta \to$ Const. This may explain why the bright-line spectrum of any given star usually corresponds to a very definite stage of excitation and does not contain a superposition of many different stages. But the absolute value of $\rho\delta$ may not be the same in all stars of the same spectral subdivision, nor is it necessary for the ratio $\rho\delta/\rho_0$ to be constant all along the spectral sequence.

Whatever the theory of bright lines may be, they are in some way excited by the radiation of the photosphere. It is therefore appropriate to arrange the bright-line spectra in order of spectral class as given by the absorption lines. This has been done in Table IV. No attempt was made to include all "normal" Be stars. Only those were included for which detailed observations were available in the literature.

Within any one subdivision there is a marked similarity in the emission spectra. There are only two very discordant stars: the companion of *o* Ceti, and β Lyrae. The first may be safely disregarded, for its spectral type was determined by Joy from the distribution of energy in the continuous spectrum. The second case is

[1] *Astrophysical Journal*, **64**, 194, 1926; *Contributions from the Mount Wilson Observatory*, No. 318, 1926.

[2] *Astrophysical Journal*, **69**, 353, 1929.

[3] Eddington, *op. cit.*, p. 489.

TABLE IV

BRIGHT LINES IN STARS OF CLASSES Oe AND Be

Star	Emission Lines	Remarks
	Spectrum O6e	
22 λ Cep	*He* II, *N* III	*He* II 4686 is broad and double; its width is 11 A; the absorption lines are broad; *N* III 4638 is also broad and double
	Spectrum O7e	
29 CMa	*He* II, *N* III	On our plates *He* II 4686 is bright and narrow (4 A), the absorption lines are narrow
	Spectrum O8e	
B.D.+6°1309	*H*, *He* II, *He* I	*H* emission broad (25 A) with strong central absorption. Absorption lines: *He* I, *Si* IV, *N* II, *Mg* II
	Spectrum Boe	
γ Cas	*H*, *Fe* II, *Mg* II, *Si* II [*Fe* II]?, *Ni* II, *Sc* II, *Cr* II? (*He* I)	Absorption lines: *He* I, *He* II, *O* II, *N* II, *Si* IV, *Si* III?; of the helium lines D_3 is bright but faint
φ Per	*H*, *Fe* II, *Ti* II?, *Ca* II?	*H* lines have strong central absorptions; all bright lines are double; *Mg* II is absent
	Spectrum B1e	
H.D. 163181	*H*, *He* I	Absorption lines *H*, *He* I, *N* II, *Mg* II, *O* II, *Si* III, *Si* IV
52 π Aqr	*H*, *Fe* II	Bright *Fe* II fainter than in φ Persei
	Spectrum B2e	
H.D. 45677	*H*, *Fe* II [*Fe* II]	Bright *H* very strong, double, variable; *Fe* II narrow, single. Strongest forbidden [*Fe* II]: 4244, 4287, 4414; *Mg* II only in absorption
κ CMa	*H*, *Fe* II	Bright *H* double, variable
−22°1874	*H*, *Fe* II	
μ Cen	*H*, *Fe* II	Bright lines variable
B.D.−6°1391	*H*, *Fe* II	*Fe* II faint
H.D. 20336	*H*, *Fe* II	*Fe* II faint

TABLE IV—*Continued*

Star	Emission Lines	Remarks
	Spectrum B3e	
31 Peg	*H*	*Fe* II absent, although bright *H* fairly strong
11 Cam	*H*, *Fe* II	
χ Oph	*H*, *Fe* II, *Mg* II, *Sc* II?	
β Mon	*H*, *Fe* II	
ω CMa	*H*	
25 Ori	*H*, *Fe* II	
ζ Tau	*H*, *Fe* II	
r Pup	*H*, *Fe* II	
δ Cen	*H*, *Fe* II	
ι Ara	*H*, *Fe* II	*H* double
υ Cyg	*H*, *Fe* II	*H* double
	Spectrum B5e	
ψ Per	*H*, *Fe* II	*H* and *Fe* II lines double
27 CMa	*H*	Variable bright, unsymmetrical *H* lines
κ Dra	*H*, *Fe* II	Variable
β Pis	*H*	Double
β Lyr	*He* I, *H*, *Ca* II, *Mg* II	Interpretation uncertain. May not belong to B5 component
κ^2 Aps	*H*, *Fe* II	*H* double, variable
	Spectrum B8e	
H.D. 50138	*H*, forbidden *O* I	Variable *H*; [*O* I]: λλ 6300, 6363. Absorption lines: *He* I, *Fe* II, *Ca* II, *Na* I, *Mg* II?
Companion of *o* Cet	*H*, *He* I, *Ca* II, *Fe* II, *Ti* II?	Bright *H* broad (9 A) with absorption centers. No absorption lines visible except those accompanying the *H* lines

somewhat more puzzling; but here, too, there is considerable uncertainty as to the origin of the bright lines. Otherwise, there is a definite progression in the state of excitation of the emission lines which runs in the same direction as that of the absorption lines. In the B's there is a lag corresponding to more than an entire spectral class. The most striking feature, however, is an apparent discontinuity between Boe and O9e. The presence of bright *He* II 4686 in B.D.+6°1309, 29 Canis Majoris, and λ Cephei, shows that for the O's the lag is much smaller. The relative infrequency of emission lines of *He* I is conspicuous. There are indications that D_3 appears more frequently in emission than any of the *He* I lines in the violet

or blue regions. It is possible that some of the discordances in the relative intensities may have their explanation in a tendency of bright lines to favor certain electronic transitions.

Bright *He* II 4686 in λ Cephei is double and very broad, while in 29 Canis Majoris it is narrow. The absorption lines are also broad in λ Cephei and narrow in 29 Canis Majoris. This agrees with our correlation between widths of emission and absorption lines.

The appearance of bright lines of *Fe* II and of other elements depends in a large measure upon the intensities of the bright hydrogen lines. Thus, failure to observe *Fe* II in a B3 star does not necessarily indicate that *Fe* II is missing, but may simply mean that all bright lines are weak. If we allow for a considerable dispersion in the total intensities of all lines, there is a suprising similarity in the bright lines of any given spectral subdivision. We have tried to ascertain whether the ratios of the intensities of the lines of *H* to those of *Fe* II are really constant within any given spectral subdivision. A very good plate of 31 Pegasi, on Process emulsion, fails to show any trace of *Fe* II, although its absorption lines are similar to those of χ Ophiuchi. But the bright hydrogen lines are appreciably stronger in χ Ophiuchi, and the test is consequently not conclusive. A comparison of 31 Pegasi with 11 Camelopardalis is more instructive. In these two stars the total intensities of the Balmer lines are not very different; but the iron lines are fairly strong in 11 Camelopardalis, while they are absent in 31 Pegasi. The absorption lines are very similar in these two stars.

Although it is probable that there exist small differences in the relative intensities of lines of different elements, it is safe to say that the effective temperature of the star is the most important factor in defining the character of the emission spectrum. We should, therefore, conclude that $\rho\delta$ remains approximately constant within each subdivision, and it is therefore permissible to retain, for the emission lines, the usual Harvard classification, provided we remember that there is a difference in the effective excitations of bright and dark lines and that this difference is probably itself a function of spectral class, being small for the O's and comparatively large for the B's.

A somewhat similar classification was suggested some years ago by Miss Payne.[1]

[1] *Harvard Observatory Bulletin*, No. 855, 1928.

III. A NEW Be STAR

60 Cygni (α $20^h57^m.7$ δ $+45°46'$, mag. 5.2, Sp. B3)

The line $H\beta$ is variable in this star. A description of the Yerkes plates is given in the accompanying tabular matter.

Date	Time	Description of $H\beta$
1919 May 12.....	21^h20^m G.M.T.	Absorption very weak; faint, widely spaced emission components probably present
Sept. 1.....	14 27 G.M.T.	Same
1920 June 7.....	20 07 G.M.T.	Same
1930 July 29.....	4 52 U.T.	Normal strong absorption line
1931 Oct. 22.....	1 56 U.T.	Absorption rather weak

Dr. Merrill writes concerning this star:[1] "$H\beta$ is nondescript on several plates, but on one taken by Mr. Joy on 1917 October 3, it appears to have two faint, widely-separated bright components."

IV. VARIATIONS IN THE SPECTRA OF Be STARS

31 Pegasi (α $22^h16^m.6$ δ $+11°42'$, mag. 4.9, Sp. B3p)

This is a well-known Be star, the spectrum of which has been described by Merrill.[2] It appears from the Yerkes observations, in the accompanying table, that the bright lines show large variations in total intensity.

Date	Time	Description	
		Bright $H\beta$	Bright $H\gamma$
1908 Oct. 16....	16^h35^m G.M.T.	Single, very strong	Single, or narrow double, fairly strong
1910 Sept. 30....	14 33 G.M.T.	Same	Same
Oct. 14....	15 02 G.M.T.	Same	Same
1918 Aug. 26....	18 06 G.M.T.	Weak, very narrow double	Weak
Sept. 16....	17 50 G.M.T.	Weak single, or very narrow double	Weak
1928 Aug. 29....	8 10 U.T.	Very strong, single	Strong, very narrow double or single
Sept. 20....	6 07 U.T.	Same	Same
1931 June 15....	8 52 U.T.	Same	Same
June 17....	9 01 U.T.	Probably slightly weaker than in 1928	Probably slightly weaker than in 1928

[1] Private communication.

[2] *Lick Observatory Bulletin*, 7, 173, 1913.

31 *o* Aquarii (α $21^h58^m.1$ δ $-2°38'$, mag. 4.7, Sp. B5p)

This is also a well-known Be star,[1] having narrow bright hydrogen components superposed over wide absorption lines. Our plates show that *o* Aquarii belongs to that small group of Be stars which have sharp and probably variable absorption lines of *Fe* II. The lines of *He* I and of *Mg* II are very broad and hazy and show no variation. A description of the Yerkes plates is given in the accompanying table.

Date	Time	Description
1908 Oct. 9.....	12^h25^m G.M.T.	*Fe* II sharp and fairly strong absorption lines; *He* I and *Mg* II very broad and faint
1910 July 8.....	20 43 G.M.T.	Same
Aug. 27.....	15 39 G.M.T.	Same? (poor plate)
Sept. 19.....	14 00 G.M.T.	Same
1928 Aug. 29.....	5 06 U.T.	*Fe* II absent or very faint
Sept. 17.....	3 03 U.T.	*Fe* II faintly visible
1930 June 27.....	8 13 U.T.	*Fe* II extremely faint
1931 Oct. 10.....	0 29 U.T.	Same

There were no appreciable changes in the emission lines of hydrogen. The simultaneous existence in the same spectrum of wide and diffuse lines of *He* I and *Mg* II and of narrow lines of *Fe* II is very unusual; there are two or three other stars, however, which show the same phenomenon; it is present in ϵ Capricorni, described below, and perhaps also in H.D. 45910,[2] except that the latter has hydrogen lines of the P Cygni type, while in *o* Aquarii they are normal, double, bright lines.

The fact that there are several stars of this kind makes it seem improbable that we are dealing with a superposition of two separate stellar spectra not resolved on the slit of the instrument.[3] The broad lines of *He* I and *Mg* II are of exactly the type which we have ascribed to rapid axial rotation.[4] We are therefore forced either to abandon

[1] *Ibid.*

[2] Merrill, *Publications of the Astronomical Society of the Pacific*, **35**, 303, 1923; J. S. Plaskett, *ibid.*, p. 145; J. S. Plaskett, *Publications of the Dominion Astrophysical Observatory* (Victoria), **4**, 1, 1927. Other stars exhibiting similar features were found by Merrill, *Astrophysical Journal*, **72**, 98, 1930.

[3] See also J. S. Plaskett's discussion of *v* Sagittarii, *Publications of the Dominion Astrophysical Observatory* (Victoria), **4**, 1, 1927.

[4] Elvey, *Astrophysical Journal*, **71**, 221, 1930; Struve, *ibid.*, **72**, 1, 1930.

the rotational hypothesis of the broadening of stellar absorption lines or to seek a new explanation for the origin of the narrow lines. The evidence in favor of the rotational explanation of dish-shaped lines is so strong that we accept the latter alternative.[1]

While we have hardly enough observational material to develop a complete theory, it is possible to affirm that our present ideas concerning the origin of some of the stellar absorption lines must be modified. In the past we have supposed that all absorption takes place within the narrow domain of the reversing layer.[2] We now believe that the strong violet absorption lines in Novae and in stars of the P Cygni type originate in an expanding nebula which surrounds the star. Similarly, we are willing to attribute the narrow and deep central absorptions in some Be stars to gases which are far removed from the photosphere. Is it not possible that the narrow metallic lines in *o* Aquarii, ϵ Capricorni, etc., are also produced in a rotating nebulous shell surrounding the star, and that they are therefore similar in nature to the central absorptions of the hydrogen lines described on page 169 for φ Persei and also observed in *o* Aquarii? Since such absorption lines would be formed by those parts of the nebulous shell which are directly in front of the star, it is clear that a rotating shell (or ring) will give rise to relatively narrow absorption lines and to broad emission lines; the star itself, on the other hand, would produce "dish-shaped" absorption lines of *He* I and of *Mg* II.

39 ϵ Capricorni (α $21^h31^m.5$ δ $-19°55'$, mag. 4.7, Sp. B5p)

Variable lines of *Fe* II and of *H* in this star have been known since 1897.[3] Our plates show a spectrum distinctly resembling that of *o* Aquarii: the hydrogen lines have variable emission components, the α Cygni lines are at times strong and narrow, while the lines of *He* I and of *Mg* II are very diffuse and broad. Our first plate, taken September 17, 1915, 16^h2^m G.M.T., shows a faint emission compo-

[1] Our reasons for believing that broad absorption lines of all elements are caused by rotation, have been explained in various papers. The evidence is so convincing that it does not seem reasonable to doubt it on the basis of the observations of the few peculiar Be stars with sharp *Fe* II lines.

[2] Excepting the lines of interstellar origin.

[3] *Harvard Annals*, **28**, 183, 1897; *Lick Observatory Bulletin*, **7**, 72, 1913.

nent on the violet side of a strong and very narrow central absorption in the normal position of $H\beta$. The absorption lines of *Fe* II and *Cr* II are fairly strong and narrow, while those of *Ti* II are faint and narrow. On the succeeding plates, taken on July 15, 1930, 6^h47^m U.T., and on various dates between May 14, 1931, and October 10, 1931, the hydrogen lines have very little (if any) emission, showing only the narrow central absorption superposed upon a broad normal absorption line. *He* I and *Mg* II are conspicuously dish-shaped, while *Fe* II can be barely seen as faint narrow lines.

V. NOTE ON THE SPECTRUM OF 17 LEPORIS

This spectrum has been described previously.[1] The lines of *Ti* II, *Sc* II, *Fe* II, *Fe* I, etc., are variable in intensity and structure. At times they show a tendency to be narrow doubles. *Mg* II 4481 is somewhat broader and more diffuse than the other lines, and does not vary in intensity; together with the lines of *Si* II, 4128 and 4131, it is unusually weak for a star which otherwise displays the characteristics of a supergiant.

The hydrogen lines consist of normal broad absorption lines over which there are unsymmetrically superposed strong and narrow absorption cores. On several plates $H\beta$ shows a faint emission line on the red side of its core.

If the presence of a normally placed emission line with strong violet absorption is to be regarded as typical for stars of the P Cygni type, 17 Leporis would belong to that class. Measurement of the radial velocity on one plate (November 28, 1930, 6^h12^m U.T.) gave the following approximate results:

Mg II (4481)	+14 km/sec.
Fe II and *Ti* II	−64 km/sec.
$H\gamma$, $H\beta$ (absorption)	−93 km/sec.
$H\beta$ (emission)	+61 km/sec.

While 17 Leporis shows little in common with P Cygni, except the structure of the hydrogen lines, it resembles in certain respects the peculiar spectrum of H.D. 45910.[2] In the latter, the bright lines of

[1] Struve, *Astrophysical Journal*, **72**, 343, 1930.

[2] J. S. Plaskett, *Publications of the Dominion Astrophysical Observatory* (Victoria), **4**, 18, 1927.

H are more pronounced than in 17 Leporis. Furthermore, in H.D. 45910 "emission at the enhanced iron lines 4233, 4352, 4549, 4584, 4922, 5015, incipient or moderately strong, is often present, which, on four occasions has developed into a complete enhanced absorption spectrum: an almost exact replica of α Cygni."[1]

Here, as in the case of o Aquarii and of ϵ Capricorni, the question might be asked whether the variable α Cygni lines should not be attributed to gaseous shells around the stars, rather than to the reversing layers.

VI. THE ROTATIONAL HYPOTHESIS OF THE ORIGIN OF BRIGHT LINES

The observational evidence that has led to our acceptance of the rotational hypothesis for the origin of bright lines in Be stars, is summarized as follows:

1. The total widths of the bright lines in nearly every case exceed those expected on theoretical grounds for a quiescent gas. Laboratory lines produced under low pressure and having total energies comparable to those of the stellar lines are invariably much narrower.

2. The objection might be raised that the stellar lines may not originate under low pressure; but this is eliminated by the fact that laboratory lines broadened by pressure show wide wings similar to the wings of stellar absorption lines which are broadened by Stark effect. No such wings are observed in the emission lines of Be stars: their contours have steep outer gradients and are frequently flat, or even depressed, at the top.

3. The theoretical emission coefficient for a quiescent gas is proportional to $1/(\lambda-\lambda_0)^2$ (in the wings), and the contour should be given by Const. $N/(\lambda-\lambda_0)^2$, where N is the total number of emitting atoms. We should therefore expect a definite correlation between line width and total intensity, but none is observed. The great widths of faint emission lines strongly suggest that we are dealing with Doppler effect.

4. The total widths of the bright lines range from about 1 to 10 A. There is no definite correlation with spectral type or temperature, nor with absolute magnitude or pressure.

5. There is, however, a very definite correlation between the

[1] *Ibid.*

widths of bright lines and of absorption lines which are not affected by emission: narrow emission lines of *H* always occur in stars with fairly sharp absorption lines of *He* I, *Mg*, II *Si* III, etc. (e.g., β Piscium, 11 Camelopardalis, χ Ophiuchi, 31 Pegasi, etc.); broad emission lines are invariably observed in stars having exceedingly diffuse and shallow absorption lines suggestive of rapid axial rotation (e.g., φ Persei, π Aquarii, β Monocerotis, ψ Persei). If the dish-shaped absorption lines are due to rotation, this establishes a connection between radial component of rotational velocity and width of emission line.

6. It might be urged that the shallow contours of the absorption lines of *He*, etc., in many Be stars are due to incipient emission. This is not probable, however, because all stars that have narrow hydrogen emission lines show normal lines of helium without any trace of incipient emission.

7. The widths of the emission lines of *H* and of *Fe* II are proportional to the wave-lengths—in agreement with the Doppler effect.

8. The widths of the emission lines of *Fe* II, *Si* II, etc., are strongly correlated with those of *H*, although in any given star they are not necessarily the same. In γ Cassiopeiae the contours determined by Higgs show that the widths of *Fe* II lines are nearly identical with those of *H*. Numerous measures by R. H. Curtiss also establish the fact for this and for other stars. No physical theory as yet proposed explains this correlation. It is, however, in agreement with the mechanical hypothesis of rotation.

9. The intensities of the Balmer emission lines agree with the hypothesis that they are produced by recombination. This suggests that they originate in a nebulous shell, sufficiently far away from the photosphere to permit large deviations from thermodynamic equilibrium.

10. The doubling of many emission lines is easily explained by the mechanism of rotation. This is also true of flat-topped contours of single emission lines.

11. The discovery of forbidden lines of *Fe* II and of *O* I by Merrill might add some weight to the hypothesis of a nebulous shell, but it is not certain whether the peculiar stars of Merrill are similar to the normal Be stars.

12. Emission lines predominate in classes B and O (if we exclude the peculiar spectra of late-type variables). This agrees with the fact that rapid axial rotation is most frequently observed in these classes.

13. The pronounced difference in the excitation conditions for bright and dark lines of the same stars (see section 1) has a logical explanation in the mechanism of recombination. It would remain wholly unexplained if the origin of the emission lines were placed in the reversing layer.

14. There might be some doubt that a star of spectral class $B3$ or $B5$ possesses enough radiant energy beyond the limit of the Lyman series to render a nebula visible. It is generally believed that stars of $T=30{,}000°$ can excite an ordinary gaseous nebula to visibility. Computation[1] shows that the ratio of energy involved in a star of $T=30{,}000°$ to that of one having $T=15{,}000°$, is approximately 400 to 1. It is clear, therefore, that the cooler star might not render a diffuse nebula visible. In a Be star, however, the nebula is practically a point-source, and it is highly probable that it would show in the spectrum. To illustrate this, imagine two large diffuse nebulae like that of Orion. Let one be excited to visibility by a star of $T=30{,}000°$ while the other surrounds a star of $T=15{,}000°$. According to our computation, the total luminosities of the two nebulae would be in the ratio of 400 to 1. But if one nebula is large while the other is 400 times more compact, we should observe the same line intensities in the spectrograph. Apparently there is no theoretical reason to doubt the possibility of hydrogen emission in a nebulous shell, produced by the mechanism of photo-electric ionization and recombination.

VII. OBJECTIONS TO THE ROTATIONAL HYPOTHESIS

In a recent paper Misses C. H. Payne and G. Maulbetsch[2] have raised several objections to the rotational hypothesis of bright lines.

[1] Struve and Schwede, *op. cit.*, p. 1195.

[2] C. H. Payne and G. Maulbetsch, *Harvard Observatory Circular*, No. 364, 1931. There is a misunderstanding on page 2 (last paragraph) of this circular. The rotational velocities in Struve's paper (*Astrophysical Journal*, **73**, 94, 1931) were estimated from the appearance of the absorption lines, and not from the bright lines, as stated by Payne and Maulbetsch. The fact that these velocities are correlated with the widths of the emission lines led to the rotational hypothesis.

We shall discuss these here in the order in which they are given in their paper.

1. The widths of the broad hydrogen absorption lines which form the background of the bright lines were measured by the authors on the original spectrograms and plotted against wave-length. The result is a straight line indicating that width is proportional to λ. The slope of the line, however, corresponds to the absurd velocity of 2000 km/sec., and the intercept on the y-axis of the extrapolated straight line is negative, instead of positive as required by Doppler-broadening. The helium lines, on the contrary, give a small slope which corresponds to fairly reasonable rotational velocities.

The test is based upon two assumptions: (*a*) that within any one spectral series the original absorption lines not broadened by rotation have the same contours; and (*b*) that, in the process of measuring line widths, settings are made upon points having equal percentage of absorption, irrespective of the structure of the line. Both assumptions are subject to doubt. The first one, especially, is known to be incorrect, for normal hydrogen lines are broadened by Stark effect and the latter depends upon serial number. Therefore, even if assumption (*b*) were correct, the data of Miss Payne and Miss Maulbetsch would merely show that the dark hydrogen lines are much more affected by causes other than rotation—a result in harmony with earlier investigations.

2. Payne and Maulbetsch also assert that the widths of the helium lines disagree with the rotational hypothesis. But within the errors of measurement their helium line widths agree well with the theoretical slopes drawn by them for velocities of 250 and 500 km/sec. The fact that slightly different results are obtained for different series proves that even for helium the assumption of equal original contours is incorrect—again in agreement with expectation. Aside from this, there is no real disagreement: on the contrary, it seems to us that their measurements agree well with the rotational hypothesis.

3. Measurements of line widths are not sufficiently sensitive for establishing rotational velocities of less than 500 km/sec. Thus, it would be difficult to choose between the theoretical lines for 250 and 500 km/sec.

4. Our objection raised in (1) to the use of the hydrogen lines

refers also to the result of Payne and Maulbetsch for the Pleiades. The helium lines give no evidence of unusual or equal velocities. The existence of bright lines in many members of the Pleiades would in itself suggest (on the basis of the rotational hypothesis) that these stars rotate rapidly. But unless all of them have emission lines of exactly the same width, there is no evidence that the rotational components in the line of sight are equal.

5. The tendency of Be stars to be more luminous than normal B's is in agreement with the rotational hypothesis: if the nebulous shell results from equatorial ejection of matter, it is clear that for constant equatorial velocity a star of small surface gravity would eject more than one of large gravity.

6. The tendency of emission lines to be more frequent in early B stars than in late may be connected with the general tendency of early-type stars to have the more dish-shaped lines (or faster rotations).

7. The remark that "narrow lined B stars are absolutely brighter than hazy lined bright line B stars, as illustrated in h and χ Persei, NGC 6231 and the cluster in Carina" does not find a ready explanation in the rotational hypothesis, but may perhaps not be contrary to it.

8. There are, as Payne and Maulbetsch remark, many B stars with high rotational velocities which do not show emission lines; V Puppis is an example. A possible explanation of this effect we owe to Dr. C. T. Elvey. The formation of a ring by rotational instability must depend not only upon the linear equatorial velocity but also upon surface gravity: a giant might be expected to shed matter at lower velocities than a dwarf. The same argument has been already used in (5). It is also possible that the companion in a *very close* system would break up any nebulous shell.

9. The occurrence of *Fe* II in the spectra of stars of early class B has been explained in section I as a consequence of the mechanism of recombination.

10. The rotational hypothesis does not provide a simple explanation for the frequent variations in the relative intensities of the emission components. It is possible that the period of the variation in intensity is equal to the orbital period in a binary system, the

presence of the secondary causing a lack of symmetry in the distribution of the nebula around the primary. It should be remembered in this connection that several Be stars are known to be binaries with fairly long periods, e.g., β Lyrae and φ Persei. Another hypothesis involving a mechanism of rotation and pulsation has recently been advanced by D. B. McLaughlin.[1]

We believe, in spite of these possible explanations, that the frequent variation of the bright lines constitutes the most vulnerable point of the rotational hypothesis.

11. The preceding paragraph refers also to those Be stars which have completely lost (Pleione, μ Centauri) or regained their emission lines for long periods of time. We doubt that it would be easier to meet these difficulties with a "physical" explanation of the emission lines.

VIII. CONCLUSIONS

In forming an opinion concerning the origin of bright lines in Be stars, it is best to consider separately two questions: (*a*) "Do we know that dish-shaped absorption lines are caused by rotation?" and (*b*) "Is it proved that the widening of emission lines is due to the rotation of a nebulous ring or shell?"

A complete answer to our first question has been given in other papers. It is certain that rapid axial rotation does exist in many stars and that it has an appreciable effect upon the line contours of such stars as Algol, V Puppis, W Ursae Majoris. For the stars in general, our evidence is of a more statistical nature; and while it seems probable that rotation is the most important cause of the broadening of lines which are not subject to Stark effect, it is not possible to prove that this is true for every individual star.

Our answer to the second question is closely connected with that given to the first one. In fact, the rotational hypothesis of the bright lines rests upon the correlation of emission and absorption line widths and upon the assumption that dish-shaped absorption lines are caused by rapid rotation. It must be admitted that this correlation is based upon a comparatively small amount of material, and future work on this subject should be directed toward testing it with

[1] D. B. McLaughlin, *Publications of the American Astronomical Society* (Delaware meeting), **7**, 31, 1931.

the aid of more extensive material. But granted the correlation, and granted that our assumption is correct, there is no escape from the conclusion that the broadening of the emission lines is due to rotation.

This does not yet prove that their origin is not in the reversing layer.[1] But the facts accumulated in section VI make it seem probable that these lines originate in a nebulous shell or ring. Perhaps the best evidence is obtained from the widths of the emission lines. It is not at present possible to compare directly the rotational velocities derived from the absorption lines with those resulting from the widths of the emission lines. But in two stars we found conclusive proof that the width of the bright *Mg* II line was almost twice that of the hydrogen lines. This could not be the case if both elements were in the same layer. Unless we abandon rotation altogether, we must assume that the bright lines originate in nebulous shells or rings and that the effective distances of the various elements from the photosphere are not exactly the same.

We are under great obligation to Professor H. N. Russell for valuable suggestions and criticisms.

YERKES OBSERVATORY
October 22, 1931

[1] A very simple method suggests itself for testing whether a bright line originates in the reversing layer or above it. Consider a member of a multiplet which happens to fall upon the wing of a strong absorption line: for example, upon one of the hydrogen lines. If the bright line originates in the reversing layer, its intensity will be cut down by the opacity which is caused by the wing of the hydrogen line. On the other hand, if the bright line originates above the reversing layer, its intensity should be normal. In order to make this test, the intensities should be measured on some absolute scale and freed from the effect of overlapping with the continuous background (see Struve and Schwede, *op. cit.*, p. 1198; Struve, *Zeitschrift für Astrophysik* [in press]). The same effect, in its application to absorption lines, has been observed for stellar and interstellar *Ca* II lines, and has been found useful in distinguishing between these two types of lines (Unsöld, Struve, and Elvey, *Zeitschrift für Astrophysik*, 1, 324, 1930). Among the stars observed by us, we have not been able to find a suitable bright line, free of blends, that could be used for this test.

MEASUREMENTS OF ULTRA-VIOLET SOLAR RADIATION[1]

By EDISON PETTIT

ABSTRACT

The ultra-violet solar radiometer.—This instrument (Pl. XI*a*) consists of a pair of quartz lenses, one silvered and one gilded, mounted on a rotating disk (Fig. 1) electrically controlled in such a manner that images of the sun in $\lambda 0.32$ and $0.5\,\mu$ are made to fall alternately upon the receivers of a compensated thermocouple for consecutive periods of one minute. A complete determination of the ratio of ultra-violet solar radiation at $\lambda 0.32\,\mu$ to green radiation at $\lambda 0.5\,\mu$ is obtained each four minutes of time, the galvanometer deflections being registered photographically (Fig. 3) together with an hour-angle scale recorded by the control clock (Pl. XI*b*).

Secular variation of the measurements.—The radiometer has been in operation on most of the clear days since June, 1924. Each galvanometer record has been measured, and the logarithms of the ratio ultra-violet to green, plotted against sec z (Fig. 3), furnish a determination of this ratio for the zenith and for no atmosphere for that day. A plot of the monthly means (Fig. 4) shows a considerable correlation with the sun-spot curve, but the amplitude (0.95–1.56) is too great to be explained by variations of solar temperature alone. Since no check observations are available, it is possible that at least a part of this amplitude is due to atmospheric or instrumental effects not understood at present.

Atmospheric and instrumental sources of error.—The effects of the variation of atmospheric ozone on the radiometer measurements were tested experimentally with an ozone tube placed over the radiometer and were found to be negligible. The small variation in atmospheric transparency (Fig. 4) does not seem to show any correspondence to the radiometer-curve. A certain white haze affects the measurements in the afternoon, and, on this account, only morning observations have been used. The transmissions of the metallic films (Fig. 2) seem not to have changed during the seven years they have been in use.

Ultra-violet light from the sky.—By means of a silvered photoelectric cell it was found that the intensity on a horizontal plane of ultra-violet sky light at $\lambda 0.32\,\mu$ is about equal to that of direct sunlight when the sun is near the zenith at Pasadena (elevation 845 ft.). The same result was obtained at $\lambda 0.31\,\mu$. Change in elevation increases the direct sunlight about as much as the intensity of sky radiation diminishes at this wave-length. Seasonal and weather effects (Fig. 5) studied with an automatic device show that we receive on a horizontal plane about 25 per cent as much radiation of $\lambda 0.32\,\mu$ on a cloudy as from sun *plus* sky on a clear day. The least amount observed was 10 per cent, recorded during a rainstorm. We receive about as much on a clear day at the winter solstice as during a cloudy day in midsummer. After the sun reaches an altitude of 6°, the intensity of sky radiation at $\lambda 0.32\,\mu$ on a horizontal plane increases proportionally with the solar altitude. The distribution of radiation at $\lambda 0.32\,\mu$ over the sky (Fig. 7) is rather uniform, being somewhat greater toward the southern horizon under the sun and less toward the northern horizon. The sudden increase near the sun takes place at greater angular distances on hazy days.

Ultra-violet limit of the spectra of skylight and direct sunlight.—A quartz spectrograph and a concave grating, crossed with a quartz monochromator, were used. In midsummer the ultra-violet limit of skylight is about $\lambda 0.296\,\mu$ and of direct sunlight a little less than $\lambda 0.290\,\mu$. In midwinter the limits are $\lambda 0.298$ and $0.296\,\mu$, respectively. It is believed that it would be difficult to detect the spectrum of the sky much

[1] *Contributions from the Mount Wilson Observatory, Carnegie Institution of Washington*, No. 445.

below $\lambda 0.295\,\mu$ for a point far from the sun. This argues for a small amount of ozone in the lower atmosphere.

Spectral energy-curve of the sun in the ultra-violet.—This was investigated at the Research Laboratory of the Desert Sanatorium at Tucson with a double arrangement of Bausch and Lomb quartz monochromators (Pl. XII*b*), fed by a siderostat (Pl. XII*a*) with stellite mirror. The thermopile alone was used for wave-lengths greater than about $0.32\,\mu$, while for shorter wave-lengths a quartz photoelectric cell was used in addition to the thermopile. Measurements were made for wave-lengths between $\lambda 0.7$ and $0.292\,\mu$. The results show that, outside the atmosphere, the energy-curve (Figs. 10 and 11) has a sudden drop of 35 per cent between $\lambda 0.40$ and $0.38\,\mu$ and a nearly constant value at about 43 per cent of the maximum between $\lambda 0.38$ and $0.325\,\mu$, nearly the entire ultra-violet spectrum. A calibration is given in watts per square meter per hundred angstroms.

Atmospheric ozone at Tucson.—The atmospheric transmissions (Fig. 9) below $\lambda 0.32\,\mu$ obtained in the course of the measurement of the solar energy-curve furnish a determination of the atmospheric ozone at Tucson. This is equivalent to a layer 0.18 cm thick at N.T.P.

The well-known eleven-year period of sun-spots strongly suggests that the solar radiation may be a variable quantity. That this variation may be most pronounced in the extreme ultra-violet is to be expected from our experience with non-eclipsing variable stars. Thus the photographic range of brightness of the Cepheid variables is, on the average, 50 per cent greater than the visual range;[1] and the visual range of the long-period variables exceeds that of their total radiation by more than 4 mags.[2] Should the sun be slightly variable, whether owing to a change in temperature, a variable emissivity, or a variable transmission of the outer solar envelope, the range in the ultra-violet radiation would probably be much greater than that in visual or infra-red radiation.

In 1922 C. G. Abbot and his colleagues[3] compared the ordinates of bolometer-curves at several selected wave-lengths recorded at times of high and low solar constant and found that the difference was most pronounced in the extreme ultra-violet, being about 5 per cent at $\lambda 0.32\,\mu$ and scaling off practically to zero in the near infra-red. About the same time, G. M. B. Dobson[4] in England, using a photographic method, measured on thirty-four days the solar radiation transmitted by silver films and found a large variation. It occurred to the writer that the defects of the photographic process

[1] Russell, Dugan, and Stewart, *Astronomy*, **2**, 761, 1927.

[2] Pettit and Nicholson, *Mt. Wilson Contr.*, No. 369, p. 486; *Astrophysical Journal*, **68**, 306, 1928.

[3] *Annals of the Astrophysical Observatory, Smithsonian Institution*, **4**, 206, 1922.

[4] *Proceedings of the Royal Society of London*, A, **104**, 252, 1923.

could be avoided by using a thermocouple as the measuring device, and that the uncertainties arising from the atmosphere and the standard of radiation could be eliminated by comparing the deflections produced by sunlight transmitted by silver with those produced by sunlight transmitted by gold. By making the apparatus automatic the number of observations could be increased and a continuous record of sky conditions obtained.

The principle of the apparatus designed to meet these specifications is illustrated in Figure 1. A spindle *A* carries a disk *D*, on which two lens cells are mounted diametrically opposite each other with their centers 6 inches apart. Cell *S* contains a crystal quartz lens and plate, both silvered chemically on their inner surfaces with two coats of silver. Cell *G* contains a similar quartz lens and plate, both coated with gold on their inner surfaces by sputtering. The lenses are of the crossed type, having minimum spherical aberration, and are of 1-inch aperture and 2-inch focal length. The separators fit the surfaces and make practically air-tight contacts. Simple copper diaphragms in contact with the outer surfaces of the plates limit the aperture of the silvered lens to 8.08 mm, and of the gold lens to 9.35 mm. These diaphragms have proved a valuable means of checking the effect of continued exposure of the apparatus to sunlight on the transmissions of the lenses and filters.

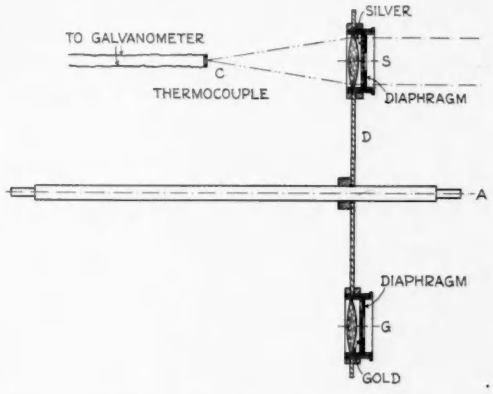

FIG. 1.—Principle of the ultra-violet solar radiometer.

Exposed to the sun, the silvered lens forms a solar image $\frac{1}{2}$ mm in diameter, in ultra-violet light of wave-length 0.32 μ, on one junction of the compensated thermocouple *C*. An escapement attached to the spindle *A*, operated electrically each minute by a contact clock, causes the image to fall first on one, then on the other blackened

receiver of the thermocouple, and then permits the disk to rotate a half-revolution and thus interchange the lenses. The process is then repeated with the gilded lens, which transmits green radiation at $\lambda 0.50\,\mu$. The galvanometer deflections produced by the thermocouple furnish a complete determination of the ratio of the ultra-violet radiation at $\lambda 0.32\,\mu$ to the green radiation at $\lambda 0.50\,\mu$ every four minutes of time. The transmissions of the gold and silver films are shown in Figure 2.

Plate XI*a* shows the ultra-violet solar radiometer attached to the 6-inch telescope on Mount Wilson. A brief description of the instrument and some of the results obtained with it have already been given.[1] The thermocouple *T* is of the air-cell type. The cell is of brass weighing about 2 kg and has a copper core provided with four windows, two forward of quartz and two at the rear of glass. The thermocouple mounted within the core is isolated in a small compartment of about 1-cc volume surrounded by thick metal walls and, in the direction of the light-beam, by air compartments. Until this year a vacuum thermocouple and rough galvanometer were used, but these have now been replaced by the air thermocouple just described and a sensitive galvanometer. The motor *M*, working through a friction disk *D*, exerts a continuous torque on the spindle, which is permitted to rotate only when the escapement *E* releases it at intervals of one minute. A cable of wires *C* carries the current from the contact clock to the escapement magnets and also the current from the thermocouple *T* to the galvanometer in the room beneath the telescope. A steel wire *W* runs over the hour-circle of the telescope and over pulleys to the registering device in the room below, where the slide

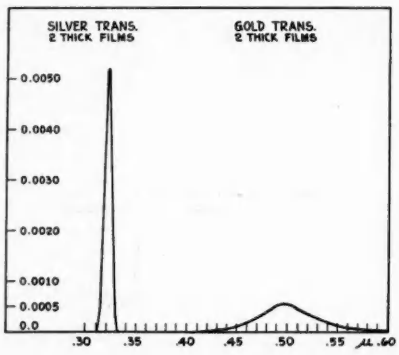

FIG. 2.—Transmissions of the silver and gold films used in the ultra-violet solar radiometer.

[1] *Publications of the Astronomical Society of the Pacific*, **38**, 26, 1926; *Mt. Wilson Comm.*, No. 98; *Proceedings of the National Academy of Sciences*, **13**, 380, 1927.

PLATE XI

a

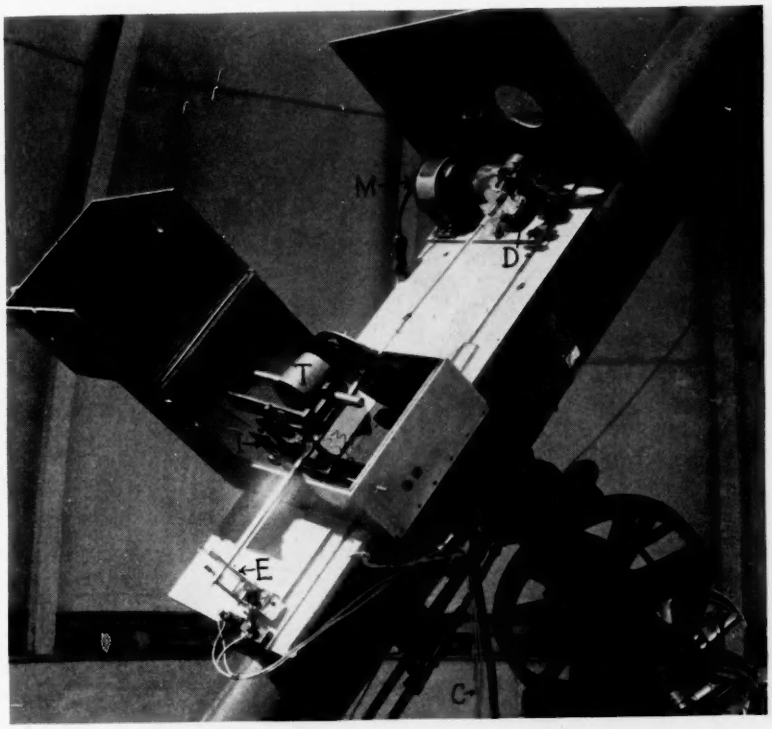

b

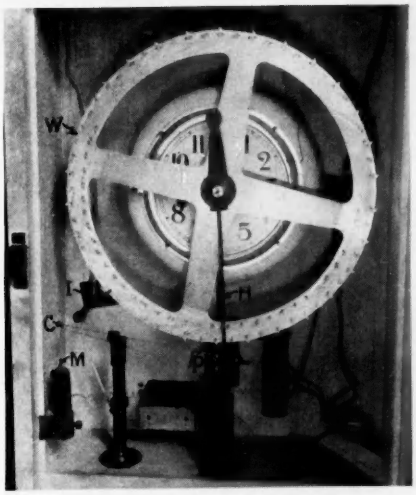

a) Ultra-Violet Solar Radiometer on Mount Wilson
b) Control Clock

UNIV. OF MICH.

carrying the photographic plate is attached directly to the end of the wire. The motion of the telescope causes the plate to fall at the rate of 27 mm per hour. A record of nine hours (135 determinations of the ratio of ultra-violet to green) can thus be put on an 8×10-inch plate. A motor re-winding automatically maintains driving-clock operation.

ADJUSTMENTS OF THE ULTRA-VIOLET SOLAR RADIOMETER

In the cycle of operations of the escapement, the movement of the image from one junction of the thermocouple to the other in order to give the galvanometer deflection occupies only a fraction of a second, while the interchange of the lenses which follows requires about nine seconds. The controlling clock must therefore give a positive instantaneous contact, followed by one which need not be so positive. To this end the clock illustrated in Plate XI*b* was constructed. The wheel *W* has thirty teeth operating against a pallet *P*, half as long as the space between the teeth. A steel wire contact *C*, which dips into mercury *M* during the minute the pallet is pressed down by a tooth, is released suddenly and remains in open circuit for the following minute. This action operates a double-throw relay which is so wired with the magnets of the radiometer escapement that the interchange of lenses takes place while the clock is depressing the pallet to make contact with the mercury, and the contact is released when the image of the sun moves from one junction to the other. With this arrangement the multiple contacts which sometimes occur at the "make" with the mercury surface do not affect the operation of the lens system. Once each hour a second contact *H* on an adjustable hand makes the circuit with a second mercury cup and lights a small flashlight bulb near the galvanometer. An hour-angle indicator is thus recorded in the form of a straight line crossing the plate at right angles to its motion. A dial on the contact wheel reads the minutes of time from the index *I*, which is a fixed hand set to correct for longitude. An inner dial corrects for equation of time by reference to the contact *H*. The observer then sets the outer dial to read standard time, after which the plate will be automatically flashed with a straight line as the sun passes each hour angle of digital value.

The adjustment of the lenses so that during operation the green and ultra-violet images shall fall alternately in the same place on the thermocouple junctions is important. Since the ultra-violet image is totally invisible, this adjustment is not easy. To accomplish it properly a fluorescent screen is used. The thermocouple is removed and a piece of uranium glass is placed at the focus of the lenses and moved about until a speck of dust centers on the image formed by the gilded lens. The escapement is then operated and the fluorescent image produced by the ultra-violet light from the silvered lens is accurately centered on the dust speck by three radial screws which hold the lens cell in position. Proper relative focusing is accomplished by the same means.

The instrument is pointed on the sun by observing the green image with a simple lens eyepiece *I* (Pl. XI*a*) focused on the thermocouple. The guiding of the instrument may be tested from time to time by checking the position of the green image or by using the image of the sun formed by the telescope on which the radiometer is mounted. After being set on the sun, the hour-circle of the telescope, which has previously been unclamped, is rotated until the plate carriage attached to the steel wire *W* is at the top of its slide. The hour-circle is clamped and the registration of the galvanometer deflections then begins.

MEASUREMENT AND REDUCTION OF THE PLATES

The upper part of Figure 3 illustrates two of the photographic records. The inside rows of dots are produced in each case by the radiation transmitted by silver, $\lambda = 0.32\,\mu$, while the outside rows are due to the radiation transmitted by gold, $\lambda = 0.50\,\mu$. The heavy lines are hour marks put on by a lamp operated by the contact clock and indicate local time. The numbers at the upper ends of these lines give the local solar time, those below, the hour angle. It will be seen that the ultra-violet light is zero for some time after sunrise and reaches a maximum at noon, while the green radiation has a large value at sunrise and more slowly approaches its maximum at noon.

Measurements of the plates with a suitable comparator[1] give the

[1] *Journal of the Optical Society of America*, **10**, 267, 1925.

galvanometer deflections and eventually the logarithms of the ratio of ultra-violet to green for each four minutes of time. The lower part of Figure 3 shows the graphical solutions for each of the plates. The logarithm of the ratio, ultra-violet to green radiation, is plotted

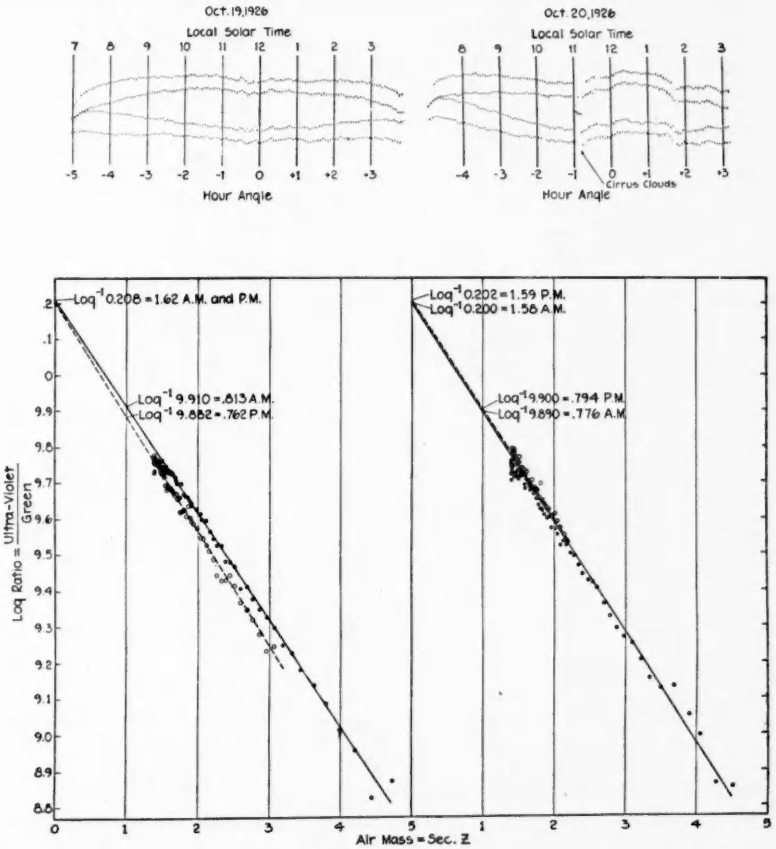
Oct. 19, 1926
Local Solar Time
7 8 9 10 11 12 1 2 3
-5 -4 -3 -2 -1 0 +1 +2 +3
Hour Angle
Oct. 20, 1926
Local Solar Time
8 9 10 11 12 1 2 3
-4 -3 -2 -1 0 +1 +2 +3
Cirrus Clouds
Hour Angle
Log⁻¹ 0.208 = 1.62 A.M. and P.M.
Log⁻¹ 9.910 = .813 A.M.
Log⁻¹ 9.852 = .762 P.M.
Log⁻¹ 0.202 = 1.59 P.M.
Log⁻¹ 0.200 = 1.58 A.M.
Log⁻¹ 9.900 = .794 P.M.
Log⁻¹ 9.890 = .776 A.M.
Log Ratio = Ultra-Violet / Green
Air Mass = Sec. Z

FIG. 3.—Records from the ultra-violet solar radiometer (above) and their graphic solutions (below).

against sec z obtained from the hour angle and a suitable conversion table. This plot defines a straight line from which two values are read, that for the zenith, sec $z = 1$, and that for no atmosphere.

The middle curve of Figure 4 shows the march of the monthly means (broken line) and the three-month running averages (full

line) of the ratio, ultra-violet to green, for the seven years beginning with June, 1924. The arbitrary scale at the left gives these values in units of the average for June, 1924. It will be noted from this curve that the monthly average of the ratio ultra-violet to green solar radiation has varied from 0.95 to 1.57 during the period

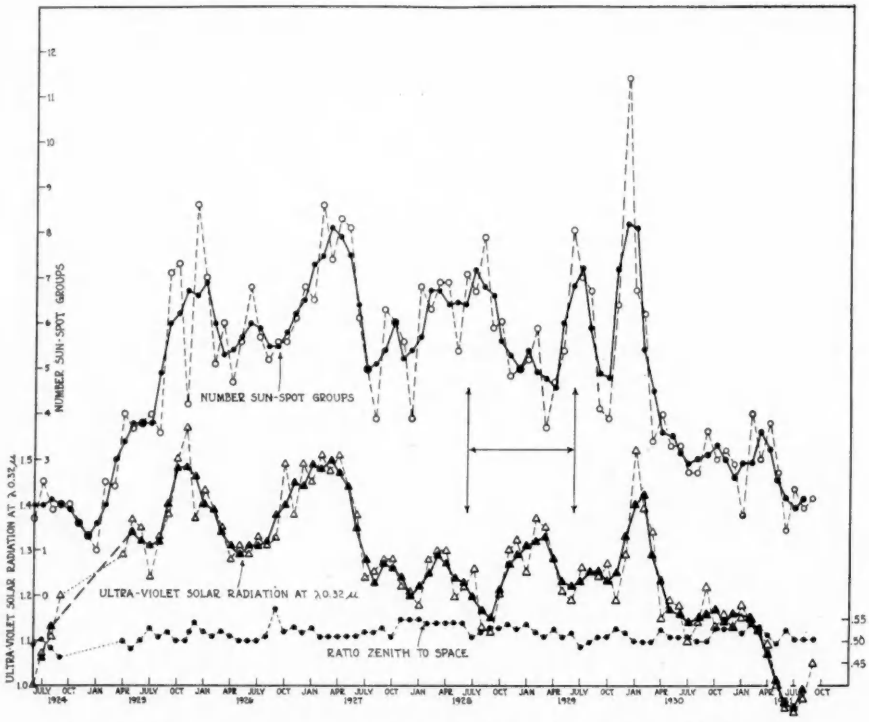

FIG. 4.—Monthly averages (middle curve, broken line) and three-month running averages (full line) of the ratio ultra-violet (λ 0.32 μ) to green (λ 0.5 μ) solar radiation for no atmosphere compared with the average daily counts of sun-spot groups treated similarly (upper curve). Below is the variation of atmospheric transmission at λ 0.32 μ (ratio zenith to space); scale at the right.

of seven years since 1924. On three occasions, namely, November and December, 1925, February and April, 1927, and January, 1930, it surpassed 1.5. It is now back to 1.0, where it stood in the beginning, and at the same point on the descending branch of the sun-spot cycle that it was on the ascending branch in the beginning. The top curve of Figure 4 gives the Mount Wilson monthly averages

of the daily number of sun-spot groups treated in similar fashion.[1] Considerable correspondence between the two curves will be noted, but it must be borne in mind that there are no independent checks on these data so much to be desired, such, for example, as another instrument, operated in the Southern Hemisphere. During the year June, 1928, to June, 1929, indicated by the arrows in the figure, the two curves ran exactly counter. No instrumental or atmospheric reason for this is known at this time, but it is significant that plots of the characteristic figures[2] of the calcium and bright hydrogen flocculi show only very slight depressions corresponding to that of the sun-spot curve for this interval. It is clear that no allowable variation in the general surface temperature of the sun will account for the variation in the ratio, ultra-violet to green, shown in Figure 4, since a range of nearly 1000° C is required if the energy-curve behaves like that of a black body. The results suggest a large atmospheric variant like the white haze shortly to be described, which may itself depend on ultra-violet sunlight. The discussion in the following section does not, however, reveal any effect of this sort to account for the phenomenon. On the other hand, the wave-length in which these measurements were made, 0.32 μ, is on a steep slope of the solar energy-curve (Fig. 11), which may be the edge of a variable absorption band in the solar spectrum.

ATMOSPHERIC AND INSTRUMENTAL SOURCES OF ERROR

The work of Dobson and D. N. Harrison[3] has shown that over the continent of Europe the atmospheric ozone varies in a seasonal cycle from a maximum of about 0.33 cm at N.T.P. in April to 0.23 cm in October. Measurements made at Table Mountain, California,[4] distant 24 miles by air-line east-northeast of Mount Wilson, show a range of approximately 0.28–0.21 cm, while in the desert climates of Arizona and South America even smaller values are found.[5]

[1] Published bimonthly by Nicholson in *Publications of the Astronomical Society of the Pacific;* complete monthly averages for the preceding year in the February number.

[2] *Bulletin for Character Figures of Solar Phenomena,* published quarterly by the Federal Observatory in Zürich.

[3] *Proceedings of the Royal Society of London,* A, **110,** 660, 1926.

[4] Dobson, *ibid.,* A, **129,** 411, 1930.

[5] F. E. Fowle, *Smithsonian Miscellaneous Collections,* **81,** No. 11, p. 13, 1929.

To provide a practical test of the question whether any possible fluctuations in the ozone content of our atmosphere might affect the measurements of the ratio of ultra-violet to green, an ozone tube 67 cm long, fitted with quartz windows, was placed in the light-path of the radiometer. Analysis by the usual iodine method showed the amount of ozone to be 1.38 cm at N.T.P., the actual pressure being 29.1 inches *Hg* in Pasadena, where the tube was filled. The ozone content was varied, by use of a pump provided with a gauge, while the sun was crossing the meridian. The experiment began at hour angle -4^m and ended at $+36^m$, sec z being 1.03–1.04 throughout the interval. The data shown in Table I were obtained with this arrangement on May 26, 1926. A plot of the ozone content against

TABLE I

Pressure	Ozone	Ratio $\frac{\text{Ultra-Violet}}{\text{Green}}$
29.1 in.	1.38 cm	0.610
19.6	0.93	0.731
10.2	0.48	0.897
4.9	0.23	0.955
0.0	0.00	1.000
Air filled	0.00	1.000

the ratio of ultra-violet to green shows that doubling the mean atmospheric ozone content[1] of 0.24 cm reduces the ratio by 5 per cent. Dobson's seasonal range of approximately 0.28–0.21 cm for Table Mountain would produce a variation in the ratio of less than 1 per cent. Since the observed variations of ultra-violet light greatly exceed this amount, it is thought the ozone effect can safely be neglected.

Whether the atmosphere in general affects the measurements may be seen from the bottom curve in Figure 4, which represents the monthly averages of the quotient of the values of the ultra-violet to green ratio for the zenith to no atmosphere. This quotient is the ratio of the atmospheric transmission for $\lambda\, 0.32\,\mu$ to that for $\lambda\, 0.50\,\mu$, and, since the transmission for $\lambda\, 0.50\,\mu$ is high, about 86 per cent, the curve is essentially a curve of variation of the atmospheric transmission at $\lambda\, 0.32\,\mu$. The range is from 0.45 to 0.55 and seems

[1] *Proceedings of the Royal Society of London*, A, **129**, 413, 1930.

not to be definitely correlated with the ultra-violet measurements. Ordinary cirrus clouds and haze apparently do not greatly affect the measurements. Indeed, some experimental runs made through such a sky give results nearly equal to the average for the month.

There is, however, a kind of white haze which fills the valley below Mount Wilson and frequently rises over the top by 11:00 A.M. that affects the measures markedly. It is noted especially on very warm days in summer and autumn, and its effect may be seen in the plots of Figure 3, where dots represent morning measurements and open circles afternoon values. The dotted line indicates the solution for the afternoon values. It will be noted that on October 19, 1926, when haze appeared in the afternoon, the values fall below the corresponding results for the morning run, while on October 20, which was free from white haze although some cirrus clouds appeared for a short time, the morning and afternoon values are nearly identical. We have made it a practice to estimate the amount of this haze by holding the thumb at arm's length to cover the sun and estimating the distance from the sun's limb to which the whiteness can be traced. The observer records the result on a scale of 1–5 when he visits the instrument approximately once an hour to examine its adjustments. On account of the prevalence of this white haze, the afternoon runs have not been used in following the variations of ultra-violet solar radiation, and only morning runs were used in the plot in Figure 4.

No tarnish has been observed on the metallic films during the seven years they have been in use without replacement. Their transmissions, determined by direct measurement on a number of occasions spread over this interval, appear to be constant. In making these determinations the cells are taken apart and each film is tested separately. The gold transmission is tested radiometrically and the silver transmission by spectrophotography, by a method already described.[1]

The effect of sunlight on the transmissions of the gold and silver films, and of the quartz lenses and plates, was tested from time to time by removing the copper diaphragms (Fig. 1) and replacing them by diaphragms of twice the aperture, exposing a previously

[1] *Mt. Wilson Contr.*, No. 336; *Astrophysical Journal*, **66**, 43, 1927.

unexposed zone of the lenses and films. This operation has always increased the deflections fourfold, showing that the transmissions of that portion of the optical system exposed by the usual diaphragms has not changed relative to the unexposed portion.

During the first two years of operation a piece of green celluloid[1] was used between the gilded lens and the plate to narrow the gold transmission band. As its density was found to be increasing, this screen was removed on September 23, 1926. The effect of the solarization of this celluloid screen was found both by direct transmission measurements and by substituting a fresh piece of the same celluloid immediately after removal of the solarized piece. Other pieces were exposed to the sun for different intervals (a maximum of two hours at noonday in September) long enough to become denser than the piece removed from the radiometer. The transmissions of these pieces were measured and found to be inversely proportional to the exposure time. The radiometer measures were then collected and corrected by an amount depending on the total number of hours the instrument had been in operation up to the time any given observation was made. The correction factor applied to each value of the ratio of ultra-violet to green varied from 0.998 on May 28, 1924, to 0.600 on September 23, 1926, after a total exposure of 2246 hours. The celluloid was removed from the machine on this date and never replaced.

ULTRA-VIOLET LIGHT FROM THE SKY

The ultra-violet radiation from the sky at $\lambda 0.32\,\mu$ was measured with vacuum sodium photoelectric cells constructed by Burt. These cells, made by the process of electrical transfusion through the glass bulb, are essentially spherical soda-glass cells, 70 mm in diameter, with a clear circular aperture of 55 mm. The thin glass readily transmits radiation at $\lambda 0.32\,\mu$.[2] The cells were coated with silver, and the deflections were produced by a shutter of thick plate glass, which does not transmit $\lambda 0.32\,\mu$, but allows longer wave-lengths to pass through.[3] Thus any pinholes in the film would not affect the observed deflections. The presence of pinholes was tested directly by comparing deflections observed with the glass plate and with a

[1] *Ibid.*, Fig. 4, curve 10. [2] *Ibid.*, Fig. 9, curve 45. [3] *Ibid.*, curve 40.

wooden shutter. No difference was noted, however. The cell was used in series with a 500-ohm galvanometer, a B-battery, and a protecting resistance. That these cells give deflections nearly proportional to the cross-section of the beam entering the circular clear aperture at any angle was tested by mounting them on a turn-table provided with a graduated circle, set 3 m from a lamp, and comparing the galvanometer deflections for various angles of incidence. The deflections when the cell is exposed to radiation from the sky with the plane of the circular window of the cell horizontal are therefore proportional to the intensity on a horizontal plane.

Measurements of the ratio of sky radiation to direct sunlight at λ 0.32 μ in Pasadena show that at this elevation, 845 feet, the intensity of sky radiation on a horizontal plane is equal to that of direct

TABLE II

	Elevation (in Feet)	Sun *plus* Sky	Sky	Sun	Ratio Sky/Sun
Pasadena	845	22.0	11	11	1.00
White Man's	3400	23.0	9	14	0.55
Mount Wilson	5700	23.3	7	16.3	0.43

sunlight when the sun is near the zenith. The sun was shaded off by a black wooden sphere, 4 inches in diameter, held 6 feet from the cell, so that the sky radiation alone was effective. The removal of the wooden sphere gave sky *plus* sun. On October 9, 1928, this ratio for λ 0.31 μ was tested by use of Eastman filter No. 52 and Corning 985B glass, which isolates a narrow band at this wave-length. Although this filter is inefficient, the deflection produced by the sky was 66 mm, and sun *plus* sky, 125 mm, showing that for a zenith distance of 44° the sun and sky contribute equally to a horizontal plane at this wave-length also.

The effect of elevation on the intensity of sun *plus* sky and on the ratio of sky to sun for λ 0.32 μ was tested on June 13, 1928, a very clear day. A silvered cell and portable galvanometer were used, a continuous record being kept in Pasadena by an automatic contrivance shortly to be described. Deflections were taken in Pasadena, elevation 845 feet; at White Man's, on the Mount Wilson trail, elevation 3400 feet; and on Mount Wilson, elevation 5700 feet. Table II shows the measurements.

It appears from this table that at λ 0.32 μ the intensity of sun *plus* sky on a horizontal plane does not vary much with elevation, the decrease in sky radiation being balanced by increased direct sunlight as the elevation increases.

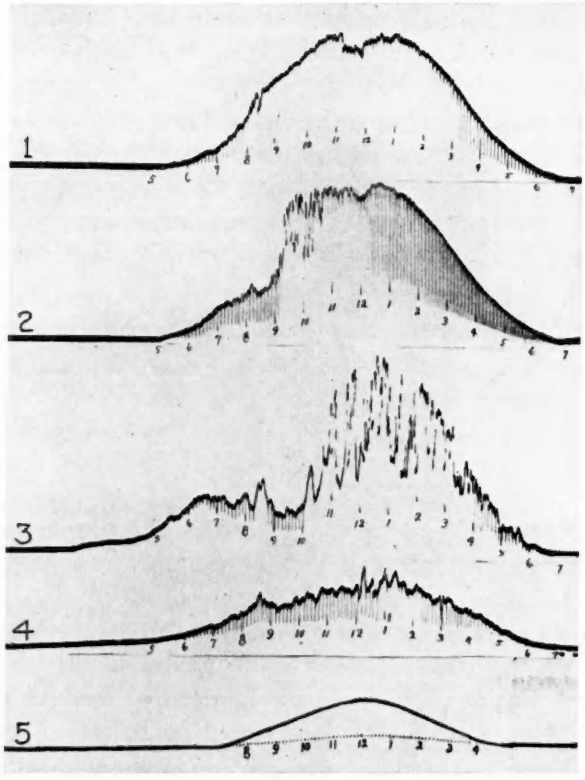

FIG. 5.—Records from the photoelectric radiometer measuring sun *plus* sky on a horizontal plane at λ 0.32 μ. Curves 1, 2, 3, 4, very clear to completely overcast days in summer. Curve 5, very clear day in midwinter.

The seasonal and weather effects on sun-*plus*-sky radiation at λ 0.32 μ were studied over a period of eighteen months with a silvered photoelectric cell and a protecting quartz cover mounted in a box with a motor-driven glass shutter. This apparatus was mounted on the roof of the instrument-shop building in Pasadena and the deflections were registered on bromide paper on a rotating

drum driven by an eight-day clock. A contact on this clock operated the shutter eight times every hour.

Figure 5 illustrates typical records, the first four taken late in May and the last late in December, 1928. The local solar time is indicated at the base of each curve. Curve 1 shows the diurnal march of the intensity of solar radiation at λ 0.32 μ incident on a horizontal plane for a clear day in early summer. The dip near noon is due to the white haze before mentioned. Curve 2 shows the effects of high fog in the morning followed by a clear afternoon. Number 3 indicates clouds in the morning and passing clouds the rest of the day. Number 4 represents a dark cloudy day such that lights were needed indoors much of the time. Even then the ultra-violet light received was nearly 25 per cent of that for a clear day. Curve 5 shows the seasonal effect of the low December sun. It will be noted that the ultra-violet radiation on a completely cloudy day in summer was as effective as a perfectly clear day in midwinter. Curve 5 also illustrates the effect of wind and rain in removing the white haze that affects the other curves near noon. Measurements were made on a number of dark days, during one of which a thunderstorm passed. The least amount of radiation observed was 10 per cent of that received at the same hour on a clear day.

The march of ultra-violet sky radiation at λ 0.32 μ during the day is illustrated in Figure 6. The ordinates are galvanometer deflections and the abscissae, altitudes of the sun. Until the sun reaches an altitude of about 6°, the amount is small. Thereafter the sky radiation is proportional to the altitude until noon. The afternoon values are higher than those of the morning on account of the additional scattering of cirrus clouds and haze.

The distribution of ultra-violet light at λ 0.32 μ over the sky was measured with a silvered photo-electric cell mounted in a cardboard cylinder, from which a second cylinder projected at right angles to receive the light. The second cylinder was 3 inches in diameter and 20 inches long, blackened inside. The 4-inch wooden ball at 6 feet distance was used to shade the opening in the tube from the sun. The tube was attached to an altazimuth mounting provided with a circle to read angular distance from the sun. The readings were made near noon in the plane of the meridian. The results for several

days, under different sky conditions, are plotted in Figure 7, in which the intensities are counted from the graduated circle representing the plane of the meridian. The rapid increase of intensity near the sun begins at greater angular distances on hazy days than on clear days. The intensity toward the southern horizon below the sun is greater than that at an equal distance above (north of) the sun.

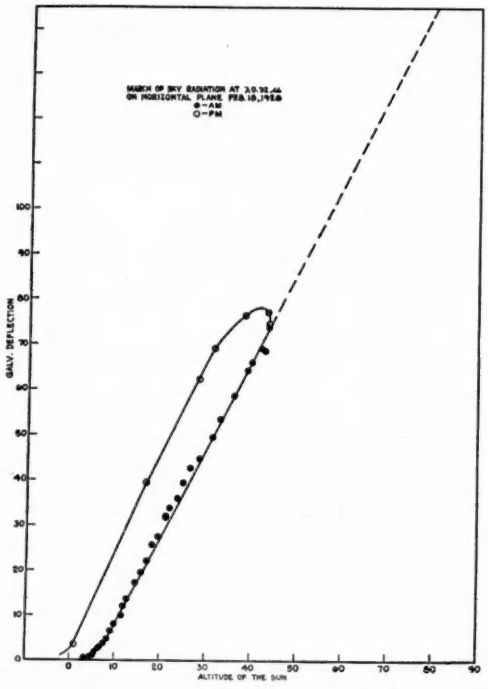

FIG. 6.—March of the sky radiation at λ 0.32 μ on a horizontal plane on a clear day in Pasadena.

THE ULTRA-VIOLET LIMIT OF THE SPECTRUM OF SKYLIGHT AND OF DIRECT SUNLIGHT

It is well known that the ultra-violet limit of the spectrum of direct sunlight photographed with a concave grating or a quartz spectrograph is about λ 0.2975 μ—the violet limit of Rowland's *Table of Wave-Lengths*. Increased exposure brings up only a fogged strip produced by scattered light in the instrument. The most effective

way to reduce the fogging is to filter out the longer wave-lengths by using a monochromator in front of the spectrograph with its dispersion along the slit. By means of this crossed spectrograph method Fabry and Buisson[1] have photographed the spectrum of direct sunlight down to $\lambda 0.2885\,\mu$. If there is any ozone in the lower atmosphere, it may be questioned whether the sky spectrum would

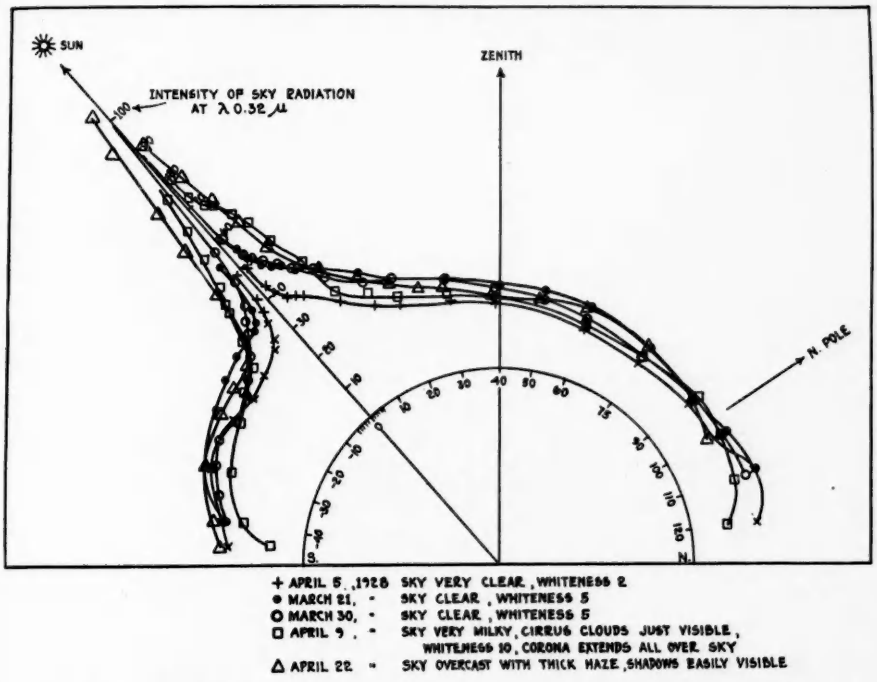
SUN
ZENITH
INTENSITY OF SKY RADIATION AT λ 0.32 μ
N. POLE
S.
N.
+ APRIL 5, 1928 SKY VERY CLEAR, WHITENESS 2
● MARCH 21, " SKY CLEAR, WHITENESS 5
○ MARCH 30, " SKY CLEAR, WHITENESS 5
□ APRIL 9, " SKY VERY MILKY, CIRRUS CLOUDS JUST VISIBLE, WHITENESS 10, CORONA EXTENDS ALL OVER SKY
△ APRIL 22 " SKY OVERCAST WITH THICK HAZE, SHADOWS EASILY VISIBLE

FIG. 7.—Distribution of radiation at $\lambda 0.32\,\mu$ over the sky at noon near the equinox, Pasadena.

reach so far into the violet, since sunlight scattered from the sky must pass through a longer air-path than direct sunlight. In order to study this problem, a Bausch and Lomb quartz monochromator used as a filtering spectroscope was crossed with two spectrographs: (1) a 1-m concave-grating spectrograph and (2) a quartz spectrograph made of the optical parts of the Bausch and Lomb quartz monochromator and designed for use with the 100-inch telescope.

[1] *Astrophysical Journal*, **54**, 297, 1921.

The relative speeds of these two arrangements depend on (*a*) the fraction of the sky included by the optical train, (*b*) the dispersion, and (*c*) the spectral efficiency of the instruments. The relative advantages of the two spectrographs are indicated by Table III.

TABLE III

	Fraction of the Sky Effective	Dispersion A per Mm	Spectral Efficiency at λ 0.302 μ
1-m grating	7×10^{-4}	17.4	0.045
Quartz spectrograph	5×10^{-3}	61	0.42

The efficiency of the 1-m concave-grating spectrograph, which was ruled with shallow lines giving a bright first order, was measured with a photoelectric cell in combination with the monochromator, the collimator lens of which was diaphragmed down so that the light entering the spectrograph just filled the grating. The ratio of the galvanometer deflections with and without the grating gives the efficiency. The results for several wave-lengths are

λ	0.435	0.406	0.366	0.313	0.302	0.254
Efficiency	0.054	0.057	0.063	0.049	0.045	0.040

A comparison of the factors given in Table III shows that for $\lambda=0.302\,\mu$ the quartz spectrograph is more than two hundred and fifty times as efficient as the grating spectrograph when used on the sky.

Since the spectral energy decreases indefinitely with decreasing wave-length, the ultra-violet limit must be defined as we observe it. Practically, this limit is determined by continuing the exposure until the fog along the spectrum strip produced by the scattered light in the instrument may easily be seen. The appearance of this fog, which was held at a minimum by maintaining the width of the spectrum (opening of the monochromator slits) at about 0.3 mm, was taken as an index of complete exposure. The minimum wave-length visible on the plates under these conditions is accepted as the ultra-violet limit. The results for the two arrangements of apparatus are given in Tables IV and V. The exposures were made in Pasadena on a point 50° above the northern horizon.

The column labeled "Fog" gives the character of the plate fog as very weak (VW), weak (W), medium (M), strong (S), or very strong (VS).

TABLE IV

ULTRA-VIOLET LIMIT OF SKYLIGHT

1-M GRATING SPECTROGRAPH AND QUARTZ MONOCHROMATOR				QUARTZ SPECTROGRAPH AND MONOCHROMATOR			
Date	Exposure Time	Limit	Fog	Date	Exposure Time	Limit	Fog
		μ				μ	
1928 July 6.....	2h	0.297	VW	1930 June 16, 17..	14h	0.296	S
7.....	5	.296	M	19, 20..	12	.296	S
8.....	5	.295	VW	21–23..	18	.296	VS
				24, 25..	16	.296	S
Dec. 20.....	6	.301	VW	26.....	7	.295*	M
21.....	6	.301	VW				
1928 Dec. 22 to 1929 Jan. 1..	60	0.298	S	July 5.....	10	.296	S
				1931 Jan. 2–8....	42	0.296†	S

* Wide slit. Burned out at λ 0.2967 μ.

† Strong at λ 0.2967 μ. Burned out at λ 0.302 μ.

TABLE V

ULTRA-VIOLET LIMIT OF DIRECT SUNLIGHT; 1-M GRATING SPECTROGRAPH AND QUARTZ MONOCHROMATOR

Date	Exposure Time	Limit	Fog	Remarks
		μ		
1929 June 26.....	1h20m	0.290	M	6-inch quartz objective; lines visible to λ 0.291 μ easily
27.....	2 0	.290	VW	Easily to λ 0.291 μ; bromine tube and Corning Purple Corex added
July 9.....	0 30	.291	W	Narrow spectrograph slit
10.....	1 0	.290	W	Very narrow monochromator slit
1929 Jan. 22.....	1 0	.297	S	Wide monochromator slit
23.....	3 0	.297	VS	Wide monochromator slit
25.....	3 0	.296	S	Easily to λ 0.297 μ
26.....	3 0	0.297	M	

A comparison of the figures in these tables shows that the ultra-violet limit of the sky spectrum near the summer solstice is about λ 0.296 μ, and that at the winter solstice the exposure required to

reach this limit is increased threefold. From a point in the sky far from the sun, it would probably be difficult to detect any sky radiation much below λ 0.295 μ. Further, the ultra-violet limit for the sky spectrum in midsummer is about the same as that for direct sunlight in midwinter.

The work of several observers[1] seems to indicate that the bulk of the atmospheric ozone is localized in a layer at a height of about 50 km above sea-level. Since nearly all the scattered light of the sky comes from far lower elevations, it follows that the screening effect of the ozone would take place before the phenomenon of scattering, thus producing the same result on both sky and direct sunlight. The observations in Tables IV and V, however, show the ultra-violet limit of direct sunlight to be λ 0.290 against λ 0.295 μ for skylight. This argues for a small ozone content in the lower atmosphere.

SPECTRAL ENERGY-CURVE OF THE SUN IN THE ULTRA-VIOLET

There are three principal methods of determining the spectral energy-curve of the sun by use of the monochromator: (1) keeping both first and second slits at constant width during the measurements and afterward correcting the results for the variable dispersion across the second slit; (2) keeping the first slit at constant width and varying the second slit proportionally to the dispersion, thus eliminating the dispersion corrections necessary in the first method; (3) varying both slits according to the dispersion, thus keeping the purity of the spectrum constant.

The first method is practically that used by the Smithsonian observers in determining the solar energy-curve in the visible and infrared spectrum by the measurement of the ordinates of bolograms. It has the disadvantage, however, that the corrections for dispersion become very large in the ultra-violet, especially if a quartz prism is used, for which the correction factor at λ 0.3 μ is about five times that at the maximum of solar energy at λ 0.5 μ. The method is advantageous in that there is no error due to uncertain action of the

[1] Lambert, Dejardin, and Chalonge, *Bulletin de l'Observatoire de Lyon*, **9**, 45, 1927; Cabannes and Dufay, *Journal de physique*, **8**, 125, 1927; Götz and Dobson, *Proceedings of the Royal Society of London*, A, **120**, 251, 1928.

PLATE XII

a

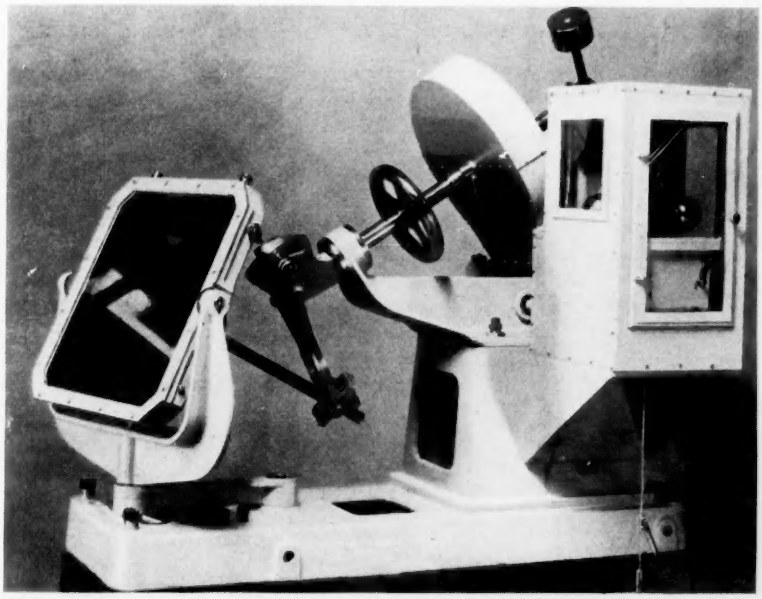

b

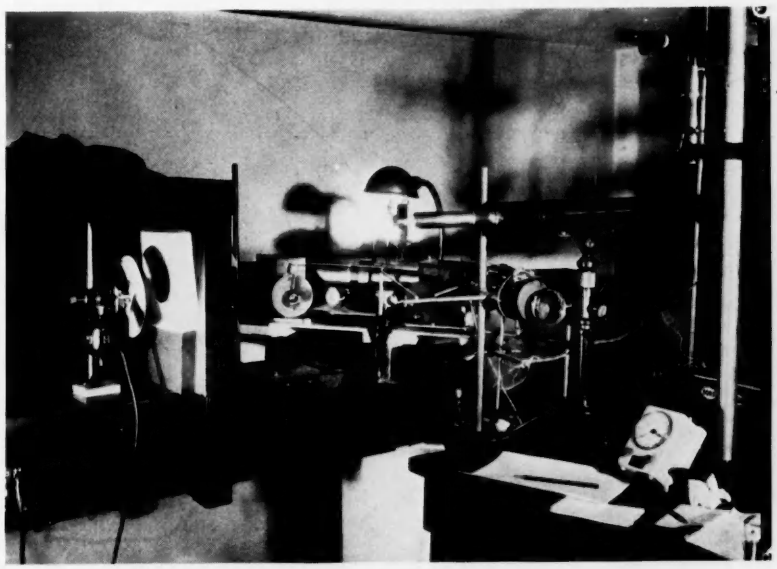

a) 12-Inch Stellite Siderostat of the Desert Sanatorium Research Laboratory, Tucson, Arizona

b) Double Bausch and Lomb Quartz Monochromator Used with the Siderostat To Measure the Ultra-Violet Spectral Energy-Curve of the Sun

OF MICH.

second slit, and, in the hands of Abbot and his colleagues, it has given an accurate determination of the form of the solar energy-curve from the near ultra-violet to the far infra-red.

The second method, principally, and in part the third were adopted by the author for the measurement of the violet slope of the solar energy-curve to the limit of atmospheric transmission, largely because of the much greater deflections resulting from these methods, and also because of the great numbers of Fraunhofer lines, which, with the first method, might lead to scattered results as the dispersion increased. In carrying the measurements into the visible spectrum it was thought that if this overlapping part were fitted to Abbot's curve, the latter would calibrate the measurements.

The spectral energy-curve of integrated sunlight and of light from the center of the solar disk was measured at the Research Laboratory of the Desert Sanatorium of Southern Arizona at Tucson in May, 1931, at the kind invitation of Drs. Davis, Pinner, and Krause. The laboratory is provided with a radiometer built after the pattern of that shown in Plate XI*a* and a Foucault siderostat of the lower arm-drive type with a 12-inch square stellite mirror (Pl. XII*a*). These instruments were designed by the writer for ultra-violet solar investigations and have been described by G. E. Davis.[1] A siderostat is superior to a coelostat or a polar heliostat for this kind of work since the light suffers only one reflection, and, as all metals are poor reflectors in the ultra-violet, the highest efficiency is thus attained with a minimum of uncertainty as to the reflection coefficients. The siderostat used feeds a beam of sunlight into a 12-inch fused-quartz crossed lens of 6-foot focal length, mounted on an I-beam, which also carries the double monochromator attached by dovetail-slides as shown in Plate XII*b*.

This double monochromator consists of two Bausch and Lomb quartz monochromators mounted on a steel plate with a common (middle) straight slit, the two outside slits (entrance and exit slits) being curved. A diagram of the optical system is shown in Figure 8. After leaving the siderostat mirror M, the light passes through the 12-inch quartz lens L and the sector X if the center of the disk is being studied; but if integrated light is used, these are eliminated.

[1] *General Electric Review*, **34**, 98, 1931.

Entering the first slit (curved) S_1, the light passes through the quartz lenses and prism train, consisting of two 30° crystal quartz prisms, of left and right quartz, of monochromator A, then through the straight slit S_2, where the scattered light of monochromator A is eliminated, into the lens and prism train of monochromator B, like that of A, and finally through the curved third (exit) slit S_3. From this slit it passes through the fused-quartz lens L_1 of 3-cm focal

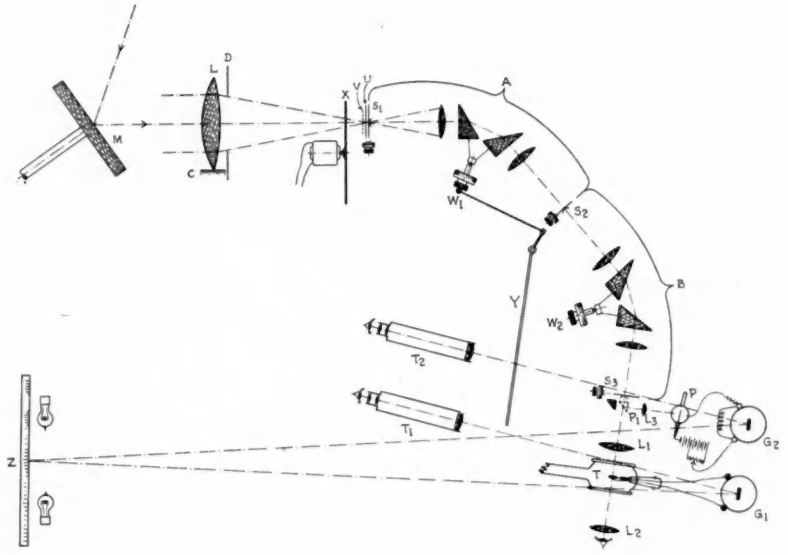

FIG. 8.—Arrangement of the double Bausch and Lomb quartz monochromator for measuring the ultra-violet spectral energy-curve of the sun with the thermopile and photoelectric cell.

length and 25-mm aperture upon one receiver of the vacuum thermopile T. A crystal-quartz prism P_1 may be moved into the beam in order to throw the light into the crystal-quartz lens L_3 of $2\frac{1}{2}$-inch focal length, and thence into the sodium photoelectric cell of quartz, P. To reduce the heating of the first slit S_1 to a minimum, a second wide slit U was used. The deflections were made with a shutter V. When the 12-inch lens, L, was used, a fixed diaphragm D of 20-cm aperture was placed behind it in part of the work, and in another part this diaphragm was attached to the lens. The lens was set for sharp focus upon the first slit S_1 by means of the focusing scale C.

The fixed diaphragm had the advantage that, when the lens was shifted in the direction of this slit, the cone of light limited by the diaphragm D remained constant, and no correction for displacement of this lens was necessary.

ADJUSTMENTS OF THE INSTRUMENT

The slits.—These are opened symmetrically by screws of 1-mm equivalent pitch, with heads divided into tenths. Since most of the measures were made with the first slit set at a fixed opening, this coarse division of the screwhead was sufficient. The second slit, however, was necessarily set at various widths in the spectrum formed by monochromator A to include a constant dispersion, i.e., a constant width in angstrom units. For the measurements on integrated sunlight this slit was always set (save on one occasion) to cover 100 A. For the center of the disk, which was observed with the 12-inch quartz lens, slit widths corresponding to 50 and 100 A were employed. The exit slit S_3 was made a half-division (0.05 mm) wider than S_2. It follows, then, that the second slit S_2 (straight) is the most important, and it was therefore provided with a graduated arc which could be read to one hundredth of a division (0.001 mm).

Slit calibration.—The width of the slit S_2 corresponding to 100 A was determined instrumentally. With this slit opened ten divisions, the lines of the mercury spectrum were shifted from one jaw to the other, the change in wave-length $\Delta\lambda$ being observed on the graduated head of the prism screw. The slit opening in divisions of the head for 100 A of the spectrum at wave-length λ is therefore one-tenth the reciprocal of $\Delta\lambda$ when $\Delta\lambda$ is expressed in μ. The observed values of $\Delta\lambda$ and the width of slit S_2 corresponding to 100 A are given in the second and third columns of Table VI.

Slit proportionality.—The proportionality of the slit opening to the galvanometer deflection was tested at intervals during the work. Narrow slits may be affected by diffraction, and zero errors of the slit screw affect the deflections from narrow slits more than those from wide slits. The monochromator prism screw was set for a flat place in the solar energy-curve or for its maximum (λ 0.5 μ), and readings of the galvanometer for screw settings of slit S_2 ranging from one to ten divisions were observed. If the deflections deviated

from simple proportionality to slit width, they were plotted and the resulting smooth curve was used to correct the solar energy measurements.

Wave-length scale.—The zero-point of the wave-length scale on the prism screw-head was checked visually at intervals on the prominent mercury lines. Errors of as much as 20 A were seldom found. The eccentric disks on the screw-nut were adjusted once to bring the

TABLE VI

SLIT WIDTHS S_2 CORRESPONDING TO 100 A, TRANSMISSION OF THE MONOCHROMATOR (T_r), REFLECTING POWER OF STELLITE (R), AND TRANSMISSION OF FUSED QUARTZ (T_R)

λ	Δλ	S_2, 100 A	R	T_r	T_r^a	T_R	T_R^a
μ	μ	div.					
0.697	0.230	0.43	0.66	0.458	0.21	.....	.....
.623	.160	0.63	.65	.....	.....	0.938	0.88
.615	.148	0.68	.65	.....	.....	.....	.....
.580	.128	0.78	.65	.....	.....	.....	.....
.546	.112	0.89	.64	.450	.20	.942	.89
.494	.082	1.22	.64	.....	.....	.....	.....
.435	.057	1.75	.62	.442	.20	.944	.89
.406	.045	2.22	.60	.440	.19	.944	.89
.386	.036	2.78	.58	.....	.....	.....	.....
.366	.031	3.23	.56	.436	.19	.932	.87
.334	.023	4.35	.53	.....	.....	.929	.86
.313	.019	5.26	.51	.426	.18	.924	.85
.297	.016	6.25	.50	.....	.....	.916	.84
.280	.014	7.14	.47	.....	.....	.900	.81
.270	.012	8.33	.44	.400	.16	.856	.73
.254	.011	9.09	.39	0.380	0.14	.661	.44
0.238	0.010	9.86	0.39	.....	.....	0.463	0.21

readings of the mercury lines into closer agreement with the known wave-lengths. Throughout the work all the settings were made by turning the screw-head in the direction of decreasing wave-length, which gave the greater wave-lengths the advantage of the greater air masses in determining the atmospheric transmissions for the morning runs.

Illumination of the optical system.—This was tested at intervals during the observing program by setting the wave-length screws for a visual wave-length and testing the illumination of the optical parts with a paper screen. The apparatus proved to be so rigid that no readjustment was required. The place where defective illumination

may be most serious in its effect is the thermopile receiver. The receiver was set visually so that the scattered light about it was symmetrical; the thermopile was then moved until maximum deflection was obtained.

Thermopile and photoelectric cell.—The thermopile was of the vacuum type, with four hot and four cold junctions of bismuth against bismuth plus 5 per cent tin, and provided with a window of fused quartz $2\frac{1}{2}$ mm thick. It was connected with a D'Arsonval galvanometer placed 8 m from the scale. The photo-cell was of quartz of the gas-filled sodium type and was used within about 5 volts of the flashing voltage (160 volts). It was put in series with a high-resistance potentiometer, a B-battery, and a second D'Arsonval galvanometer also at 8 m distance from the scale. This galvanometer was of 86 ohms resistance with 100 ohms damping resistance in shunt. The two galvanometers were read by suitable telescopes T_1T_2 (Fig. 8) placed near the monochromator.

TABLE VII

COLOR SENSITIVITY OF THE SODIUM PHOTOELECTRIC CELL

λ	Sensitivity	λ	Sensitivity
μ		μ	
0.546	5	0.313	100
.435	20	.302	87
.406	33	.270	36
.366	55	0.254	27
0.334	93		

The current-sensitivity of the photoelectric cell for various wave-lengths was measured in the mercury spectrum by direct comparison with the thermopile, with the results for a potential within 5 volts of the flashing voltage shown in Table VII. The maximum of sensitivity appears to be near λ 0.32 μ, and it is this property which makes it desirable as an instrument for investigating the solar spectrum in the extreme ultra-violet. The idea was to use the photoelectric cell to extend the measurements made with the thermopile beyond the point near λ 0.30 μ where the deflections dropped to 2 or 3 mm.

Setting the wave-length scale.—After some experiment it was decided to use the galvanometer deflections themselves to indicate

accurate settings of the monochromator prism screws W_1W_2. A slow motion consisting of levers (Y, etc., Fig. 8; also Pl. XII) was attached to the prism screw of monochromator A in such a manner that the observer could operate it while looking through either of the galvanometer telescopes. By shifting the lever Y a condition of maximum deflection was reached, which indicated that the two monochromators were set for exactly the same wave-length. The actual wave-length setting was thus made to depend on monochromator B alone.

METHODS OF OBSERVING

The observations consisted, briefly, in determining the intensity of solar energy at different wave-lengths over a constant dispersion at known hour angles. These measures provided at once a determination of the atmospheric coefficients of transmission and of the form of the solar energy-curve.

Since the walls of the dome extend above the siderostat mirror, the observable air mass was limited to 2.9. The coefficients of atmospheric transmission for the longer wave-lengths are therefore not so well determined as might be wished; but the values for the extreme ultra-violet are satisfactory.

Generally speaking, the observing program proceeded approximately as follows. A sheet similar to Table VIII was prepared giving the slit settings for each 100 A between λ 0.4 and 0.33 μ, for greater intervals above λ 0.4 μ, and for each 50 A below λ 0.33 μ. Columns were provided for entering the deflection and hour angle. The wave-length scale and illumination of each optical part, and also the slit zeros, were tested. Two small beams of light taken from the sides of the siderostat mirror produced on cardboard screens in the observing-room and on the wall of the dome images of the sun which were used for guiding. These images were set after the illumination had been tested. When integrated light was being used, a cardboard diaphragm of 4-inch aperture was placed 8 feet from the entrance slit S_1 to limit the sky effective on the monochromator. This slit was customarily set at the one-division opening. These adjustments were maintained throughout the observing program.

The measurements began at the longer wave-lengths, λ 0.6 or

0.7 μ, and proceeded to the ultra-violet limit of the spectrum. For each individual wave-length the following adjustments were required: focusing of four monochromator lenses by setting the focusing heads for the particular wave-length; setting of two prism-box screws, W_1W_2, for the particular wave-length; and setting of the second slit S_2 for the proper opening, as indicated by the observing sheet, and of the third slit S_3 for the same opening plus one half-division to allow for a margin of error. The shutter was then opened, and the slow motion, Y, of the prism screw of monochromator A was moved until maximum deflection was reached. If on closing the shutter the zero was found to have shifted sensibly, a second deflection was read. The hour angle was read directly from a clock having a dial graduated to read in both directions from the noon hour as zero. Observation of the deflection on each wave-length and of the corresponding hour angle proceeded in this manner until the galvanometer deflections had fallen to about 25 mm, which occurred at λ 0.32 μ for large hour angles and at λ 0.31 μ for small ones. From this point on, both photoelectric cell and thermopile were read until the limit of the solar spectrum was reached. The photoelectric cell was adjusted to give a deflection of about 700 mm when the thermopile gave about 30 mm. The efficiency of the monochromator in eliminating scattered light is indicated by the fact that no deflection whatever was observable below λ 0.29 μ with either photo-cell or thermopile, even at noonday.

When the radiation at the center of the disk was measured, the 12-inch quartz lens provided with a 7-inch diaphragm was focused at each wave-length setting of the monochromator. A sector reducing the deflections to one-tenth their undiminished values was used until the point was reached where the photo-cell measurements normally began, when it was removed, thereby increasing the deflections tenfold. An obstruction prevented the focusing of the 12-inch quartz lens for wave-lengths shorter than λ 0.33 μ. About one hour was required to complete a set of observations on the twenty-two wave-lengths observed between λ 0.7 and 0.29 μ, twelve of which were duplicated by the photoelectric cell.

After the apparatus was erected and put in working order, eight clear days were available for the observations. Generally the sky was

excellent in the mornings, but by late afternoon on four of these days clouds accompanying distant desert storms made observing conditions poor.

TRANSMISSION COEFFICIENTS AND ATMOSPHERIC OZONE

In reducing the measurements we have to consider (1) the atmospheric transmissions, (2) the reflecting power of the siderostat mirror, (3) the transmission of the monochromator, (4) the transmission of the fused quartz lens L_1 (which projects the image of the exit slit S_3 upon the thermopile receiver), and of the 12-inch lens L (when this was used for the work on the center of the disk). These will be discussed in the order named.

1. *The atmospheric transmissions.*—As already mentioned, the observable air mass was limited to 2.9. The time of starting the observations was therefore limited to an hour angle of approximately -5^h12^m for the season in which the observations were made. Since a complete set of measurements required an hour, only three or four sets could be obtained while the air mass was changing rapidly. The logarithms of the deflections for each wave-length were plotted against sec z (air mass) obtained from a table with the hour angle and the declination as arguments. A straight line was passed through these points and projected to the axis of air mass 0. The difference in the readings for air masses 1 and 0 is the logarithm of atmospheric transmission. Because of the small range in the air mass, it was thought best to reduce the deflections for a given wave-length for each day with the aid of the mean atmospheric transmission obtained from all the observations at that wave-length on all the days. For this reason the logarithms of the averages of the observed transmissions were plotted against values of $-(u-1)^2/\lambda^4$, which occurs in the right-hand member of Rayleigh's equation of molecular scattering,

$$\log T_r = -\left(\frac{32\pi^3}{3N}\right)\frac{(u-1)^2}{\lambda^4}, \qquad (1)$$

and which depends on both wave-length λ and index of refraction u. This plot (the filled circles and heavy line) is shown in Figure 9. Two additional points (the open circles) at λ 0.32 and 0.5 μ were furnished by the radiometer, which operated at the same time.

If only Rayleigh scattering were involved, we should expect this plot to be a straight line passing through the upper right corner of the diagram. Probably because of scattering by large particles, however, it actually passes below this point, thus indicating that Rayleigh's equation should be modified, as Dobson and Harrison[1] have done, by adding a constant term δ to the right member of equation (1).

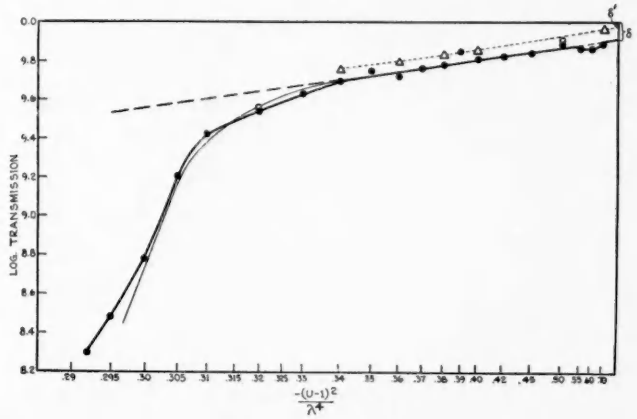

FIG. 9.—Atmospheric transmission (the heavy full line and dots) at Tucson (elevation 760 meters).

It will be noted that the plot is well represented by a straight line above λ 0.34 μ. The rapid fall of the line for wave-lengths less than λ 0.33 μ is due to the Huggins absorption band of ozone. Some indication of the Chappuis band in the orange is seen in the slight hook at the other end of the line.

Atmospheric ozone at Tucson.—We may compute the thickness of the ozone content of the atmosphere at N.T.P., which would account for this deviation of the observed transmissions from the formula of pure scattering with the aid of the coefficients of absorption as given by Fabry and Buisson[2] for 1 cm:

$$\log a = 17.58 - 0.00564\,\lambda\,, \qquad (2)$$

where λ is in angstroms.

[1] *Op. cit.*

[2] *Journal de physique*, **3**, 196, 1913.

If, following Dobson and Harrison,[1] we extend the straight part of the atmospheric transmission-curve in Figure 9 to the violet, as shown in the heavy broken line, we obtain the curve corresponding to an atmosphere free from ozone. The thickness t of the ozone layer at N.T.P. for any λ can then be found from the difference between the ordinates of the dotted line ($\log tr$) and the full (observed) line ($\log tR$) by means of the equation

$$t = \frac{\log tr - \log tR}{a}. \qquad (3)$$

From several points on the rapidly changing part of the curve near λ 0.31 μ we find an average of 0.18 cm of ozone. The light line represents the transmission-curve which would be given by this thickness of atmospheric ozone and which probably represents the observed atmospheric transmissions fairly well. Possibly 0.17 or 0.16 cm would be a little better. Dobson's values for ozone at Table Mountain, California, average 0.24 cm, while Fowle's values[2] for Harqua Hala, Arizona, for the years 1921–1924, during which measurements were made at this station on the Chappuis band, average very nearly 0.18 cm, as found by the writer. It follows that the transmissions observed at Tucson are probably reasonable preliminary values. The dotted curve with triangles in Figure 9 represents the values given by Abbot[3] for Mount Wilson, the difference in δ probably being due in part at least to the greater elevation.

2. *Reflecting power of the siderostat mirror.*—On account of the difficulty of manipulating so large a piece of stellite, only a few measurements of the reflecting power of the siderostat mirror were made. The work of Coblentz and Emerson[4] on this subject is so complete that their results were adopted when it was found that their measured reflection coefficients for the mercury lines $\lambda\lambda$ 0.313, 0.366, 0.402, and 0.546 μ were substantially the same as those of the author. The values of the reflecting power, R, of stellite are given in Table VI.

[1] *Op. cit.*

[2] *Op. cit.*, pp. 12–13; see also table on p. 8.

[3] *Ibid.*, **74**, No. 7, p. 21, 1923; see also *Smithsonian Physical Tables* (7th rev. ed., 1921), p. 418.

[4] *Bulletin of the Bureau of Standards*, **14**, 307, 1917, Table 2.

3. *Transmission of the monochromator.*—The intensities of the mercury lines were observed with monochromator A alone, then with A and B together, as shown in Figure 8. The ratios of the deflections observed with A and B together to those observed with A alone are the transmissions of monochromator B. These results agree substantially with the values supplied by Bausch and Lomb. Since the two instruments are identical, the transmission of the whole instrument A and B together is the square of that for B alone. The observed values of the transmissions T_r of A alone and their squares T_r^2 are given in Table VI.

4. *Transmission of fused quartz.*—The fused quartz lens L is approximately $2\frac{1}{2}$ cm thick; L_1 is 1 cm thick at the center, and the window of the thermocouple T, which is also of fused quartz, is $2\frac{1}{2}$ mm thick. To determine the transmissions of fused quartz, a plane-parallel interferometer plate of this substance, 15.3 mm thick, was furnished by King. Light from a mercury arc was collimated between two lenses and the transmission measured in the parallel beam. The results T_R are given in Table VI. Tests were made on the lens L used as a condenser for the mercury arc alternately with a 6-inch crystal quartz lens of the same focal length. The results of this determination were in general the same as those for the plane-parallel piece, but more scattered, probably on account of the difficulty of exact replacement when the lenses were interchanged. When lens L was employed, the square of the measured transmission, T_R^2, was used as a correcting factor. Its values are also included in Table VI.

REDUCTION OF THE MEASUREMENTS

The observations of May 16, 17, 18, and 19 were made on integrated light by the method of constant purity of spectrum (all slits varied); those of May 19 (P.M.), 20, and 23, on integrated light by the method of constant dispersion (second and third slits varied); and those of May 21 and 22, on the center of the solar image by the method of constant dispersion. The measurements of May 23 on integrated light were made with the same slit width (50 A) and slit length (reduced from 10.8 to 4.5 mm) as were used in the measures on the center of the disk. This arrangement decreased the de-

flections to approximately one-fourth those previously observed for integrated light and perhaps best represents the use of the photoelectric cell. The results of the first run of the morning of May 23 are shown in Table VIII.

The first step in the reduction was to plot the deflections with the photoelectric cell (marked *P* in the Table) against those obtained

TABLE VIII

MEASURES OF THE SPECTRAL ENERGY OF THE SUN, MAY 23, 1931
(Slit S_2, 50 A wide; slit S_1, 1 div. wide and 4.5 mm long)

λ	S_2	H.A.	Defl.	λ	S_2	H.A.	Defl.
μ	Div.		mm	μ	Div.		mm
0.70.....	0.22	-4^h33^m	64	0.35.....	1.85	-4^h06^m	17
.60.....	0.36	4 30	106	.34.....	2.08	4 00	17
.55.....	0.45	4 28	106	.33.....	2.28	3 52	540*P*
						3 50	14
.50.....	0.58	4 24	99	.325.....	2.39	3 47	530*P*
						3 48	13
.45.....	0.81	4 23	91	.32.....	2.50	3 45	450*P*
						3 44	9
.42.....	1.00	4 21	61	.315.....	2.63	3 37	358*P*
						3 36	7.5
.40.....	1.10	4 19	54	.31.....	2.78	3 34	274*P*
						3 33	4.5
.39.....	1.28	4 17	46	.305.....	2.94	3 31	170*P*
						3 30	2
.38.....	1.39	4 14	25	.30.....	3.12	3 27	84*P*
							(0.7)
.37.....	1.50	4 12	25	.295.....	3.33	3 25	27*P*
							(0.19)
0.36.....	1.60	−4 10	21	0.292.....	3.55	−3 23	8*P*
							(0.06)

with the thermopile for the same wave-length and to extend to the origin the smooth curve representing them. The thermopile deflections corresponding to those of the photoelectric cell were then read off and smoothed by second differences. The smoothed values appear in the last column of Table VIII, where the last three thermopile deflections, given in parentheses, are computed in this manner from the photoelectric-cell deflections.

The observations of a given day were reduced to the zenith and to no atmosphere by Bouguer's formula, which may be written

$$\left.\begin{aligned} \log d_o &= \log d - \sec z \log Tr, \\ \log d_z &= \log d_o + \log Tr, \end{aligned}\right\} \qquad (4)$$

where log d is the average of the logarithms of the observed deflections; d_z and d_o, the corresponding deflections at the zenith and for no atmosphere; Tr, the mean atmospheric transmission obtained as already described; and sec z is the average air mass.

These values of d_o and d_z were then corrected for the instrumental losses described under "Transmission Coefficients and Atmospheric

TABLE IX

ENERGY IN THE SOLAR SPECTRUM AND OBSERVATIONAL CORRECTING FACTORS

λ	Tr_a	$\frac{1}{Tr_a}$	Tr_i	F_1	F_2	F_3	Energy in Arbitrary Units (Deflections in mm)								Energy in 100 A	
							Integrated I		Integrated II		Center		Average		Watts per Square Meter	
							Z	No Atm.	Z	No Atm.	Z	No Atm.	Z	No Atm.	Z	No Atm.
μ																
0.700...	0.79	1.26	1.00	....	1.00	2.22	.....	.....	70.1	88.4	79.3	99.9	74.7	94.2	8.3	10.5
.600...	.79	1.27	0.96	1.83	1.00	1.67	97.7	123.5	115.5	146.8	121.6	154.6	111.6	141.6	12.4	15.7
.550...	.78	1.29	0.94	1.85	1.08	1.57	124.4	160.3	128.3	165.4	129.3	166.5	127.4	164.1	14.2	18.2
.500...	.76	1.31	0.91	1.56	1.13	1.33	.....	.....	137.5	179.9	135.6	177.5	136.6	178.7	15.2	19.9
.450...	.74	1.36	0.87	1.15	1.15	1.15	132.6	180.0	132.6	180.0	132.7	180.0	132.6	180.0	14.7	20.0
.420...	.71	1.41	0.85	....	1.18	1.20	.....	.....	101.0	142.6	107.7	151.9	104.3	147.2	11.6	16.4
.400...	.68	1.47	0.82	0.81	1.19	1.25	99.7	146.8	95.7	140.8	98.6	145.0	98.0	144.2	10.9	16.0
.390...	.66	1.52	0.81	0.76	1.23	1.29	71.1	107.7	68.5	103.7	57.8	87.6	65.8	99.7	7.3	11.1
.380...	.64	1.57	0.79	0.74	1.27	1.36	54.5	85.4	52.6	82.6	51.2	80.2	52.8	82.7	5.9	9.2
.370...	.61	1.64	0.78	0.70	1.32	1.42	52.5	85.8	55.2	90.5	52.5	86.0	53.4	87.4	5.9	9.7
.360...	.58	1.73	0.76	0.63	1.33	1.46	46.9	81.0	52.2	90.3	50.7	87.6	49.9	86.3	5.5	9.6
.350...	.54	1.84	0.74	0.58	1.35	1.50	37.5	68.9	41.8	76.8	45.7	84.2	41.7	76.6	4.6	8.5
.340...	.49	2.02	0.72	0.55	1.37	1.54	36.1	73.1	39.0	78.9	39.6	80.2	38.2	77.4	4.2	8.6
.330...	.43	2.32	0.71	0.54	1.42	1.63	32.1	74.7	34.7	80.6	34.9	80.7	33.9	78.7	3.8	8.7
.325...	.39	2.56	0.69	....	1.45	1.67	.....	.....	31.0	79.6	31.6	80.8	31.3	80.2	3.5	8.9
.320...	.35	2.85	0.68	0.44	1.48	1.73	17.7	49.9	26.5	75.8	20.4	57.8	21.5	61.2	2.4	6.8
.315...	.30	3.29	0.67	....	1.51	1.80	.....	.....	18.9	62.4	14.3	47.1	16.6	54.8	1.8	6.1
.310...	.25	3.97	0.66	0.39	1.54	1.86	6.3	25.1	14.0	55.6	10.3	40.8	10.2	40.5	1.1	4.5
.305...	.17	5.88	0.64	....	1.56	1.91	.....	.....	7.6	44.7	5.1	29.5	6.4	37.1	0.71	4.1
.300...	.07	14.49	0.63	0.38	1.59	1.96	2.2	30.0	4.0	58.7	1.5	21.2	2.6	36.6	0.29	4.1
.295...	.03	30.30	0.61	0.38	1.63	2.05	0.7	19.4	1.3	40.3	0.1	4.4	0.7	21.4	0.08	2.4
0.292...	0.02	50.00	0.59	0.36	1.63	2.06	0.2	9.6	0.5	20.6	0.1	1.1	0.3	10.4	0.03	1.1

Ozone" and, in addition, for certain corrections that apply to the individual days. The measurements made by the method of constant purity of spectrum were reduced to constant dispersion with the aid of the data on the relation of slit width to galvanometer deflection. In some cases a slit-zero correction was also applied. In the case of measurements on the center of the disk, the reciprocal square of the focal length of L was applied to reduce all the measurements to constant angular aperture when the diaphragm was used on the lens.

Table IX shows the results of all the measurements. This table

gives the wave-length λ; the atmospheric transmission coefficients Tr_a and their reciprocals $1/Tr_a$ to show the effect of this function as a correcting factor; the instrumental transmission coefficients Tr_i; the complete instrumental correcting factors F_1, F_2, and F_3 applied to the three methods of measurement (constant purity, constant dispersion, and center of the disk); the values of the deflections at the zenith and for no atmosphere, the latter reduced to a mean value of 180 mm at λ 0.45 μ; and, in the last two columns, the average of all these measurements in units of watts per square meter per hundred angstroms.

The results of the measurements are plotted separately in Figure 10, and the average of the three methods in Figure 11. One of the interesting features of these curves is the sudden drop of 35 per cent in the solar energy outside the atmosphere between λ 0.40 and 0.38 μ, and the nearly constant value of the solar energy, about 43 per cent of the maximum, between λ 0.38 and 0.325 μ, which covers nearly the entire ultra-violet spectrum.

The scale on the left is in millimeters of deflection, and on the right, in watts per square meter per hundred angstroms. The latter scale is derived as follows: The energy-curves for no atmosphere are plotted in Figure 10 on a scale to fit Abbot's curve for the longer wave-lengths. Now if Abbot's entire solar energy-curve be plotted to a wave-length scale, where 1 μ is equivalent to 15.2 cm and the maximum of energy is 25.4 cm, the area is found to be 257 cm^2. This area is equivalent to the solar constant, 1.95 cal cm^{-2} min^{-1}, or 1355 watts per square meter. From these data an area 100 A wide by 1.25 cm high was found to be equivalent to 1 watt. A height of 1.25 cm is therefore the unit of watts per square meter per hundred angstroms. It may be seen from the curve that the galvanometer deflections divided by 9 also give the radiation in these units. For the maximum of the curve the rate of emission is 20.3 watts per square meter per hundred angstroms.

We should expect the measures on the center of the disk to show a richer ultra-violet content than those on integrated light, and that these measurements give a result which is about the same as the mean value for the two groups of measures on integrated light is a little puzzling. The Smithsonian work on drift-curves of the sun

forms a basis for calculating the energy-curve for the center of the disk. If we divide the solar disk into concentric zones and use the Smithsonian[1] values of the energy at the center of area of each zone

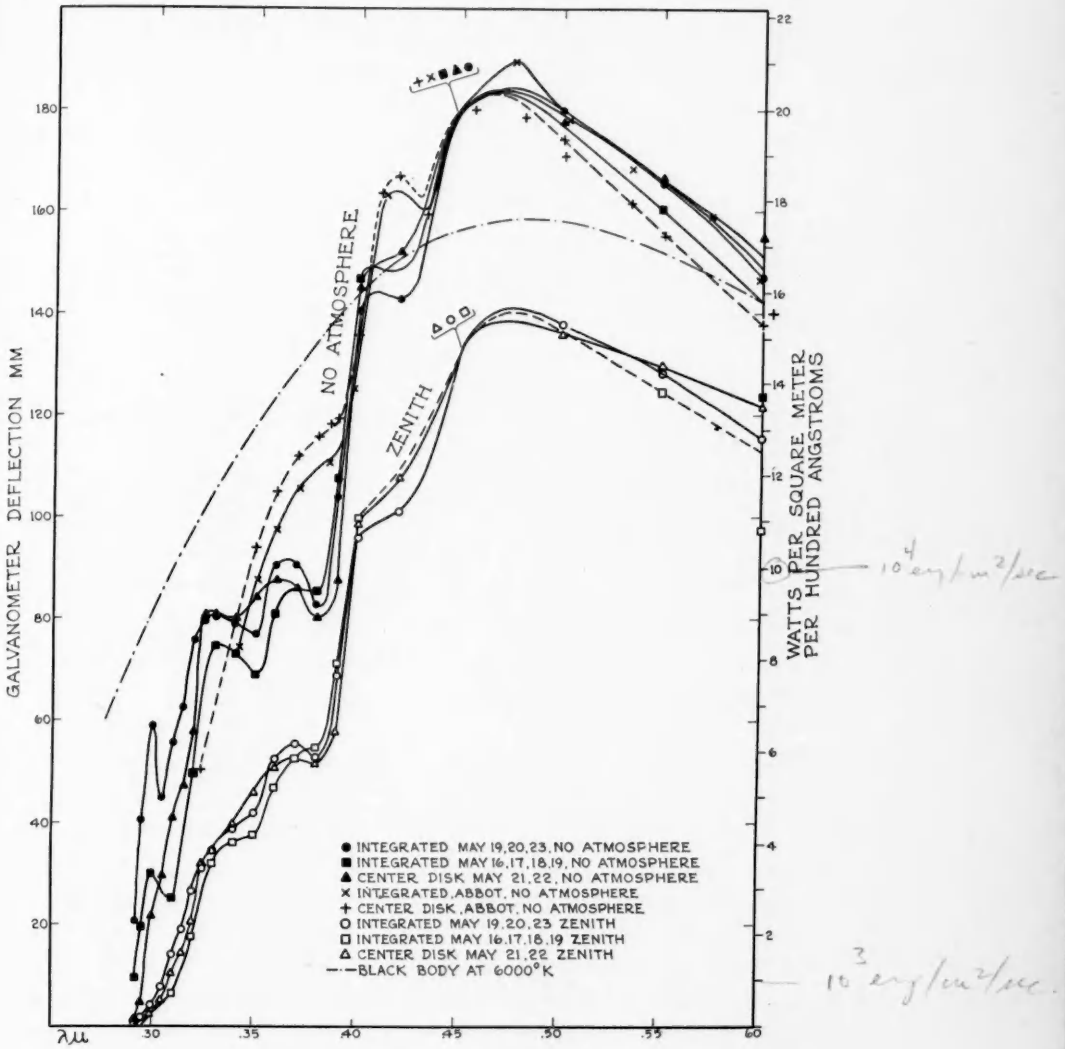

FIG. 10.—Solar energy-curve in the visible and ultra-violet outside the earth's atmosphere and for the sun in the zenith at Tucson.

[1] Abbot, *The Sun* (1926), pp. 106–107.

as weights, we may obtain by summation a series of coefficients by which the energy in integrated light for various wave-lengths must be multiplied in order to give the energy-curve of radiation from the center of the disk. Abbot[1] gives some of these coefficients; others

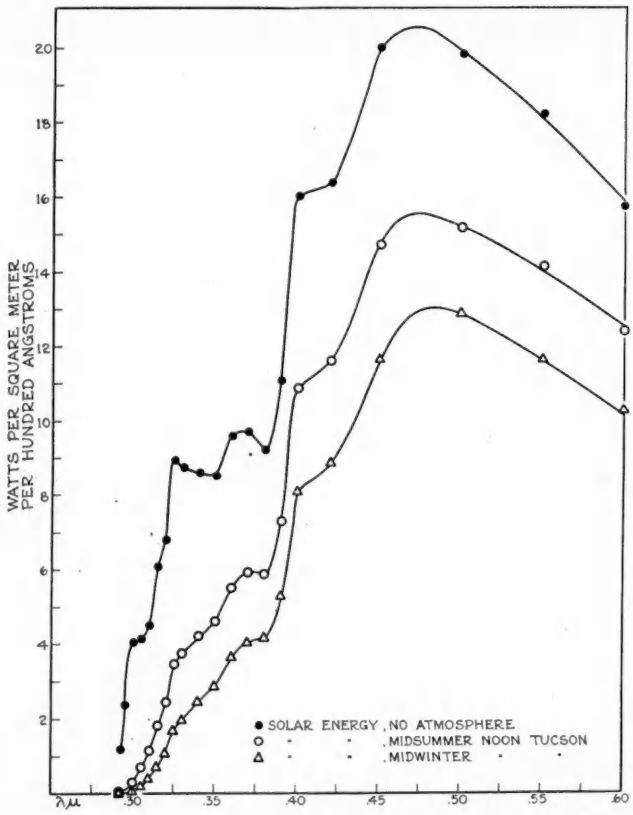

FIG. 11.—Mean curve of solar energy in the visible and ultra-violet, outside the earth's atmosphere and for noonday sun in midsummer and midwinter at Tucson.

have been calculated to obtain the form of the curve in the ultra-violet. Figure 10 shows the results when they are applied to Abbot's curve for integrated solar radiation. The black-body curve for 6000° K has been made to coincide with the solar energy-curve at λ 0.7 μ, because the curve to the red of this wave-length fits the observa-

[1] *Ibid.*, Table VII.

tions of the Smithsonian observers the best. It will be noted that for wave-lengths shorter than λ 0.4 μ the black-body curve lies considerably above the violet slope of the observed curve.

Figure 11 is a plot of the mean values of the solar energy for no atmosphere and for the zenith at Tucson. The zenith-curve is also essentially that for the noonday sun in midsummer. The noonday curve for midwinter at that latitude has been computed from equation (4). These curves are particularly interesting in showing the extremes of the seasonal effect of atmospheric absorption on ultra-violet solar radiation. For example, the energy in the 100 A between λ 0.3 and 0.29 μ at Tucson in midsummer (see col. 16, Table IX, at λ 0.295 μ) is 0.08 watts per square meter; while in midwinter, equation (4) shows that it would fall to only 0.0017 watts, about one-fiftieth part of the energy in midsummer.

The writer is indebted to the other members of the solar department, S. B. Nicholson, F. Ellerman, R. S. Richardson, J. Hickox, L. H. Humason, and N. Perrakis, for assistance in taking the radiometer plates, now numbering nearly two thousand, and to Miss Richmond for the measurement and reduction of this extended series of observations. He is also indebted to G. E. Davis and J. H. McCarthy of the Desert Sanatorium at Tucson for much assistance in the measurement of the ultra-violet energy-curve of the sun, and to Miss Ware for the complicated reduction of these measurements.

CARNEGIE INSTITUTION OF WASHINGTON
MOUNT WILSON OBSERVATORY
October 1931

SOME RESULTS FROM A STUDY OF THE ATOMIC LINES IN THE SUN-SPOT SPECTRUM[1]

By CHARLOTTE E. MOORE

ABSTRACT

A detailed study of the atomic lines in the sun-spot spectrum has resulted in a determination of the effective temperature of sun-spots and the pressure and amount of material above them.

Intensities for 6312 lines of atomic origin in the spot spectrum have been estimated on the Rowland scale on original negatives and on prints made from them. The plates were those taken with the 150-foot tower telescope and 75-foot spectrograph for the Mount Wilson map of the spot spectrum. The third order was used from λ 3900 to λ 5400; the second order from λ 5400 to λ 6000. The spectrum of the disk appears on each side of the spot spectrum. The use of a quarter-wave plate and Nicol prism gives the lines subject to Zeeman effect a dentate appearance in the spectrum of the spot, which makes it possible to select the atomic lines. Intensities estimated from the prints agree systematically with those from the plates.

The *identifications* of lines in the solar spectrum from λ 2975 to λ 6635 and in the spot spectrum from λ 3894 to λ 6635 have been revised and extended. Lines of Lu^+ have been identified for the first time. The principal criteria employed have been laboratory wave-lengths and intensities, the multiplet relations and excitation potentials, which are now available for almost all elements except the rare earths, and the behavior of the lines in the spectrum of γ Cygni, a giant star of class F8. Nine hundred and thirty-six faint solar lines not previously identified and 21 spot lines have been recognized as faint members of multiplets not yet observed in the laboratory, but accurately predictable. Of these, 437 are due to *Fe*, 122 to *Cr*, 89 to *Ni*, 73 to Cr^+, 67 to *Ti*, 50 to Fe^+, 43 to Ti^+, 21 to *Co*, 20 to Zr^+, 12 to *V*, 9 to V^+, 7 to Sc^+, and 7 to *Mn*. Three hundred and ninety-six new atomic lines which appear only in the spot spectrum have been measured and 193 identified.

A *quantitative* study of the composition of the atmosphere above sun-spots has been based on the calibration of the Rowland intensity scale. This gives a quantity Y, which is the logarithm of the ratio of the number of atoms producing a line in the spot spectrum to that effective in the formation of the same line in the solar spectrum. From thermodynamic theory $Y = Y_0 + SE_x$, where Y_0 is the logarithm of the ratio of the numbers of neutral atoms above equal areas of the photospheres of spot and disk, E_x the excitation potential, and $S = 5040\,(1/T - 1/T')$. T and T' are the effective temperatures of disk and spot, respectively. For enhanced lines, Y_0 must be replaced by Y_1, the corresponding quantity for ionized atoms. The observed data from 6 elements give a weighted mean value of S equal to -0.190 ± 0.010. Taking $T = 5740°$ K, $T' = 4720° \pm 40°$ K, where the probable error is a measure of the accordance of the observations. From the observed values of Y_0 and Y_1 and the Saha equation as modified by Pannekoek and Fowler, the ratio of the electron pressures P'_e (spot) and P_e (disk) can be found. Eight elements have a sufficient number of arc and spark lines present in both solar and spot spectra to be used. The weighted mean value of $\log (P'_e/P_e)$ is -0.22 ± 0.07, i.e., the electron pressure over the spot is 0.60 ± 0.10 times that over the disk.

Russell has defined the "level of ionization" as the ionization potential of an atom which would be just 50 per cent ionized under given conditions. For the spot this level is 7.0 ± 0.1 volts, as compared with 8.5 ± 0.1 for the disk. From these quantities the percentages of ionization for disk and spot were calculated for 28 elements. By comparing these percentages with Y_0 and Y_1, it was found that the amount of material per unit

[1] *Contributions from the Mount Wilson Observatory, Carnegie Institution of Washington*, No. 446.

area above the spot is greater than that above the disk. The ratio of these amounts, C, was determined for 19 elements in the neutral state and for 11 in the ionized state, the result being

$$\log C = +0.23 \pm 0.03,$$

or

$$C = 1.70 \pm 0.11 .$$

Checks upon these results may be obtained in two ways: First, the mean percentage of ionization can be computed for both disk and spot from Russell's data for the composition of the solar atmosphere; this gives the ratio of the number of ions per square centimeter above disk and spot, which should equal the ratio of electron pressures. The calculated value of $\log (P'_e/P_e)$ is -0.17, as against -0.22 observed. Second, from Gaunt's relation that the absorption coefficient κ varies as $P_e T^{-3/2}$, it is possible to calculate the increased transparency above the spot and to determine both C and P'_e/P_e theoretically when T' is given. For $T' = 4720°$, $\log C = +0.13$ and $\log (P'_e/P_e) = -0.26$. The agreement with observation is satisfactory, in view of the approximate nature of the theory.

Adams and Russell, in determining the temperatures of stars by the method used here, introduced an empirical correction X to care for a supposed departure from thermodynamic equilibrium. If applied to the spot spectrum, this correction gives $T' = 4290°$, $\log (P'_e/P_e) = -1.09$, and $\log C = +0.31$. The first theoretical check gives $\log (P'_e/P_e) = -0.11$; the second gives $\log (P'_e/P_e) = -0.38$ and $\log C = +0.19$. This discordance indicates decisively that no such empirical correction is applicable in the case of the sun-spot spectrum.

From the three constants T', P'_e/P_e, and C derived from observation, the intensities of the atomic lines in the spot spectrum may be calculated for all lines of known energy relations. These calculations have been made for a number of the most difficult cases in the whole spectrum—the lines of *H*, *O*, *Si*, *Si*$^+$, *Mg*, and *Mg*$^+$. Aside from a few lines so strong that estimates are meaningless, the average discordance of observed and calculated spot intensities is ± 1 unit of the Rowland scale. Similar calculations made for all lines in a selected region in the red show good agreement between observed and calculated values, except in the case of certain lines due to *Ti*, *V*, *Y*, and *Zr* which are very faint in the spectrum of the disk. Further study of such cases is desirable. Apart from this difficulty, the intensities of lines in the sun-spot spectrum have been quantitatively explained by physical and thermodynamic theory.

Sun-spots have long attracted the attention of astronomers. In particular, the sun-spot spectrum has played an interesting part in the interpretation of stellar spectra and has yielded much valuable information in support of the theory of ionization. In 1874 Norman Lockyer noticed the increased width of the D lines in the spot and attributed it to the presence of an increased amount of *Na*.[1] In 1887 he noted that many spot lines were seen at low temperatures in the laboratory and that these lines were not intensified in passing from the temperature of the electric arc to that of the electric spark.[2] Since spot lines occur in stellar spectra, he suggested the existence of similar physical conditions in sun-spots and in stellar atmos-

[1] *Contributions to Solar Physics* (1874), pp. 227, 327, 388, 535.

[2] *Chemistry of the Sun* (1887), p. 314.

pheres. Later, A. Fowler estimated intensities of lines in the spot spectrum and showed that lines of *Fe*, *Ti*, *V*, and *Sc* that were strong in the arc or flame were strengthened in the spot spectrum, while many enhanced lines were weakened.[1]

In 1906 Hale and Adams[2] published a list of 345 lines whose intensities varied in passing from disk to spot. Their estimates were made on photographs taken in the second order with the Snow telescope on Mount Wilson, with a dispersion of 1.5 A per millimeter. A comparison of lines of *Ti*, *V*, *Cr*, *Mn*, and *Fe* which differed in intensity in disk and spot with those in the laboratory spectra of these elements taken with a strong arc, a weak arc, and a spark[3] indicated that a difference in temperature would explain the behavior of the lines in the sun-spot spectrum and initiated the long series of investigations made at Mount Wilson on the temperature classification of spectral lines. The conclusion respecting the influence of temperature was further verified by the appearance of *Ti* flutings in the spot spectrum and their absence from the spectrum of the disk.[4] *A Preliminary Catalogue of Lines Affected in Sun-Spots* in the region λλ 4000–4500 was published by Adams in 1908,[5] and the discovery of the magnetic field in sun-spots was announced by Hale in the same year.[6] With the 60-foot tower telescope on Mount Wilson, completed in 1907, it became possible to obtain better photographs; and a revised list of lines from λ 4005 to λ 6495, including disk and spot intensities, a discussion of the behavior of the various elements to which these lines were due, and a list of lines broken up into doublets and triplets by the magnetic field appeared in 1909.[7] Further, the presence of *TiO*, *MgH*, and *CaH* in the spot accounted for most of the band lines appearing in the spot spectrum and confirmed the conclusions concerning temperature.

[1] *Transactions of the International Astronomical Union for Co-operation in Solar Research*, **1**, 201, 1906.

[2] *Mt. Wilson Contr.*, No. 5; *Astrophysical Journal*, **23**, 11, 1906.

[3] Hale, Adams, and Gale, *Mt. Wilson Contr.*, No. 11; *Astrophysical Journal*, **24**, 185, 1906.

[4] Hale and Adams, *Mt. Wilson Contr.*, No. 15; *Astrophysical Journal*, **25**, 75, 1907.

[5] *Mt. Wilson Contr.*, No. 22; *Astrophysical Journal*, **27**, 45, 1908.

[6] *Mt. Wilson Contr.*, No. 30; *Astrophysical Journal*, **28**, 315, 1908.

[7] Adams, *Mt. Wilson Contr.*, No. 40; *Astrophysical Journal*, **30**, 86, 1909.

1. OBSERVATIONAL MATERIAL

With the completion of the 150-foot tower telescope and the 75-foot Littrow spectrograph, excellent large-scale photographs of the sun-spot spectrum became available. From the best of the negatives taken in 1915–1917 a series was selected for the preparation of the Mount Wilson map of the sun-spot spectrum. The data from these photographs, which are listed in Table I, form the basis of the present investigation. From λ 3900 to λ 5400 third-order plates were used, having a dispersion of 0.224 A per millimeter at λ 3930 and 0.215 A per millimeter at λ 5100; from λ 5400 to λ 6600 the photographs were of the second order, with a dispersion of 0.345 A per millimeter at λ 5400 and 0.333 A per millimeter at λ 6500. A quarter-wave plate and Nicol prism were placed before the slit of the spectrograph to show the Zeeman effect in the sun-spot region. Since the spectrum of the disk appears on each side of the spot spectrum, intensity comparisons between disk and spot can readily be made.

When the *Revision of Rowland's Table of Solar Spectrum Wave-Lengths*[1] was in preparation, all available spot intensities were included; but it was not then possible to utilize the wealth of material on the original plates taken with the 150-foot tower telescope. This circumstance was a serious handicap in identifying the many thousands of solar lines. The behavior of lines of various elements was known, and many additional lines could have been identified on this basis had the spot intensities been available. For this reason, upon the suggestion of Mr. W. S. Adams, the writer undertook the present work. The problem is complicated by the fact that the sun-spot spectrum also contains many band lines, but, interesting as they are, they have not been included because of the vast possibilities offered by the atomic lines alone.

The intensities were first estimated on a series of excellent prints made for the writer from the original negatives by Mr. F. Ellerman. About 6000 lines of atomic origin in the spot spectrum between λ 3894 and λ 6635 were examined. The λ 3900 region is rich in band lines, and very few of the atomic lines show a change of

[1] St. John, Moore, Ware, Adams, and Babcock, *Carnegie Institution of Washington, Publication* No. 396; *Papers of the Mount Wilson Observatory*, 3, 1928.

intensity in the spot spectrum, because the overlapping solar spectrum masks the real spot spectrum in the violet. In this region it is therefore difficult to establish a clear picture of the Rowland intensity scale and of the changes of intensity in the spot spectrum. Near the red limit of the map are lines which have a large range of intensity in the disk, are undisturbed by band lines in disk and spot, and are perceptibly changed in intensity in the spot. With the

TABLE I

OBSERVATIONAL MATERIAL

Plate	Region	Date	Spot No.
T′ 1953	λλ 3900–4100	Jan. 4, 1917	7926
T′ 1954	4100–4300	Jan. 4, 1917	7926
T′ 1955	4300–4500	Jan. 4, 1917	7926
T′ 1956	4500–4700	Jan. 4, 1917	7926
T′ 1969	4700–4800	Feb. 7, 1917	7977
T′ 1970	4800–4900	Feb. 7, 1917	7977
T′ 1971	4900–5000	Feb. 7, 1917	7977
T′ 1972	5000–5100	Feb. 7, 1917	7977
T′ 2050	5100–5200	Feb. 13, 1917	7977
T′ 2049	5200–5300	Feb. 13, 1917	7977
T′ 2050	5300–5400	Feb. 13, 1917	7977
T′ 1779	5400–5550	May 5, 1916	7708
T′ 1783	5550–5850	May 26, 1916	7727
T′ 1778	5850–6000	May 3, 1916	7709
T′ 1713*	6000–6150	July 12, 1915	7330
T′ 1709	6150–6300	July 11, 1915	7330
T′ 1713*	6300–6450	July 12, 1915	7330
T′ 1974	6450–6600	Feb. 8, 1917	7977

* Contact copy from original plate.

experience gained by estimating the intensities of such lines, the difficult regions toward the violet could be handled much more satisfactorily. For this reason it seemed advisable to work from the red toward the violet. The spot estimates have been made on the Rowland scale throughout, but in cases where Rowland's estimates of disk intensities seemed inconsistent with his own scale, the disk intensities have been changed. The atomic lines were selected principally by means of the Zeeman effect, which shows as a dentate appearance in the spot spectrum owing to the use of the quarter-wave plate and Nicol prism, the red component being cut off from one strip and the violet components from the two adjacent strips. The estimates were made on those strips of the map on which lines

strengthened in the spot have the maximum intensity. For faint lines it is very difficult in many instances to distinguish between the atomic and the band lines. Some atomic lines are so little affected by the magnetic field that this criterion alone is not sufficient; but in doubtful cases the policy has been to include possible band lines rather than to exclude possible atomic lines. Lines neither showing perceptible Zeeman effect nor having the general appearance of the other band lines in the region have been retained. On the other hand, solar lines masked in the spot spectrum by band lines have not been included.

Although the successive strips of the map overlap considerably and the disk intensities check the uniformity of the intensity scale within each region, the possibility that photographic errors may have been introduced by making estimates on prints rather than on plates made it advisable to examine the original negatives, a privilege granted through the courtesy of the Mount Wilson Observatory. On comparing the prints with the negatives it was immediately evident that the plates, when strongly illuminated, show more detail. They reveal more faint solar lines and more atomic spot lines, and are also more useful than the map in resolving close pairs. The entire region was therefore again examined, and much material added from the plates alone. Although the estimates from the negative and the map do not always agree, it has not been possible to apply any systematic correction. In many instances the discordance arises from an attempt to keep the estimates consistent with both the Rowland scale and the neighboring lines. Such consistency is difficult to attain and is largely a matter of judgment. Both the print and the plate were considered, and whenever the estimates differed, that from the plate was adopted. Very rarely do the differences exceed one unit of the Rowland scale. It is noteworthy that in some cases the character of the line seems to show better on the print, that is, the degree of blackness of two lines may vary considerably, while no difference can be detected on the illuminated negative.

Adams[1] has pointed out some of the influences that affect visual estimates of sun-spot intensities, among them the tendency to make

[1] *Mt. Wilson Contr.*, No. 40; *Astrophysical Journal*, 30, 86, 1909.

the estimates too high because of the influence of line width. He also notes that the presence of light from the sky and the solar photosphere always tends to make the spot intensity too high for weakened lines and too low for those which are strengthened. Other factors also enter, such as the definition at the time the spectrogram is taken, the influence of the continuous background in disk and spot, and the possible effect of actual spectral differences in different spots. Until accurate microphotometric curves are obtained for lines of different intensities in various regions, no significant corrections can be made for some of these errors.

Some material bearing on the effect of different spots on the same line is available, however, for seven different spots were observed in taking the photographs used for this work. Fortunately, the plates show considerable overlap, and the intensities of lines observed in two different spots can therefore be compared. If the overlapping region includes lines having considerable range in intensity, the comparison should reveal any appreciable difference. In the cases examined no systematic difference could be detected. The greatest discordances occur in the overlapping interval λλ 5999–6013 (plates T' 1713 and T' 1778); but a plot of the estimates from one plate against those from the other is well represented by a line drawn at 45° and therefore no correction has been made. The lines on the plate toward the red, T' 1713, seem wider and sharper than those on T' 1778; but it is difficult to say whether this is to be attributed entirely to the use of different spots. On the present evidence, therefore, it is impossible to derive a correction for differences between spots; but more work must be done to prove that such differences do not exist. The available data are limited and indicate only that for the few lines examined the effect of using different spots is not serious.

Finally, the writer's estimates of spot intensities have been compared with those made by Adams and included in the *Revised Rowland Table*. After omitting all intensities which correspond to blends of two solar lines, a total of 3295 lines remained, distributed as tabulated. (See table on opposite page.)

A plot of the two spot intensities of every line against each other shows that from λ 3900 to λ 4200 the new estimates are in general one unit stronger than those of Adams for lines ranging from the

faintest to intensity 4 on the Rowland scale. From λ 4200 to λ 6000, by far the greater part of the interval studied, no systematic difference is evident, and the deviations from a straight line are not serious. In the red, the revised spot intensities have been lowered a little in order to keep them more nearly on the scale used by Rowland for the lines in the spectrum of the disk. This shows in the plot of the region between λ 6000 and λ 6635 for lines of intensity 9 and greater. The greatest discordances occur among the faint lines, several of which are now recorded as having intensity −1 (00) and −2 (000), which previously had been marked "obliterated." This is possibly to be explained by differences in seeing conditions when the two sets of plates were made, as poor seeing tends to equalize

Region	No.	Region	No.	Region	No.
λλ 3900–4000.....	238	λλ 4400–4500....	211	λλ 5100–5400....	301
4000–4100.....	220	4500–4600....	206	5400–5526....	118
4100–4200.....	245	4600–4700....	175	5526–5800....	247
4200–4300.....	243	4700–4900....	266	5800–6000....	89
4300–4400.....	210	4900–5100....	241	6000–6635....	285
				Total.....	3295

disk and spot intensities. Since the spectrograms taken for the spot map are excellent and have greater dispersion than the older ones, the newer intensities have been adopted.

2. IDENTIFICATIONS

Recent work in spectroscopy is particularly advantageous for the identification of lines in solar and spot spectra, where the possibility of using high dispersion minimizes the problem of blends. It is also of great assistance when many faint lines are to be considered. At the time the *Rowland Table* was revised a wealth of spectroscopic material had been collected; but since then much more has accumulated, and with the list of spot intensities now available the way is open to revise many of the identifications. The close alliance between disk and spot spectra makes it undesirable to separate the two in any such undertaking. Hence, although the spot intensities start at λ 3894, the discussion of the identifications begins with the violet limit of the solar spectrum, λ 2975, and extends to λ 6635, the red

limit to which the spot intensities have been revised. It is hoped soon to extend the investigation to the limit of the original *Rowland Table* at λ 7330. Beyond this, a revision of the infra-red spectrum, extending as far as the photographic method permits, is in progress at Mount Wilson. This will give *all* observed lines and include revised identifications and spectroscopic data similar to those in the *Revised Rowland*. Unfortunately, at the time that volume was published it was possible to include *only* those lines measured with the interferometer between λ 7330 and λ 7958.[1] Even with all the unpublished grating measures beyond this limit added and with those by F. S. Brackett[2] between λ 9000 and λ 9801, the material was still fragmentary.

As soon as the spectrum of an element has been analyzed, the strong low-level multiplets can be selected and the behavior of the lines in the solar spectrum determined. Indeed, for those elements represented here by a large number of lines, identifications can be made without knowledge of the multiplets, merely by comparing solar and laboratory intensities and wave-lengths. The information supplied by multiplets becomes very important, however, in dealing with the fainter lines and with those of elements whose presence in the sun is doubtful. For instance, if strong laboratory lines which arise from the lowest atomic levels and are on the main diagonals of multiplets lie in the observable region of the solar spectrum but are absent from this spectrum, the coincidence of other lines of the element with the solar wave-lengths does not indicate its presence.

Multiplets of all the elements have been collected, as far as possible, and the identifications in the present work have been made primarily on the basis of this material. With the aid of the spot intensities, the intensities in the spectrum of γ Cygni, which were kindly furnished by Mr. Adams, and the intensities in the flash spectrum, much can be told about identifications; for the spot presents a more advanced spectral type for comparison with an earlier type in the flash spectrum or in that of γ Cygni. In the spot spectrum, arc lines are strengthened and spark lines weakened, while in the spectrum of earlier type the reverse is generally true.

[1] Babcock, *Mt. Wilson Contr.*, No. 328; *Astrophysical Journal*, **65**, 140, 1927.

[2] *Mt. Wilson Contr.*, No. 197; *Astrophysical Journal*, **53**, 121, 1921.

Notation, etc.—A uniform procedure has been followed in preparing the tables. The wave-lengths of the solar lines are taken from the *Revised Rowland* and are the original Rowland values reduced to the International System by means of the *Fe* standards adopted by the International Astronomical Union in 1922. In 1928 the Union adopted a slightly different set of *Fe* standards and, *de novo*, a set of solar standards, both of which were referred to the primary *Cd* standard.[1] The corrections to the wave-lengths published in the *Revised Rowland* which reduce them to the 1928 standards are only −0.002 A in the violet; but they increase linearly from λ 5600 to the red, being −0.005 A at λ 6050 and −0.009 A at λ 6678; that is, according to the present standards, the wave-lengths in the *Revised Rowland* are too long by these amounts.

With one exception, the identification, notation, and symbols are those used in the *Revised Rowland*. If a line is strongly dominant in the production of a solar blend to which a weaker line contributes slightly, the stronger element is doubly underlined. If one element dominates to a lesser degree, a single underline is used. The other symbols are:

Fe, Co	Coincidences are of like order.
Fe Co	Coincidence closer for preceding element.
Fe-Co	*Fe* line coincides with violet portion of the solar line; *Co* with the red portion.
Fe–	Solar line is too strong to be produced by *Fe* alone and probably has an unidentified component to the red; or *Fe* is displaced too far to the violet.
–Fe	Solar line is too strong to be produced by *Fe* alone and probably has an unidentified component to the violet; or *Fe* is displaced too far to the red.
Fe?	Identification is somewhat doubtful.

In giving the disk and spot intensities of lines, as in the *Revised Rowland*, −3 is substituted for 0000, −2 for 000, and −1 for 00 on the Rowland scale. Disk intensities which differ from Rowland's value are underlined.

The following symbols are used with the intensities:

N = Diffuse	Bd? = May be a band line
d = Double	ob = Line is obliterated
d? = May be double	

[1] *Transactions of the International Astronomical Union*, **3**, 81, 1928.

The multiplet designations are tabulated in the form recently recommended by a committee on spectroscopic notation and now generally adopted.[1] For elements whose lines belong to well-known series, the series notation is employed.

The older series notation can be used only for the simplest spectra. In general, the prefixes a, b, c, etc., are adopted for the successive low terms of any one L-value, multiplicity, and set (e.g., ^{4}F) in the order of increasing excitation potential; and e, f, g for the similar high terms. These terms combine with terms of the opposite set, which are denoted successively by the prefixes z, y, x, etc., z being the lowest. For most elements the low and high terms are "even," and the intermediate ones "odd." *Ti*, for example, has two low ^{3}F-terms and five high ones. These are labeled a^{3}F, b^{3}F, e^{3}F, f^{3}F, etc. There are seven odd ^{3}P-terms, called z^{3}P°, y^{3}P°, x^{3}P°, etc. In a few instances a compromise notation was adopted, which indicates in abbreviated form the electron configuration that produces the terms. In case the multiplicity is even (doublets, quartets, etc.), half-quantum numbers are used.

For the convenience of those working with the more complex spectra, Table II has been prepared. This table gives the transformation of the notation originally published for the individual spectra into that recently adopted and used throughout the present work. Eight elements are included: *Sc*, *Sc*$^+$, *Ti*, *Ti*$^+$, *Fe*, *Fe*$^+$, *Y*, *Y*$^+$. The types of terms are listed in the order S, P, D, F, G, H, etc., corresponding to the values 0, 1, 2, 3, 4, 5, respectively, of the quantum number L of Hund's theory. The terms of lower multiplicity precede those of higher, i.e., those of even multiplicity are in the order: doublets, quartets, etc.; and those of odd multiplicity in the order: singlets, triplets, quintets, etc. Further, the even terms of any multiplicity precede the odd ones. The first column gives the new notation, and the second, the published notation under the heading of the respective authors. For example, the e^{2}P-term of *Sc* in the new notation has been published as b^{2}P′.

A comprehensive compilation, entitled "Table of Atomic Lines in the Sun-Spot Spectrum," includes the revised identifications and laboratory data for practically all the stronger solar lines and for

[1] Russell, Shenstone, and Turner, *Physical Review*, **33**, 900, 1929.

TABLE II

Transformation of Notation

*Sc***

Doublet Terms				Quartet Terms			
Even		Odd		Even		Odd	
New	Russell and Meggers†	New	Russell and Meggers	New	Russell and Meggers	New	Russell and Meggers
^2P	$^2P'$	$^2S°$	$^2S'$	^4P	$^4P'$	$^4S°$	$^4S'$
a	a	z	a	a	a	z	a
e	b			e	b		
		$^2P°$	^2P			$^4P°$	^4P
^2D	^2D	z	a	^4D	^4D	z	a
a	a	y	b	e	a	y	b
b	b	x	c	f	b		
e	c	w	d	g	c	$^4D°$	$^4D'$
f	d					z	a
g	e	$^2D°$	$^2D'$	^4F	$^4F'$	y	b
h	f	z	a	a	a		
		y	b	e	b	$^4F°$	^4F
^2F	$^2F'$	x	c	f	c	z	a
a	a	w	d	g	d	y	b
e	b	v	x	h	e		
		u	y	i	f	$^4G°$	$^4G'$
^2G	^2G					z	a
a	a	$^2F°$	^2F	^4G	^4G		
e	b	z	a	e	a		
		y	b				
		x	c				
		w	d				
		$^2G°$	$^2G'$				
		z	a				
		y	b				
		$^2H°$	^2H				
		z	a				

** The published values of the inner-quantum numbers should be diminished by one-half.

† *Scientific Papers of the Bureau of Standards*, **22**, 340 (No. 558), 1927.

TABLE II—*Continued*

Sc+

Singlet Terms				Triplet Terms			
Even		Odd		Even		Odd	
New	Russell and Meggers‡	New	Russell and Meggers	New	Russell and Meggers	New	Russell and Meggers
^1S	^1S	$^1P^\circ$	^1P	^3S	^3S	$^3P^\circ$	^3P
a	a	z	a	e	a	z	a
e	b	y	b			y	b
				^3P	$^3P'$		
^1P	$^1P'$	$^1D^\circ$	$^1D'$	a	a	$^3D^\circ$	$^3D'$
e	a	z	a	e	b	z	a
				f	c		
^1D	^1D	$^1F^\circ$	^1F			$^3F^\circ$	^3F
a	a	z	a	^3D	^3D	z	a
b	b			a	a		
e	c			e	b		
f	d			f	c		
^1F	$^1F'$			^3F	$^3F'$		
e	a			a	a		
				e	b		
^1G	^1G						
a	a			^3G	^3G		
e	b			e	a		

‡ *Ibid.*, p. 331.

TABLE II—*Continued*

Ti

Singlet Terms				Triplet Terms				Quintet Terms			
Even		Odd		Even		Odd		Even		Odd	
New	Russell§	New	Russell	New	Russell	New	Russell	New	Russell	New	Russell
^1S	^1S	$^1S^\circ$	$^1S'$	^3P	$^3P'$		$^3S'$	^5P	$^5P'$	$^5S^\circ$	$^5S'$
a	a	z	a	a	a	z	a	a	a	z	a
				b	b	y	b	e	b	y	b
^1P	$^1P'$	$^1P^\circ$	^1P	c	c	x	c				
a	a	z	a	e	d	w	d	^5D	^5D	$^5P^\circ$	^5P
e	b	y	b					e	b	z	a
		x	c	^3D	^3D	$^3P^\circ$	^3P	f	c	y	b
^1D	^1D	w	d	a	a	z	a	g	d		
a	a	v	e	e	b	y	b	h	e	$^5D^\circ$	$^5D'$
b	b			f	c	x	c			z	a
e	c	$^1D^\circ$	$^1D'$			w	d	^5F	$^5F'$	y	b
f	d	z	a	^3F	$^3F'$	v	e	a	a	x	c
		y	b	a	a	u	f	e	b	w	d
^1F	$^1F'$	x	c	b	b	t	g	f	c	v	e
a	a	w	d	e	c			g	d		
e	b	v	e	f	d	$^3D^\circ$	$^3D'$	h	e	$^5F^\circ$	^5F
f	c			g	e	z	a	i	f	z	a
		$^1F^\circ$	^1F	h	f	y	b	j	g	y	b
^1G	^1G	z	a	i	g	x	c	k	h		
a	a	y	b			w	d			$^5G^\circ$	$^5G'$
b	b	x	c	^3G	^3G	v	e	^5G	^5G	z	a
e	c	w	d	a	a	u	f	e	a	y	b
f	d	v	e	e	b	t	g	f	b		
		u	f	f	c	s	h	g	c		
^1H	$^1H'$					r	i	h	d		
a	a	$^1G^\circ$	$^1G'$	^3H	$^3H'$	q	j				
e	b	z	a	a	a	p	k	^5H	$^5H'$		
		y	b	e	b	o	l	e	a		
		x	c			n	m	f	b		
		w	d					g	c		
		v	e			$^3F^\circ$	^3F				
		u	f			z	a				
						y	b				
		$^1H^\circ$	^1H			x	c				
		z	a			w	d				
		y	b			v	e				
		x	c			u	f				
						t	g				
		$^1I^\circ$	$^1I'$			s	h				
		z	a			r	i				
						q	j				
						$^3G^\circ$	$^3G'$				
						z	a				
						y	b				
						x	c				
						w	d				
						v	e				
						u	f				
						t	g				
						$^3H^\circ$	^3H				
						z	a				
						y	b				
						x	c				
						w	d				
						$^3I^\circ$	$^3I'$				
						z	a				

§ *Mt. Wilson Contr.*, No. 345; *Astrophysical Journal*, **66**, 347, 1927.

TABLE II—*Continued*

Ti+**

Doublet Terms				Quartet Terms			
Even		Odd		Even		Odd	
New	Russell[|]	New	Russell	New	Russell	New	Russell
^2S	^2S	$^2S^\circ$	$^2S'$	^4P	$^4P'$	$^4S^\circ$	$^4S'$
a	a	z	a	a	a	z	a
^2P	$^2P'$	$^2P^\circ$	^2P	b	b	$^4P^\circ$	^4P
a	a	z	a	^4D	^4D	z	a
b	b	y	b	e	a	y	b
^2D	^2D	x	c	^4F	$^4F'$	$^4D^\circ$	$^4D'$
a	a	$^2D^\circ$	$^2D'$	a	a	z	a
b	b	z	a	b	b	y	b
c	c	y	b	e	c	x	c
^2F	$^2F'$	x	c	f	d	$^4F^\circ$	^4F
a	a	w	d	^4G	^4G	z	a
b	b	v	e	e	a	$^4G^\circ$	$^4G'$
e	c	$^2F^\circ$	^2F	^4H	$^4H'$	z	a
f	d	z	a	e	a		
^2G	^2G	y	b				
a	a	x	c				
b	b	w	d				
e	c	v	e				
^2H	$^2H'$	$^2G^\circ$	$^2G'$				
a	a	z	a				
e	b	y	b				
		$^2H^\circ$	^2H				
		z	a				

** The published values of the inner-quantum numbers should be diminished by one-half.

|| *Mt. Wilson Contr.*, No. 344; *Astrophysical Journal*, **66**, 283, 1927.

TABLE II—*Continued*

Fe

Triplet Terms				Quintet Terms				Septet Terms			
Even		Odd		Even		Odd		Even		Odd	
New	Burns and Walters¶	New	Burns and Walters	New	Burns and Walters	New	Burns and Walters	New	Burns and Walters	New	Burns and Walters
^3P	^3P	$^3S°$	$^3S*$	^5P	^5P	$^5S°$	$^5S*$	^7D	^7D	$^7P°$	$^7P*$
a	a	z	a	a	a	z	a	e	a	z	a
b	b										
e	c	$^3P°$	$^3P*$	^5D	^5D	$^5P°$	$^5P*$			$^7D°$	$^7D*$
		z	a	a	a	z	a			z	a
^3D	^3D	y	b	e	b	y	b				
e	a			f	c	x	c			$^7F°$	$^7F*$
f	c	$^3D°$	$^3D*$			w	d			z	a
		z	a	^5F	^5F		6R				
^3F	^3F	y	b	a	a	v	5R				
a	a	x	c	e	b		3R				
b	b	w	d								
e	c										
		$^3F°$	$^3F*$			$^5D°$	$^5D*$				
^3G	^3G	z	a			z	a				
a	a	y	b			y	b				
b	b		15R			x	c				
e	c	x	12R			w	d				
			9R								
^3H	^3H					$^5F°$	$^5F*$				
a	a	$^3G°$	$^3G*$			z	a				
		z	a			y	b				
		y	b			x	c				
							50R				
		$^3H°$	$^3H*$				49R				
		z	a			w	48R				
							51R				
							47R				
						$^5G°$	$^5G*$				
						z	a				
						y	b				
						x	c				

¶ *Publications of the Allegheny Observatory*, **6**, 159 (No. 11), 1929.

TABLE II—*Continued*

Fe^{+***}

Quartet Terms				Sextet Terms			
Even		Odd		Even		Odd	
New	Russell***	New	Russell	New	Russell	New	Russell
^4P	$^4P'$	$^4P°$	^4P	^6S	^6S	$^6P°$	^6P
a	a	z	a	a	a	z	a
b	b						
		$^4D°$	$^4D'$	^6D	^6D	$^6D°$	$^6D'$
^4D	^4D	z	a	a	a	z	a
a	a						
b	b	$^4F°$	^4F			$^6F°$	^6F
		z	a			z	a
^4F	$^4F'$	y	b				
a	a						
b	b						
^4G	^4G						
a	a						

** The published values of the inner-quantum numbers should be diminished by one-half.

*** *Mt. Wilson Contr.*, No. 318; *Astrophysical Journal*, **64**, 194, 1926.

TABLE II—*Continued*

*Y***

Doublet Terms				Quartet Terms			
Even		Odd		Even		Odd	
New	Meggers and Russell††	New	Meggers and Russell	New	Meggers and Russell	New	Meggers and Russell
^2S	^2S	$^2S°$	$^2S'$	^4P	$^4P'$	$^4S°$	$^4S'$
e	a	z	z	a	a	z	z
f	b			e	b		
g	c	$^2P°$	^2P	f	c	$^4P°$	^4P
		z	z	g	d	z	z
^2P	$^2P'$	y	y	h	e	y	y
a	a	x	x				
e	b	w	w	^4D	^4D	$^4D°$	$^4D'$
f	c			e	a	z	z
		$^2D°$	$^2D'$	f	b	y	y
^2D	^2D	z	z	g	c	x	x
a	a	y	y	h	d		
b	b	x	x			$^4F°$	^4F
e	c	w	w	^4F	$^4F'$	z	z
f	d	v	v	a	a	y	y
g	e			e	b		
		$^2F°$	^2F	f	c	$^4G°$	$^4G'$
^2F	$^2F'$	z	z	g	d	z	z
a	a	y	y	h	e		
		x	x	i	f		
^2G	^2G	w	w				
a	a	v	v	^4G	^4G		
				e	a		
		$^2G°$	$^2G'$				
		z	z				
		y	y				
		$^2H°$	^2H				
		z	z				

** The published values of the inner-quantum numbers should be diminished by one-half.

†† *Bureau of Standards Journal of Research*, **2**, 745 (Reprint No. 55), 1929.

TABLE II—*Continued*

Y^+

Singlet Terms				Triplet Terms			
Even		Odd		Even		Odd	
New	Meggers and Russell‡‡	New	Meggers and Russell	New	Meggers and Russell	New	Meggers and Russell
^1S	^1S	$^1P^\circ$	^1P	^3S	^3S	$^3P^\circ$	^3P
a	a	z	z	e	a	z	z
e	b	y	y	f	b	y	y
f	c						
		$^1D^\circ$	$^1D'$	^3P	$^3P'$	$^3D^\circ$	$^3D'$
^1P	$^1P'$	z	z	a	a	z	z
e	a			e	b		
		$^1F^\circ$	^1F	f	c	$^3F^\circ$	^3F
^1D	^1D	z	z			z	z
a	a			^3D	^3D		
b	b			a	a		
e	c			e	b		
f	d			f	c		
g	e			g	d		
h	f						
				^3F	$^3F'$		
^1F	$^1F'$			a	a		
e	a			e	b		
^1G	^1G			^3G	^3G		
a	a			e	a		
e	b						

‡‡ *Ibid.*, p. 737.

many faint ones. This table is too extensive to present here, but it is hoped that eventually it may be published. Meanwhile, the material will be made available, as far as possible, to those interested.

Table III summarizes the contents of the large unpublished table. Spot intensities have been estimated for 6312 lines between λ 3894 and λ 6635, most of which also appear in the spectrum of the disk. A total of 1818 lines in this region remains unidentified. The number of identified lines attributed to each element is listed in Table III as follows: The second column gives the number of unblended lines of each element found among the lines for which spot intensities have been estimated. The third column contains the number of lines attributed somewhat doubtfully to the various elements. Thus the number of identifications given in the large table as *Ti?* is 28. The

fourth column lists the number of lines of each element which contributes to the production of blended atomic lines in the solar or spot spectrum. For example, in the case of a solar line identified as *Fe-Ti*, a blend of *Fe* and *Ti*, each element is included in the counts in this

TABLE III

NUMBER OF LINES BETWEEN λ 3894 AND λ 6635 DUE TO VARIOUS ELEMENTS

El.	Id.	Id.?	Id. Bl.	Id. Bl. and Id.?	Total	El.	Id.	Id.?	Id. Bl.	Id. Bl. and Id.?	Total
H	5	.....	.....	.....	5	*Sr*$^+$	3	.....	1	.....	4
C	2	.....	1	.....	3	*Y*	20	1	8	.....	29
Na	10	1	1	.....	12	*V*$^+$	22	.....	10	.....	32
Mg	12	2	.....	1	15	*Zr*	44	11	15	7	77
Mg$^+$	2	.....	.....	.....	2	*Zr*$^+$	19	1	25	2	47
Al	3	.....	.....	.....	3	*Cb*	.....	.....	.....	2	2
Si	14	.....	.....	.....	14	*Mo*	2	2	.....	1	5
Si$^+$	2	.....	.....	.....	2	*Mo*$^+$	.....	.....	1	2	3
K	2	.....	.....	.....	2	*Ru*	4	1	.....	.....	5
Ca	67	.....	5	1	73	*In*	1	.....	.....	.....	1
Ca$^+$	2	.....	.....	.....	2	*Ba*$^+$	5	.....	3	.....	8
Sc	48	3	8	2	61	*Hf*$^+$	1	.....	.....	.....	1
Sc$^+$	31	.....	6	.....	37	*W*	2	.....	1	3	6
Ti	484	28	127	14	653	*Pb*	1	.....	.....	.....	1
Ti$^+$	81	1	32	2	116	*La*$^+$	16	1	17	2	36
V	214	14	71	19	318	*Ce*$^+$	40	4	48	7	99
V$^+$	17	.....	15	4	36	*Pr*$^+$	.....	.....	1	5	6
Cr	342	47	154	26	569	*Nd*$^+$	13	4	46	12	75
Cr$^+$	45	4	16	1	66	*Sa*$^+$	5	1	21	5	32
Mn	81	17	36	8	142	*Eu*$^+$	4	.....	1	.....	5
Mn$^+$	.....	.....	1	6	7	*Gd*$^+$	.....	2	3	8	13
Fe	1291	31	225	5	1552	*Dy*$^+$	3	1	3	1	8
Fe$^+$	65	.....	4	.....	69	*Er*$^+$	1	.....	1	.....	2
Co	99	17	48	9	173	*Lu*$^+$	.....	.....	.....	1	1
Ni	238	18	79	13	348	*Atm.*	2	6	25	4	37
Ni$^+$	1	.....	2	1	4	*Atm.O*	1	.....	5	.....	6
Cu	4	.....	1	1	6	*Atm.wv*	.....	2	12	2	16
Zn	4	.....	.....	.....	4	C_2	.....	7	15	3	25
Ga	.....	.....	1	.....	1	*CH*	2	15	25	17	59
Sr	10	.....	1	.....	11	*CN*	2	3	13	8	26

column. When the identification is listed as a blend, but questioned, the entry appears in the fifth column. Thus for the identification *Ti-Co?*, *Co* is entered in this column. Finally, the last column gives the total number of entries for each element listed.

Certain elements not in the table should, however, be mentioned. For example, *Li* and *Rb* have strong spot lines to the red of λ 6635 which are the only evidence for the presence of these elements in the sun. Similarly, the infra-red *O* lines are present in the solar spec-

trum and are weakened in the spot spectrum. Several other elements whose lines are known to occur in the solar spectrum are also omitted from Table III because the lines lie to the violet of λ 3894.

A few band lines are included in the table. Most of these are blended with atomic lines.

New lines.—An interesting outcome of the work is a large number of new atomic spot lines. Many of these are faint, but show a decided Zeeman effect in the spot region. Others are not weak, but heretofore have been overlooked because they lie in the wings of strong lines. Here the illuminated negative yields much information. An interesting case is the *Cr* line at λ 4861.19, in the wing of *Hβ*, but clearly visible on the negative. In all, 75 spot lines were entered in the *Revised Rowland*, a number now extended to 469, although doubtless some band lines are included. From λ 6617 to the red but one new line has been added, namely, the second line of the *Li* pair at λ 6707, a strong spot line clearly double on the plate.

Table IV gives all known spot lines, those formerly listed being marked with a dagger. The measured wave-lengths are in the first column. The positions of the new lines relative to neighboring lines were measured to two decimal places by using scales which fit the map. An interesting check on these results is afforded by R. S. Richardson's[1] measures of all the lines in the sun-spot spectrum between λ 4900 and λ 5403. Most of these are band lines, but some atomic lines were detected by means of the Zeeman effect. A total of 82 atomic lines was found by both Mr. Richardson and the writer. A comparison of the two sets of measures gives an average difference of ±0.01 A. Three lines, λλ 5048, 5295, and 5377, were found by Mr. Richardson alone; but a large number that he thought might possibly show some Zeeman effect have been omitted from the table as they are exceedingly faint and have not been found on both sets of plates. He has kindly consented to the inclusion of his measures in Table IV, where they are indicated by an "R" following the wave-length. They are the only three-place measures in the table.

The second column of Table IV gives the adopted identification; the third, the spot intensity. An intensity followed by "Bl" signifies a blend and does not therefore apply to the spot line alone. The

[1] Unpublished material.

TABLE IV

ATOMIC LINES PRESENT ONLY IN THE SUN-SPOT SPECTRUM

λ I.A.	Ident.	Int. Spot	T.C.	E.P.	Multiplet Designation
3900.44	.....	0	.....	.....	.....
4007.20?	*Ti*	−2	IV	2.083	$z^5F^\circ_2 - e^5H_3$
4047.23	*K*	0	.....	0.000	$4^2S_{1/2} - 5^2P^\circ_{1/2}$
4069.84	*V?*	−1	.....	.....	.....
4071.21	.....	−1	.....	.....	.....
4077.16	*Ti*	0	IV	2.151	$a^3D_2 - u^3P^\circ_1$
4078.89?	.....	−1	.....	.....	.....
4080.69	.....	−1	.....	.....	.....
4093.48	*V*	0	III	1.178	$a^4P_{1/2} - x^4D^\circ_{1/2}$
4116.60	*V*	0	Pred	0.261	$a^6D_{1/2} - y^6D^\circ_{1/2}$
4117.56	.....	0	.....	.....	.....
4144.33	.....	0	.....	.....	.....
4152.36	*Sc?*	0	III	1.961	$z^4F^\circ_{3\frac{1}{2}} - e^4G_{4\frac{1}{2}}$
4167.52	*Y*	1	II	0.065	$a^2D_{2\frac{1}{2}} - y^2F^\circ_{2\frac{1}{2}}$
4174.15	*Y*	0	II	0.065	$a^2D_{2\frac{1}{2}} - y^2P^\circ_{1\frac{1}{2}}$
4179.86	*Ti*	0	.....	2.165	$a^3D_3 - s^3F^\circ_3$
4186.84	.....	−1	.....	.....	.....
4278.79	*Ti*	0	III	2.295	$z^5D^\circ_3 - e^5D_2$
4281.71	.....	−2	.....	.....	.....
4294.49	.....	−2Bd?	.....	.....	.....
4306.18	*V*	0	I	0.017	$a^4F_{2\frac{1}{2}} - z^4F^\circ_{3\frac{1}{2}}$
4306.91	*Ti*	−2	III A	0.809	$a^5F_1 - w^3D^\circ_2$
4308.54	*Ti*	0	III A	1.062	$a^3P_2 - y^3P^\circ_2$
4311.63	*Ti*	1	IV	2.144	$a^3D_1 - r^3D^\circ_1$
4314.36	*Ti*	0N	III A	0.832	$a^5F_4 - x^3G^\circ_3$
4314.77	*Ti*	0	II*	0.815	$a^5F_2 - w^3D^\circ_2$
4345.21?	.....	−N	.....	.....	.....
4363.54?	*V*	(	II A	0.274	$a^6D_{2\frac{1}{2}} - z^4P^\circ_{2\frac{1}{2}}$
4368.92	*Ti*	0	IV	2.258	$b^3G_4 - u^3G^\circ_3$
4378.97	.....	0N	.....	.....	.....
4387.20	*V*	−2	III A	.....	.....
4393.33	.....	0	.....	.....	.....
4394.51	.....	−2N	.....	.....	.....
4397.22	*Cr?*	0	III	2.999	$b^5D_1 - u^5P^\circ_1$
4418.63	.....	−2	.....	.....	.....
4420.46	*Zr?*	−1	III	1.360	$a^5P_2 - w^5D^\circ_2$
4425.85	*Ti*	−1	III A	1.062	$a^3P_2 - v^3D^\circ_2$
4433.97	*Ti*	1	III A*	1.424	$b^3F_2 - v^3F^\circ_3$
4438.25	*Ti*	−1	IV	2.240	$b^3P_2 - r^3D^\circ_2$
4439.01	*V*	−2	IV	.....	.....
4449.60	*V*	−1	III	.....	.....
4449.97	*Ti*	−1	IV	1.871	$a^3G_4 - x^1F^\circ_3$
4475.50	*Ti*	−1	IV	2.108	$z^5F^\circ_4 - f^5F_5$
4476.62	*Ti*	−2	Pred	2.076	$z^5F^\circ_1 - f^5F_2$
4491.18	*V*	−2	III	.....	.....
4497.73	*Na*	−1	.....	2.095	$3^2P^\circ_{1\frac{1}{2}} - 7^2D$
4505.73†	*Ti*	−1	IV	2.094	$z^5F^\circ_3 - f^5F_2$
4511.31†	*In*	−1	.....	0.273	$5^2P^\circ_{1\frac{1}{2}} - 6^2S_{1/2}$
4511.82	.....	−2	.....	.....	.....
4527.98	*V*	−1	IV	.....	.....
4535.86?	.....	−2	.....	.....	.....
4537.05†	.....	−1	.....	.....	.....

* Blend. † Not new; included in the *Revised Rowland Table.* ‡ Mostly band.

TABLE IV—*Continued*

λ I.A.	Ident.	Int. Spot	T.C.	E.P.	Multiplet Designation
4541.35	*V*?	−1			
4541.61		−1			
4542.90		−2			
4543.13		−2			
4547.30	*Ti*?	−1	IV		
4563.66†	*Cr*	0	IV		
4564.23†	*Ti*	−1	III A	1.454	$b^3F_4 - w^3F_3^\circ$
4573.09		−2N			
4575.48	*Zr*	0	I	0.000	$a^3F_2 - z^3G_3^\circ$
4578.47		0			
4581.30	*V*	−1	IV		
4582.43?		−2Bd?			
4583.90	*Cr*	−1		3.000	$b^5D_2 - y^3D_2^\circ$
4586.93	*Ti*	−2	Pred	2.416	$z^3F_4^\circ - f^3G_4$
4588.76		−1			
4589.35		−2			
4590.55	*Zr*?−	−1	II	0.540	$a^3P_1 - x^3D_1^\circ$
4594.50?	*Ti*	−2	Pred	2.335	$c^3P_2 - r^3D_2^\circ$
4595.87		−2			
4599.79		−2			
4606.13	*V*	2	I	0.017	$a^4F_{2\frac{1}{2}} - z^4G_{2\frac{1}{2}}^\circ$
4609.97		−1			
4626.49?	*V*	−1	III	1.039	$a^4D_{\frac{1}{2}} - y^4P_{\frac{1}{2}}^\circ$
4627.24		−1			
4636.12	*V*?	−1NBd?	IV		
4640.44	*Ti*	−1	IV?	2.324	$c^3P_1 - v^3P_0^\circ$
4643.72	*V*	2	I	0.000	$a^2D_{1\frac{1}{2}} - z^2F_{2\frac{1}{2}}^\circ$
4643.94		−1			
4644.86	*Zr*?	−1	V	1.814 1.437	$a^3D_3 - t^3D_3^\circ$ $b^3F_2 - u^3F_2^\circ$
4661.92?		−1			
4663.28?		0			
4665.76		−2			
4677.53?	*Ti*?	−1	IV?	3.049	$z^1G_4^\circ - e^1G_4$
4679.73	*Ti*	0	Pred	1.048	$a^3P_1 - x^5D_1^\circ$
4683.44	*Zr*?	−1	V?	1.524	$b^3F_4 - v^3F_4^\circ$
4684.28		−1			
4684.50	*Ti*	0	IV?	2.151	$a^3D_2 - t^3D_3^\circ$
4685.17		−2			
4692.45†	*Ti*	0	Pred	1.062	$a^3P_2 - x^5D_2^\circ$
4698.83	*Ti*	0		2.151	$a^3D_2 - t^3D_2^\circ$
4706.17	*V*	−1	?		
4707.69?		−1Bd?			
4711.68		−1			
4711.91	*Zr*?	−1	V	1.524	$b^3F_4 - u^3F_4^\circ$
4714.12	*V*	−1	?		
4719.12	*Zr*?	−2	V	1.850	$a^3H_5 - z^3I_6^\circ$
4724.68	*Ti*	−1		2.165	$a^3D_3 - t^3D_2^\circ$
4729.54	*V*	−1N	III		
4730.60		−2			
4737.66	*Sc*	2	III	1.427	$a^4F_{2\frac{1}{2}} - y^4D_{1\frac{1}{2}}^\circ$
4742.64	*V*	−2	IV		
4746.64	*V*	−1N	IV	2.020	$z^6G_{1\frac{1}{2}}^\circ - e^6F_{1\frac{1}{2}}$
4747.27	*Ti*	0	III A	1.062	$a^3P_2 - w^3D_1^\circ$

TABLE IV—*Continued*

λ I.A.	Ident.	Int. Spot	T.C.	E.P.	Multiplet Designation
4747.96	*Na*?	0	.....	2.093	$3^2P^\circ_{\frac{1}{2}} - 7^2S_{\frac{1}{2}}$
4748.50	*V*	−2	III	2.031	$z^6G^\circ_{2\frac{1}{2}} - e^6F_{2\frac{1}{2}}$
4751.00	*V*	−1	III	2.046	$z^6G^\circ_{3\frac{1}{2}} - e^6F_{3\frac{1}{2}}$
4751.29	.....	−1N	.....	.....	.....
4751.58	*V*	−1	III	.....	.....
4753.18†	*Sc*	2	I A	0.000	$a^2D_{1\frac{1}{2}} - z^2F^\circ_{2\frac{1}{2}}$
4757.48	*V*	−1	III	2.020	$z^6G^\circ_{1\frac{1}{2}} - e^6F_{1\frac{1}{2}}$
4760.97†	*Y*	0	I	0.065	$a^2D_{2\frac{1}{2}} - z^2F^\circ_{2\frac{1}{2}}$
4764.87	.....	−2N	.....	.....	.....
4766.33	*Ti*	0?	III	2.239	$a^3H_5 - x^3H^\circ_4$
4779.34†	*Sc*	1N	I A	0.021	$a^2D_{2\frac{1}{2}} - z^2F^\circ_{3\frac{1}{2}}$
4784.45	*V*	0	II A	0.017	$a^4F_{2\frac{1}{2}} - z^4D^\circ_{3\frac{1}{2}}$
4784.94	*Zr*	0	II	0.684	$a^5F_4 - y^3G^\circ_5$
4787.64	.....	−1	.....	.....	.....
4789.79†	*Ti*	1	.....	0.832	$a^5F_4 - y^3G^\circ_4$
4791.53	*Sc*	0	I A	0.021	$a^2D_{2\frac{1}{2}} - z^2F^\circ_{2\frac{1}{2}}$
4805.89†	*Zr*	0	II	0.684	$a^5F_4 - y^5G^\circ_4$
4811.89†	*Sr*	−1	I	1.839	$5^3P^\circ_2 - p^2\,{}^3P_2$
4816.46	.....	0N	.....	.....	.....
4818.29	.....	−1	.....	.....	.....
4821.29	*Ti*	−2	.....	2.151	$a^3D_2 - u^3D^\circ_3$
4824.29	*Zr*	0	II	0.648	$a^5F_3 - y^5G^\circ_3$
4828.06	*Zr*	−1	II	0.620	$a^5F_2 - y^3G^\circ_3$
4833.03	*V*	−2N	IV A	.....	.....
4839.25	*Ti*	−1	.....	2.222	$b^3P_0 - t^3D^\circ_1$
4846.33	*Cr*?	−1N	IV	.....	.....
4851.35	*Zr*	0	II	0.620	$a^5F_2 - y^5G^\circ_2$
4852.68	*Y*	−1	II	1.368	$a^4F_{2\frac{1}{2}} - y^4F^\circ_{2\frac{1}{2}}$
4854.76	*Ti*	−1	.....	2.230	$b^3P_1 - t^3D^\circ_1$
4861.19	*Cr*	1?	III	2.533	$a^5G_3 - y^5F^\circ_3$
4862.26	.....	0d?	.....	.....	.....
4862.90	.....	−1	.....	.....	.....
4863.75	*Ti*	−1	Pred	2.240	$b^3P_2 - t^3D^\circ_2$
4864.85	*V*	−1	Pred	1.178	$a^4P_{\frac{1}{2}} - y^4P^\circ_{1\frac{1}{2}}$
4866.07	*Zr*	−1	II	0.727 2.167	$a^5F_5 - y^3G^\circ_5$ $z^3F^\circ_4 - e^3F_4$
4874.85	.....	−1N	.....	.....	.....
4875.26	.....	−1N	.....	.....	.....
4880.59†	*V*	0	III	1.190	$a^4P_{1\frac{1}{2}} - y^4P^\circ_{2\frac{1}{2}}$
4881.24	*Zr*	−1	III	0.648	$a^5F_3 - y^3G^\circ_3$
4893.13	*Zr*?	−2	IV	1.575 0.684	$a^3G_4 - v^3F^\circ_3$ $a^5F_4 - y^5G^\circ_3$
4893.92	*Ti*	−2	.....	2.151	$a^3D_2 - u^3D^\circ_1$
4895.99	.....	−2	.....	.....	.....
4896.94	.....	−2	.....	.....	.....
4897.65	.....	−2	.....	.....	.....
4898.27	.....	−1	.....	.....	.....
4900.02?	*Ti*	−2?	Pred	2.650	$z^3G^\circ_3 - g^3F_2$
4904.30	.....	−1	.....	.....	.....
4908.44	*Ti*	−2	.....	2.684	$z^3G^\circ_5 - g^3F_4$
4910.44	.....	−2Bd?	.....	.....	.....
4912.39?	*Co*	−2?	I A	0.579	$b^4F_{2\frac{1}{2}} - z^6F^\circ_{1\frac{1}{2}}$
4918.503R	.....	0Bd?	.....	.....	.....
4924.56	.....	1N	.....	.....	.....

TABLE IV—*Continued*

λ I.A.	Ident.	Int. Spot	T.C.	E.P.	Multiplet Designation
4925.72	*V*—	0NBd?	III	1.213	$a^4P_{2\frac{1}{2}}-y^4P^\circ_{2\frac{1}{2}}$
4927.592R		−2			
4928.892R	*Ti*	−2		0.832	$a^5F_4 - x^3F^\circ_4$
4930.21		−2			
4930.66†		−1			
4931.50†		−1			
4932.29†		−1			
4937.16		−1			
4937.612R		−1			
4937.881R		−2			
4937.995R	*Ti*	−2		1.988	$z^5G^\circ_4 - e^5F_5$
4940.304R		−1			
4941.02	*Ti*	−1		1.972	$z^5G^\circ_3 - e^5F_4$
4941.38		−2			
4943.06	*Ti*	−2	(III A)	0.896	$a^1D_2 - x^3D^\circ_3$
4944.824R		−2			
4947.334R		−2?			
4947.98†	*Ti*	1	III A	0.815	$a^5F_2 - x^3F^\circ_2$
4948.782R		−2			
4948.874R		−2			
4953.361R	*Ti*	−2	Pred	0.845	$a^5F_5 - x^3F^\circ_4$
4953.488R		−2			
4953.576R		−2			
4959.122R		−2			
4962.26	*Sr*	−1	I	1.839	$5^3P^\circ_2 - 5^3D_3$
4967.32	*Ti*	−1	(III A)	0.000	$a^3F_2 - z^3D^\circ_3$
4967.80?†		0			
4971.626R		−1Bd?			
4973.06	*Ti*	0	III	1.988	$z^5G^\circ_4 - e^5F_4$
4994.990R		−1			
4995.08	*Ti*	−1	(III)	2.240	$b^3P_2 - u^3D^\circ_3$
4995.566R		−1?			
4997.74		−1			
5019.22†	*Cr*	−1	Pred	0.964	$a^5D_1 - y^7P^\circ_2$
5020.350R		−2Bd?			
5033.61		−1Bd?			
5042.580R	*Mn*?	−2		2.940	$a^4D_{\frac{1}{2}} - z^6F^\circ_{1\frac{1}{2}}$
5046.550R	*Zr*?	−2	V	1.524	$b^3F_4 - w^3G^\circ_5$
5048.642?R	*Ti*?	−3?			
5048.76	*Cr*	1	II A	0.979	$a^5D_2 - y^7P^\circ_2$
5058.280R	*Ti*?	−1Bd?			
5064.339R	*Sc*	−1	III	1.433	$a^4F_{3\frac{1}{2}} - y^4F^\circ_{4\frac{1}{2}}$
5069.360R	*Ti*	−1	IV	2.144	$a^3D_1 - w^3P^\circ_0$
5069.466R		−1			
5070.23	*Sc*?	−2Bd?	III	1.427	$a^4F_{2\frac{1}{2}} - y^4F^\circ_{3\frac{1}{2}}$
5077.548R		−2			
5078.284R	*Zr*	−2	V?	1.437	$b^3F_2 - w^3G^\circ_3$
5095.030R		−2			
5108.852R		−1Bd?			
5119.25		−2			
5124.866R		−1Bd?			
5142.25		−2			
5144.612R	*Cr*?	−1N	II?		
5158.304R		0N			

TABLE IV—*Continued*

λ I.A.	Ident.	Int. Spot	T.C.	E.P.	Multiplet Designation
5158.928R		−1			
5161.78	*Cr*	−1	III?		
5169.430R		−2			
5170.46	*Ti*	−2		2.258	$b^1G_4 - x^1F^\circ_3$
5177.32		oBd?			
5185.750R		o			
5187.11†		−1			
5190.188R		−1			
5194.772R		−2			
5201.823R		−2			
5212.27	*Ti*	−1	III		
5218.090R	*Ti*	−1	IV		
5222.67	*Cr*	−1N	IV	2.696	$a^5P_3 - x^5P^\circ_2$
5222.980R		−2Bd?			
5224.16	*Ti*	−1	(IV A)	0.822	$a^5F_3 - y^5D^\circ_3$
5228.59		−2			
5231.254R		−2Bd?			
5231.526R		−2			
5232.82?		−1N			
5233.72		−2			
5234.820R		−3			
5238.52	*Ti*	o	III A*	2.083	$z^5F^\circ_2 - e^5F_1$
5239.95	*Ti*	−1		0.809	$a^5F_1 - y^5D^\circ_1$
5246.651R	*Ti*	−1			
5251.49†	*Ti*	o	(III A)	0.815	$a^5F_2 - y^5D^\circ_1$
5252.365R		−2N			
5258.334R	*Sc*	−2	IV	2.498	$a^2G_{4\frac{1}{2}} - z^2H^\circ_{5\frac{1}{2}}$
5273.43	*Cr*	−1	III	3.435	$z^7D^\circ_5 - f^7D_4$
5277.422R	*Zr*	−1	III	0.540	$a^3P_1 - y^3D^\circ_2$
5286.072R		−1NBd?			
5288.40		−1			
5288.988R		−2N			
5291.604R		−2Bd?			
5292.809R	*Cr*?	−2	Pred	3.874	$a^5F_4 - x^5D^\circ_3$
5293.638R		−3N			
5294.314R		−2Bd?			
5295.584R		−3?			
5298.46	*Cr*	o	Pred	2.887	$z^7P^\circ_3 - e^7D_2$
5304.00?		−2			
5311.20		−1Bd?			
5311.43	*Zr*	−1	III	0.518	$a^3P_0 - y^3D^\circ_1$
5314.574R		−1N			
5317.266R		−1Bd?			
5317.734R		−1NBd?			
5317.896R		−1NBd?			
5318.58		−2			
5320.486R		−3Bd?			
5321.288R		−2N			
5321.84		−1			
5323.928R	*Ti*	o	(III A)	0.822	$a^5F_3 - y^3D^\circ_2$
5326.414R		−1Bd?			
5329.487R		−3Bd?			
5331.980R		−2			
5332.140R		−1			

TABLE IV—*Continued*

λ I.A.	Ident.	Int. Spot	T.C.	E.P.	Multiplet Designation
5334.134R		−1N			
5334.439R		−3			
5335.094R		−2			
5335.24		−2			
5335.434R		−2N			
5336.07†		0			
5337.163R		−2			
5339.349R		0N			
5339.651R		−2N			
5339.82?		−2			
5342.88?		−2			
5343.666R		−1N			
5344.16?		−2N			
5347.892R		−2			
5354.684R		−1			
5356.429R		−1			
5356.607R		−2			
5359.05		−2			
5361.71†	*Ti*	−1	(III A)	0.832	$a^5F_4 - y^3F^\circ_4$
5362.570R	*Zr*	−2	III	0.540	$a^3P_1 - y^3D^\circ_1$
5376.60†	*Ti*	−1		0.000	$a^3F_2 - z^5D^\circ_3$
5377.356R		−2NBl			
5382.921R	*Ti*	−2	Pred	1.865	$a^3G_3 - w^3F^\circ_3$
5391.350R	*Cr*?	−1	IV	3.355	$b^3P_1 - y^3P^\circ_1$
5392.066R	*Sc*	−1NBl	III	1.979	$z^4F^\circ_{4\frac{1}{2}} - e^4D_{3\frac{1}{2}}$
5401.39†	*Ti*	−1	(III A)	0.815	$a^5F_2 - y^3F^\circ_2$
5401.92	*V*	−1	III		
5403.984R	*Ti*	−1?	IV	2.324	$c^3P_1 - w^3P^\circ_2$
5432.33?	*Ti*	−1		2.398	$z^3F^\circ_3 - e^3F_4$
5444.85		−1Bd?			
5453.40		−2			
5463.89		−2			
5465.75		0			
5470.48	*Ti*	−1	Pred	1.437	$b^3F_3 - x^3G^\circ_3$
5470.97		−2			
5481.71		−2Bd?			
5497.98		−1			
5517.18	*V*?	−2	II A	0.000	$a^4F_{1\frac{1}{2}} - z^6F^\circ_{\frac{1}{2}}$
5547.06	*V*	1	II	1.076	$a^4D_{3\frac{1}{2}} - y^6D^\circ_{4\frac{1}{2}}$
5548.76?		−2			
5558.77	*V*	−1N	III	1.039	$a^4D_{\frac{1}{2}} - y^6D^\circ_{\frac{1}{2}}$
5560.56	*V*	−2	Pred	0.040	$a^4F_{3\frac{1}{2}} - z^6D^\circ_{3\frac{1}{2}}$
5574.04	*V*?	−1	II A	0.040	$a^4F_{3\frac{1}{2}} - z^6F^\circ_{2\frac{1}{2}}$
5579.91		0N			
5586.91		−1			
5592.97	*V*	−1N	II A	0.040	$a^4F_{3\frac{1}{2}} - z^6D^\circ_{2\frac{1}{2}}$
5597.69	*Ti*?	−1NBd?			
5597.86	*Cr* *V*?	−1NBd?	Pred III A	3.823 1.059	$z^5F^\circ_3 - e^5D_4$ $a^4D_{2\frac{1}{2}} - y^6D^\circ_{1\frac{1}{2}}$
5598.86?		−2			
5618.38		0Bd?			
5620.17?	*Zr*	−2	IV?	2.151 0.517	$z^5F^\circ_3 - e^5F_2$ $a^3P_2 - z^3S^\circ_1$
5659.16		−2			

TABLE IV—*Continued*

λ I.A.	Ident.	Int. Spot	T.C.	E.P.	Multiplet Designation
5664.26		−2			
5664.52†	*Zr*	−1	II	0.630	$a^1D_2 - y^1D^\circ_2$
5680.91†	*Zr*	−1	II	0.540 2.313	$a^3P_1 - z^3S^\circ_1$ $a^1H_5 - x^1G^\circ_4$
5708.20	*Ti*	0	IV	2.308	$z^5D^\circ_4 - e^5F_4$
5711.76	*Sc*	2N	III A	1.422	$a^4F_{1\frac{1}{2}} - z^4G^\circ_{2\frac{1}{2}}$
5725.36		−2Bd?			
5741.20	*Ti*	0	IV	2.495	$b^1D_2 - x^1F^\circ_3$
5751.42		−2N			
5752.86	*Ti*	−2	IV	2.230	$b^3P_1 - y^3S^\circ_1$
5756.40?		−2			
5759.02?		−2			
5785.94	*Cr*	0	I A	0.964	$a^5D_1 - z^7F^\circ_2$
5788.61	*V*	−1	III	2.731	$z^4G^\circ_{4\frac{1}{2}} - e^4F_{3\frac{1}{2}}$
5790.15		0			
5790.64	*V*	1	III A		
5797.43	*Ti*	−1	(IV)	3.291	$y^5G^\circ_4 - f^5H_4$
5797.55	*Cr*	−2	Pred	3.088	$z^7F^\circ_1 - e^7D_2$
5797.75†	*Zr*	0	II	0.070	$a^3F_3 - z^3D^\circ_2$
5799.90	*V*	−2			
5807.14†	*V*	−1	III		
5807.30		−2			
5813.97†	*Ti*	0	(III A)	1.062	$a^3P_2 - y^5D^\circ_3$
5839.53†		−1			
5839.77†		−1			
5848.03		−2			
5852.34	*Ti*?	0			
5879.79	*Zr*	1	II	0.153	$a^3F_4 - z^3D^\circ_3$
5915.55†	*Co*	0	III	2.127	$a^2G_{3\frac{1}{2}} - y^2G^\circ_{3\frac{1}{2}}$
5944.68†	*Ti*	2		0.000	$a^3F_2 - z^5F^\circ_1$
5955.16		−1			
5962.53		−1			
5978.13		−2			
5980.93	*Ti*?	0N	(III A)	1.062	$a^3P_2 - y^3D^\circ_1$
5982.53		0			
5999.05		0			
6002.31†	*V*	1	II A	1.213	$a^4P_{2\frac{1}{2}} - y^4D^\circ_{3\frac{1}{2}}$
6007.69		−1Bd?			
6012.99?		−2N			
6017.00		−1			
6017.56		−2			
6017.93	*V*	−2	III A	1.190	$a^4P_{1\frac{1}{2}} - y^4D^\circ_{1\frac{1}{2}}$
6018.41†	*Ti*	0		2.144	$a^3D_1 - v^3F^\circ_2$
6018.66†	*Ti*	1		1.048	$a^3P_1 - z^5S^\circ_2$
6023.42†	*V*	0	I A	0.000	$a^2D_{1\frac{1}{2}} - z^4D^\circ_{1\frac{1}{2}}$
6025.44	*V*	−1	III A		
6030.69†		0N			
6032.61	*Zr*?	−1	IV?	1.476	$b^3F_3 - w^3F^\circ_4$
6057.08		−2			
6058.77	*Ti*	0	Pred	1.062	$a^3P_2 - z^5S^\circ_2$
6063.14		−1			
6077.38		−2			
6082.55		−2			
6087.50	*V*	−2	III A	1.046	$a^4D_{1\frac{1}{2}} - y^6F^\circ_{2\frac{1}{2}}$

TABLE IV—*Continued*

λ I.A.	Ident.	Int. Spot	T.C.	E.P.	Multiplet Designation
6097.47	*V*	−2	.....	1.076	$a^4D_{3\frac{1}{2}}-y^6F^\circ_{4\frac{1}{2}}$
6106.79?	.....	−2	.....	.....	.....
6106.99†	*V*	0	III A	.....	.....
6107.27	.....	−1	.....	.....	.....
6124.83†	*−Zr*	0	III?	0.518	$a^3P_0-z^3P^\circ_1$
6128.34†	*V*	−1	III A	1.046	$a^4D_{1\frac{1}{2}}-y^6F^\circ_{\frac{1}{2}}$
6134.57	*Zr*	3	II	0.000	$a^3F_2-z^3F^\circ_2$
6134.72	.....	−2	.....	.....	.....
6138.44†	*V* / *Ti*?	1	I A IV	0.065 2.144	$a^2D_{2\frac{1}{2}}-z^4D^\circ_{3\frac{1}{2}}$ $a^3D_1-w^3F^\circ_2$
6140.47†	*Zr*	0	II	0.517	$a^3P_2-z^3P^\circ_2$
6163.50?	.....	1?Bd?	.....	.....	.....
6170.34	*V*	3	I A	0.285	$a^6D_{3\frac{1}{2}}-z^6F^\circ_{4\frac{1}{2}}$
6175.12	.....	−1	.....	.....	.....
6186.15	*Ti*	2	III	2.165	$a^3D_3-w^3F^\circ_4$
6191.75†	*Y*	3	I A	0.000	$a^2D_{1\frac{1}{2}}-z^2D^\circ_{1\frac{1}{2}}$
6192.96	*Zr*	−1N	III?	0.540	$a^3P_1-z^3P^\circ_1$
6193.70	*Sc*	0	II A	0.000	$a^2D_{1\frac{1}{2}}-z^4D^\circ_{2\frac{1}{2}}$
6205.24	.....	1	.....	.....	.....
6213.13	*Zr*?−	−1	IV?	0.540	$a^3P_1-z^3P^\circ_2$
6214.51?	.....	−2	.....	.....	.....
6215.23†	*Ti*	2	III	2.684	$z^3G^\circ_5-e^3F_4$
6221.73	*Fe*	−1	.....	0.855	$a^5F_5-z^7F^\circ_4$
6222.62	*Y*	0	I A	0.000	$a^2D_{1\frac{1}{2}}-z^2D^\circ_{2\frac{1}{2}}$
6230.86	.....	2	.....	.....	.....
6241.32?	.....	−2	.....	.....	.....
6249.92	.....	−2N	.....	.....	.....
6257.64	*Ti*	−2?	[III A]	0.000	$a^3F_2-z^5G^\circ_3$
6257.82†	.....	1	.....	.....	.....
6261.24	*V*	1	II A	0.266	$a^6D_{1\frac{1}{2}}-z^6F^\circ_{\frac{1}{2}}$
6268.54	*Ti*	1	Pred	1.424	$b^3F_2-x^3D^\circ_1$
6273.40†	*Ti*	1	[II A]	0.020	$a^3F_3-z^5G^\circ_4$
6276.33	*Sc*	1	II A	0.021	$a^2D_{2\frac{1}{2}}-z^2D^\circ_{1\frac{1}{2}}$
6285.43	.....	−2	.....	.....	.....
6295.29†	*Ti**	−1	[III A]	0.048 1.741	$a^3F_4-z^5G^\circ_5$ $a^5P_3-x^5D^\circ_3$
6296.67†	*Ti*	3	[II A]	0.000	$a^3F_2-z^5G^\circ_2$
6306.05†	*Sc*	1	I A	0.021	$a^2D_{2\frac{1}{2}}-z^4D^\circ_{1\frac{1}{2}}$
6308.63	.....	−2	.....	.....	.....
6313.04	*Zr*	−1	V	1.577	$a^3G_5-z^3H^\circ_6$
6339.93	.....	−2N	.....	.....	.....
6342.27	.....	−2	.....	.....	.....
6344.83	*Sc*	0	II A	0.000	$a^2D_{1\frac{1}{2}}-z^4F^\circ_{2\frac{1}{2}}$
6349.49†	*V*	1	III	.....	.....
6357.30†	*V*	1	III	.....	.....
6359.92†	*Ti*	2	[II A]	0.048	$a^3F_4-z^5G^\circ_4$
6361.08	.....	−1	.....	.....	.....
6367.83	.....	−2N	.....	.....	.....
6367.93	.....	−1	.....	.....	.....
6370.62	.....	0Bd?	.....	.....	.....
6374.74	.....	1	.....	.....	.....
6378.86†	*Sc*	2	I A	0.000	$a^2D_{1\frac{1}{2}}-z^4F^\circ_{1\frac{1}{2}}$
6379.40	*V*?	2Bd?	III	.....	.....
6380.94	.....	−2	.....	.....	.....

TABLE IV—*Continued*

λ I.A.	Ident.	Int. Spot	T.C.	E.P.	Multiplet Designation
6381.45	.....	2Bd?	.....	.....	.....
6383.45	.....	−1	.....	.....	.....
6385.39	.....	0Bd?	.....	.....	.....
6386.81	.....	0Bd?	.....	.....	.....
6395.48	.....	0	.....	.....	.....
6401.96	−*Y*	−1	I A	0.065	$a^2D_{2\frac{1}{2}}-z^2D^\circ_{1\frac{1}{2}}$
6406.08	.....	−1Bd?	.....	.....	.....
6408.48†	*Sr*	−1	II	2.262	$4^3D_3-dp^3F^\circ_4$
6413.08?	*Ti*	−1	Pred	0.048	$a^3F_4-z^5G^\circ_3$
6413.33†	*Sc*	2	I A	0.021	$a^2D_{2\frac{1}{2}}-z^4F^\circ_{2\frac{1}{2}}$
6419.10†	*Ti*	0	.....	.....	.....
6430.51	*V*	−1	III	.....	.....
6431.65?	*V*?	−2	III A	.....	.....
6433.20	.....	−2	.....	.....	.....
6445.73?	*Zr*	−2	IV	0.995	$a^1G_4-y^3F^\circ_3$
6452.09	.....	−3?	.....	.....	.....
6467.84?	.....	−1	.....	.....	.....
6470.03	.....	−2	.....	.....	.....
6470.24	*Zr*	−2	IV	1.575	$a^3G_4-z^3H^\circ_5$
6497.70†	*Ti*	2	III A	1.437	$b^3F_3-x^3F^\circ_4$
6504.01†	*Sr*	−1	II	2.249	$4^3D_2-dp^3F^\circ_3$
6506.40	*Zr*	−2	IV?	0.630	$a^1D_2-z^3P^\circ_2$
6527.31	.....	−2	.....	.....	.....
6536.48	*Ti*?	−1Bd?	.....	.....	.....
6543.52†	*V*	0	III A	1.190	$a^4P_{1\frac{1}{2}}-z^4P^\circ_{1\frac{1}{2}}$
6548.35	*Ti*?	−1	.....	.....	.....
6550.27	*Sr*	−1	III?	2.679	$5^1P^\circ_1-p^{2\,1}D_2$
6557.38	*Y*	−1	I A	0.000	$a^2D_{1\frac{1}{2}}-z^4F^\circ_{2\frac{1}{2}}$
6558.04	*V*?	0N	III A	.....	.....
6563.42†	*Co*	0	II	2.032	$a^2G_{4\frac{1}{2}}-z^2G^\circ_{4\frac{1}{2}}$
6575.19	*Ti*	−1	V	2.567	$a^1H_5-y^1G^\circ_4$
6576.60	.....	−2	.....	.....	.....
6578.97	*V*	−2	III A	.....	.....
6579.09?	.....	−2?	.....	.....	.....
6580.93	*Cr*	−1	.....	1.026	$a^5D_4-z^7P^\circ_4$
6601.45?	.....	−2	.....	.....	.....
6607.90	.....	−1	.....	.....	.....
6617.28†	*Sr*	−2	III?	2.242	$4^3D_1-dp^3F^\circ_2$
6621.12‡†	.....	2	.....	.....	.....
6624.78†	.....	0	.....	.....	.....
6637.23†	.....	0	.....	.....	.....
6649.48†	.....	0	.....	.....	.....
6665.48†	.....	0	.....	.....	.....
6707.77†	*Li*	2N	.....	0.000	$2^2S_{\frac{1}{2}}-2^2P^\circ_{1\frac{1}{2}}$
6707.94	*Li*	1N	.....	0.000	$2^2S_{\frac{1}{2}}-2^2P^\circ_{\frac{1}{2}}$
7800.29†	*Rb*	1	.....	0.000	$5^2S_{\frac{1}{2}}-5^2P^\circ_{1\frac{1}{2}}$
7947.63†	*Rb*	0	.....	0.000	$5^2S_{\frac{1}{2}}-5^2P^\circ_{\frac{1}{2}}$

temperature classes in the fourth column are by A. S. King, except when in parentheses or brackets, the latter being used for a few lines of *Ti* observed in the furnace spectrum. "Pred" indicates a line not observed in the laboratory but identified from its predicted position obtained from the multiplet. The fifth column gives the excitation potential. This quantity is the energy, expressed in volts, required to raise an atom from the lowest energy state to that in which it can absorb the line, one volt corresponding to 8100 wave-number units *in vacuo*. The multiplet designation appears in the last column. For example, the *Ti* line at λ 4007.20 has the designation $z^5F^\circ_2 - e^5H_3$. The superscripts denote the multiplicity of the terms involved in the production of the line, both quintets in this instance. The subscripts give the inner-quantum numbers of the two respective levels. The symbol (°) indicates the term belonging to the odd set; "z" shows that the low term involved is the lowest odd term of the ^{5}F-type; and "e," that the high term is the lowest high even term of the ^{5}H-type. "F" and "H" indicate the values of the Hund quantum number *L*.

The new spot lines can in general be identified as the fainter members of multiplets of those elements which are greatly strengthened in the spot spectrum. Among them are lines of *Li*, *Na*, *K*, *Sc*, *Ti*, *V*, *Cr*, *Mn*?, *Fe*, *Co*, *Rb*, *Sr*, *Y*, *Zr*, and *In*. Three of these elements, *Li*, *Rb*, and *In*, are identified in the sun by the presence of their lines in the spot spectrum alone. Some other interesting identifications may be cited. *V* is weak in the solar spectrum and strong in the spot spectrum. Therefore the fainter *V* lines occur only in the spot spectrum. With the exception of one line, $a^6D_{\frac{1}{2}} - y^6D^\circ_{\frac{1}{2}}$, all the lines of one strong multiplet of *V* are present in the spectra of both disk and spot. The calculated position of the exceptional line is λ 4116.62; but the nearest laboratory line is λ 4116.700, classified by King as 4 IA, which is present in both disk and spot spectra. A spot line has been measured at λ 4116.60, which undoubtedly is the faint *V* line. In another *V* multiplet the line $a^4P_{\frac{1}{2}} - y^4P^\circ_{1\frac{1}{2}}$ has been marked as masked by the strong *V* arc line at λ 4864.76 (40 I). The position calculated from the multiplet is λ 4864.82, and a spot line has been measured at λ 4864.85. Many such instances might be mentioned, but these suffice to show the importance of the new spot lines in

confirming solar identifications and in supplementing incomplete laboratory material. Of the 206 spot lines of known multiplet designation in Table IV, 129 are faint members of multiplets whose stronger lines appear in the spectrum of the disk.

TABLE V

NEW SOLAR LINES

λ I.A.	IDENT.	INTENSITY		T.C.	E.P.	MULTIPLET DESIGNATION
		Disk	Spot			
3917.36*	.....	0	0	.....	.....	.....
3939.29*	.....	−1N	−1N	.....	.....	.....
4036.26*	.....	−2	−2	.....	.....	.....
4113.98?	.....	−2	−2	.....	.....	.....
4114.09†	.....	0	0Bd?	.....	.....	.....
4114.14†	.....	0	0Bd?	.....	.....	.....
4121.06*	.....	−1	−1	.....	.....	.....
4146.24*‡	$\left\{\begin{matrix}Ce^{+}\\Cr\end{matrix}\right\}$	0	1d	$\left\{\begin{matrix}\text{IV}\\\text{IV}\end{matrix}\right\}$	.....	.....
4236.78	.....	0N	0N	.....	.....	.....
4326.97	*Ti*	0?	1	III A	0.809	$a^5F_1 - w^3D^\circ_1$
4372.41	*Ti*	0Bl	1Bl	IV	2.477	$a^1P_1 - v^1P^\circ_1$
4402.85*	.....	−1	−1Bd?	.....	.....	.....
4428.52	$\left\{\begin{matrix}V\\Cr\end{matrix}\right\}$	0?	2	$\left\{\begin{matrix}\text{I}\\\text{III}\end{matrix}\right.$	0.266 3.001	$a^6D_{1\frac{1}{2}} - z^6P^\circ_{2\frac{1}{2}}$ $b^5D_3 - u^5P^\circ_3$
4431.04*	.....	−1	−1	.....	.....	.....
4686.87§	*Ti*	−1d?	0	IV?	2.144	$a^3D_1 - t^3D^\circ_2$
4686.96§	*V*		0	?	.....	.....
4763.89‖	Ti^{+}	2	2	V	.....	.....
4763.93‖	*Ni*	2	2	III	3.639	$z^3F^\circ_4 - f^3F_4$
4776.32	−*Co*	−1?	1	III	3.283	$z^6G^\circ_{1\frac{1}{2}} - e^6F_{\frac{1}{2}}$
5220.300R*	−*Ni*?	0	0	V	3.724	$z^5F^\circ_2 - e^3F_3$
5258.84	.....	−2N	0b	.....	.....	.....

* Error of 0.1 A in Rowland wave-length suspected.

† One line measured by Rowland at λ 4114.120; intensity, −1d.

‡ Band line on violet side.

§ One line measured by Rowland at λ 4686.942.

‖ One line measured by Rowland at λ 4763.921; intensity, 4d.

During the investigation 21 new solar lines have been measured. These are listed in Table V, arranged similarly to Table IV, except that a column containing the intensities of the lines in the disk spectrum has been added. In two cases lines noted as double by Rowland have been resolved. For 8 lines, Rowland's wave-length appears to be in error by ±0.1 A. These are marked with an asterisk in the table.

Predicted lines in the solar spectrum.—The use of calculated wave-lengths for identification purposes is particularly applicable to elements such as *Fe*, for which practically every observed laboratory line is present in the solar spectrum. If the spectrum of an element has been analyzed, the spectral terms are known. By selecting the combinations permitted by the quantum rules, a calculated position for every classified line and also predicted positions for lines not yet detected in the laboratory can be determined from the term values. Many of these predicted wave-lengths are found among the solar lines. In 1928[1] several faint solar lines were identified as *Fe* and Cr^+ by this method, and a number of the predicted *Fe* lines were measured on an arc plate of long exposure on which fairly good standards could nevertheless be obtained. The tabulated multiplet of *Fe* will illustrate the procedure:

	$z^3F^\circ_4$ 31307.277	z^3F_3 31805.100	$z^3F^\circ_2$ 32134.020
e^3D_3 51294.262	5001.864 12V	5129.63 (1)	5217.677 (−3N)
	19986.988	19489.17	19160.301
	6.985	9.162	0.242
e^3D_2 51739.964		5014.942 10V	5099.07 (1)
		19934.866	19605.97
		4.864	5.944
e^3D_1 52039.939			5022.235 6V
			19905.919
			5.919

The values of the lower and higher terms, z^3F° and e^3D, respectively, appear at the top and on the left. The observed wave-length, intensity, and temperature class, and the observed and calculated wave-numbers for each permitted transition are given below. For example, the observed line λ 5001.864 is of intensity 12 and temperature class V. Its wave-number *in vacuo* is 19986.988, and the calculated wave-number, $z^3F^\circ_4 - e^3D_3$, is 19986.985. The combination $z^3F^\circ_2 - e^3D_3$, calculated wave-number 19160.242, gives a predicted line at λ 5217.692. This line has not been observed in the laboratory, but the solar line λ 5217.677, intensity −3N, may be identified as

[1] Moore and Russell, *Mt. Wilson Contr.*, No. 365; *Astrophysical Journal*, **68**, 151, 1928; Dunham and Moore, *Mt. Wilson Contr.*, No. 360; *Astrophysical Journal*, **68**, 37, 1928.

predicted *Fe*, because the coincidence in wave-length is good and all the observed lines of the group are present in the solar spectrum.

Multiplets of the spectra of 13 elements, Sc^+, *Ti*, Ti^+, *V*, V^+, *Cr*, Cr^+, *Mn*, *Fe*, Fe^+, *Co*, *Ni*, and Zr^+, have been examined in this way. The predicted lines found in the solar spectrum are distributed as tabulated:

El.	No.	El.	No.	El.	No.
Sc^+	7	*Cr*	122	*Co*	21
Ti	67	Cr^+	73	*Ni*	89
Ti^+	43	*Mn*	7	Zr^+	20
V	12	*Fe*	437		
V^+	9	Fe^+	50	Total	957

Table VI lists all the solar lines thus identified which have not previously been published at Mount Wilson. With the exception of a few lines of *Fe*, Fe^+, *Ti*, and Cr^+, the material in this table is new. *Fe* and Cr^+ lines for which the identifications differ from those published are included here. The solar wave-length from the *Revised Rowland* is in the first column. The second column contains the difference between the solar and predicted wave-length. For *Fe* this quantity is given to three decimal places for lines included in the list of Burns and Walters.[1] The disk and spot intensities are in the third and fourth columns. If underlined, the disk intensity differs from that in the *Revised Rowland*. Spot intensities marked "Bl" refer to two solar lines. "N" and "d," as usual, indicate diffuse and double lines, respectively. The last four columns give the excitation potential, the wave-number *in vacuo* of the solar line, the multiplet designation, and the suggested identification.

For *Fe*, a number of levels are verified by several combinations, but the types of the terms S, P, D, etc., have not yet been assigned. Provisionally they are designated by numbers, a symbol (°) being added to those of the odd set. Subscripts, as usual, denote the inner-quantum numbers and are given when known. The numbers assigned by Burns and Walters[1] have been retained, as have also their labels for the three low even levels $2M_4$, $3M_2$, and $4M_2$. For the

[1] *Publications of the Allegheny Observatory*, **6**, 159 (No. 11), 1929.

TABLE VI

PREDICTED LINES IN THE SOLAR SPECTRUM

SUN I.A.	Δλ O−C	INTENSITY		E.P.	WAVE NO. VAC.	MULTIPLET DESIGNATION	SUGGESTED SOLAR ID.
		Disk	Spot				
			Sc⁺				
3902.106.....	+0.02	0	0	0.314	25619.95	$a^1D_2 - z^3D^\circ_3$	*Cr Sc⁺*
3939.520.....	+ .01	−1	−1	0.314	25376.64	$a^1D_2 - z^3D^\circ_1$	*Sc⁺*
4008.424.....	+ .01	−2	−1Bl	0.603	24940.44	$a^3F_3 - z^3P^\circ_2$	*Sc⁺*
4008.604.....	+ .01	0	0	0.593	24939.31	$a^3F_2 - z^3P^\circ_1$	*Sc⁺−*
4716.143.....	+ .01	−3N	.....	0.603	21197.86	$a^3F_3 - z^1D^\circ_2$	*Sc⁺*
5854.324.....	+ .01	−2	.....	1.351	17076.67	$b^1D_2 - z^3D^\circ_2$	*Sc⁺*
6059.276.....	+0.03	−3	.....	1.351	16499.07	$b^1D_2 - z^3F^\circ_2$	*Sc⁺?*
			Ti				
3056.796.....	−0.01	1	.....	2.398	32704.51	$z^3F^\circ_3 - f^1G_4$	*Fe⁺? Ti?*
3143.017.....	+ .02	1	.....	1.988	31807.37	$z^5G^\circ_4 - g^5H_4$	*OH? Ti?*
3143.157.....	.00	−1	.....	0.000	31805.96	$a^3F_2 - y^3P^\circ_2$	*Ti?*
3203.613.....	+ .03	−3	.....	0.000	31205.77	$a^3F_2 - v^3D^\circ_3$	*Ti?*
3245.279.....	− .01	−2N	.....	2.385	30805.13	$z^3F^\circ_2 - f^1D_2$	*Ti*
3431.073.....	− .01	−3	.....	1.496	29137.08	$a^1G_4 - u^3G^\circ_3$	*Ti?*
3555.618.....	− .03	−3	.....	2.239	28116.50	$a^3H_5 - u^1G^\circ_4$	*Ti?*
3582.332.....	+ .01	2	.....	0.000	27906.84	$a^3F_2 - y^1D^\circ_2$	*Ti−*
3613.606.....	+ .03	2	.....	0.000	27665.33	$a^3F_2 - z^5P^\circ_1$	*Ti−*
3665.851.....	− .01	−3	.....	1.960	27271.06	$z^5G^\circ_2 - g^5F_3$	*Ti?*
3674.924.....	.00	−3	.....	1.960	27203.73	$z^5G^\circ_2 - g^5F_2$	*Ti*
3679.113.....	− .03	−2N	.....	1.972	27172.76	$z^5G^\circ_3 - g^5F_3$	*Ti*
3687.761.....	− .03	−3	.....	2.398	27109.04	$z^3F^\circ_3 - h^3F_4$	*Ti*
3698.018.....	− .02	1N	.....	1.496	27033.85	$a^1G_4 - x^3H^\circ_5$	*−V? Ti?*
3794.090.....	+ .02	−2	.....	1.865	26349.33	$a^3G_3 - s^3F^\circ_3$	*CN? Ti?*
3886.157.....	+ .01	−1d	.....	2.650	25725.10	$z^3G^\circ_3 - i^3F_4$	*Ti?−*
3904.175.....	− .02	−2	.....	2.665	25606.38	$z^3G^\circ_4 - i^3F_4$	*Ti?*
3928.986.....	+ .01	−2N	.....	2.032	25444.68	$z^5G^\circ_6 - e^5G_5$	*Ti*
3975.693.....	− .02	−1d?	.....	2.094	25145.76	$z^5F^\circ_3 - g^3F_4$	*Ti?*
3980.823(1)*..	− .03	−2	−1	2.083	25113.36	$z^5F^\circ_2 - g^3F_3$	*Ti*
3985.604(1)...	+ .01	−1	0	2.083	25083.23	$z^5F^\circ_2 - e^5D_2$	*Ti−*
4013.241.....	− .01	−1	0	2.094	24910.50	$z^5F^\circ_3 - g^3F_2$	*Ti*
4021.091.....	− .02	−2	.....	2.094	24861.87	$z^5F^\circ_3 - e^5H_3$	*Ti*
4024.332.....	− .02	−2	.....	2.108	24841.85	$z^5F^\circ_4 - e^5H_4$	*Ti*
4047.191.....	+ .01	−1d?	.....	2.125	24701.54	$z^5F^\circ_5 - e^5H_4$	*Ti?*
4287.721.....	+ .01	−2	−1	0.815	23315.88	$a^5F_2 - x^3G^\circ_3$	*Ti*
4299.141.....	− .03	1	1?	0.822	23253.94	$a^5F_3 - x^3G^\circ_3$	*−Ti*
4326.224.....	− .01	−3	.....	1.988	23108.37	$z^5G^\circ_4 - f^5F_3$	*Ti*
4410.767.....	− .01	−3	.....	2.385	22665.45	$z^3F^\circ_2 - g^3F_3$	*Ti?*
4460.932.....	+ .02	−2N	.....	2.240	22410.57	$b^3P_2 - r^3D^\circ_1$	*Ti?*
4475.173.....	− .01	−3	−2	2.083	22339.26	$z^5F^\circ_2 - f^5F_3$	*Ti Cr*
4476.62.....	+ .01	.....	−2	2.076	22332.04	$z^5F^\circ_1 - f^5F_2$	*Ti*
4540.409.....	.00	−1	od?	2.324	22018.30	$c^3P_1 - x^3S^\circ_1$	*Ti*
4586.93.....	− .02	.....	−2	2.416	21794.99	$z^3F^\circ_4 - f^3G_4$	*Ti*
4594.50?.....	− .01	.....	−2	2.335	21759.08	$c^3P_{2'} - r^3D^\circ_2$	*Ti*
4599.010.....	+0.02	−1	−1	2.323	21737.74	$c^3P_0 - r^3D^\circ_1$	*Ti*

* Superior figures in first column refer to notes at the end of the table.

TABLE VI—*Continued*

Sun I.A.	Δλ O−C	Intensity		E.P.	Wave No. Vac.	Multiplet Designation	Suggested Solar Id.
		Disk	Spot				
			Ti—continued				
4679.73.....	0.00	.....	0	1.048	21362.79	$a^3P_1 - x^5D^\circ_1$	*Ti*
4692.45.....	.00	.....	0	1.062	21304.89	$a^3P_2 - x^5D^\circ_2$	*Ti*
4797.629.....	+ .02	−3	−2NBl	0.822	20837.82	$a^5F_3 - y^3G^\circ_3$	*Ti*
4837.402.....	− .02	−3	−2	2.282	20666.50	$z^5D^\circ_1 - f^5F_2$	*Ti*
4842.590.....	+ .01	−3	.....	2.279	20644.36	$z^5D^\circ_0 - f^5F_1$	*Ti*
4854.76(1)....	+ .02	.....	−1	2.230	20592.60	$b^3P_1 - t^3D^\circ_1$	*Ti*
4863.75.....	.00	.....	−1	2.240	20554.55	$b^3P_2 - t^3D^\circ_2$	*Ti*
4900.02?.....	− .01	.....	−2?	2.650	20402.40	$z^3G^\circ_3 - g^3F_2$	*Ti*
4953.361.....	− .01	.....	−2	0.845	20182.70	$a^5F_5 - x^3F^\circ_4$	*Ti*
4997.964.....	.00	−2N	−2	4.155	20002.58	$z^1P^\circ_1 - e^1P_1$	*Ti?*
5001.212.....	− .01	−3	.....	2.144	19989.59	$a^3D_1 - y^5S^\circ_2$	*Ti*
5081.360.....	− .01	−3N	.....	1.424	19674.30	$b^3F_2 - v^3D^\circ_3$	*Ti*
5093.050.....	+ .01	−3	.....	2.684	19629.14	$z^3G^\circ_5 - f^3G_4$	*Ti?*
5382.921.....	+ .02	.....	−2	1.865	18572.13	$a^3G_3 - w^3F^\circ_3$	*Ti*
5391.071.....	.00	−3	−2	1.871	18544.05	$a^3G_4 - w^3F^\circ_4$	*Ti*
5394.207.....	− .01	−3	.....	2.324	18533.27	$c^3P_1 - y^5S^\circ_2$	*Ti?*
5440.503.....	− .03	−3	−1	1.424	18375.56	$b^3F_2 - x^5D^\circ_2$	*Ti*
5470.48.....	+ .02	.....	−1	1.437	18274.87	$b^3F_3 - x^3G^\circ_3$	*Ti*
5494.709(1)...	− .01	−2	−1Bd?	1.454	18194.28	$b^3F_4 - x^3G^\circ_4$	*Ti*
5497.902.....	+ .01	−2	.....	0.896	18183.72	$a^1D_2 - y^3D^\circ_2$	*Ti?*
5518.099.....	− .02	−2	−1	2.398	18117.16	$z^3F^\circ_3 - e^3F_2$	*Ti*
5734.360.....	+ .03	−3N	.....	2.287	17433.91	$z^5D^\circ_2 - e^5F_1$	*Ti?*
5739.064.....	− .01	−2	−1N	2.295	17419.62	$z^5D^\circ_3 - e^5F_2$	*Ti*
5774.550.....	+ .01	−3N	.....	2.239	17312.58	$a^3H_5 - y^3H^\circ_4$	*Ti?*
6018.41(1)....	− .02	.....	0	2.144	16611.10	$a^3D_1 - v^3F^\circ_2$	*Ti*
6058.77.....	+ .01	.....	0	1.062	16500.44	$a^3P_2 - z^5S^\circ_2$	*Ti*
6268.54.....	+ .02	.....	1	1.424	15948.28	$b^3F_2 - x^3D^\circ_3$	*Ti*
6413.08?.....	− .05	.....	−1	0.048	15588.83	$a^3F_4 - z^5G^\circ_3$	*Ti*
6921.599.....	+ .02	−3	.....	3.554	14443.55	$y^5F^\circ_4 - g^5F_4$	*Atm? Ti?*
6922.304.....	+ .01	−3	.....	3.535	14442.08	$y^5F^\circ_2 - g^5F_2$	*Atm Ti?*
7084.268.....	+0.02	−3	.....	1.424	14111.90	$b^3F_2 - y^3D^\circ_3$	*Ti?*
			Ti+				
3109.929.....	+0.01	−1	.....	1.216	32145.78	$a^2P_{½} - z^4P^\circ_{½}$	*Ti+*
3140.017.....	− .02	−3	.....	1.079	31837.77	$a^2D_{2½} - y^4D^\circ_{2½}$	*Ti+?*
3205.654.....	+ .01	−2	.....	1.160	31185.90	$a^4P_{1½} - y^4D^\circ_{2½}$	*Ti+−Zr+*
3212.691.....	− .01	−1	.....	0.112	31117.60	$b^4F_{1½} - z^2D^\circ_{2½}$	*Ti+*
3218.451.....	+ .02	−2	.....	1.156	31061.91	$a^4P_{½} - y^4D^\circ_{1½}$	*Ti+*
3221.761.....	+ .01	−3	.....	1.160	31029.99	$a^4P_{1½} - y^4D^\circ_{1½}$	*Ti+*
3228.388.....	+ .03	−2	.....	1.156	30966.30	$a^4P_{½} - y^4D^\circ_{½}$	*Ti+*
3283.162.....	+ .02	−1	.....	1.232	30449.70	$a^2P_{1½} - y^4D^\circ_{1½}$	*Ti+*
3293.479.....	.00	−1	.....	1.232	30354.32	$a^2P_{1½} - y^4D^\circ_{½}$	*Ti+*
3323.396.....	.00	1	.....	1.160	30081.08	$a^4P_{1½} - y^2D^\circ_{2½}$	*Ti+*
3360.125.....	− .03	0	.....	1.216	29752.28	$a^2P_{½} - z^2P^\circ_{1½}$	*NH−Ti+*
3383.574.....	+ .01	0	.....	1.226	29546.09	$b^4P_{1½} - y^2D^\circ_{2½}$	*Ti+?−*
3549.243.....	− .02	1	.....	3.081	28167.01	$c^2D_{1½} - x^2P^\circ_{1½}$	*−Ti+?*
3613.333.....	+0.03	−3	.....	1.575	27667.42	$b^2D_{2½} - y^4D^\circ_{1½}$	*Ti+?*

TABLE VI—*Continued*

Sun I.A.	Δλ O−C	Intensity		E.P.	Wave No. Vac.	Multiplet Designation	Suggested Solar Id.
		Disk	Spot				
			Ti⁺—continued				
3634.006.....	+0.01	−3N	.....	3.081	27510.03	$c^2D_{1\frac{1}{2}}-x^4D^\circ_{2\frac{1}{2}}$	*Ti⁺?*
3635.353.....	.00	−1	.....	1.226	27499.83	$b^4P_{1\frac{1}{2}}-z^2S^\circ_{\frac{1}{2}}$	*Ti⁺ Cr?*
3635.653.....	+ .01	−2N	.....	3.081	27497.57	$c^2D_{1\frac{1}{2}}-x^4D^\circ_{1\frac{1}{2}}$	*Ti⁺?*
3664.829.....	− .03	−2N	.....	3.110	27278.66	$c^2D_{2\frac{1}{2}}-x^4D^\circ_{2\frac{1}{2}}$	*−Ti⁺?*
3679.686(2)...	+ .02	2	.....	1.575	27168.52	$b^2D_{2\frac{1}{2}}-y^2F^\circ_{2\frac{1}{2}}$	*Ti⁺*
3786.331.....	.00	1	.....	0.605	26403.32	$a^2F_{3\frac{1}{2}}-z^4F^\circ_{4\frac{1}{2}}$	*Ti⁺*
4174.082(3, 4).	.00	0	0	2.586	23950.64	$b^2F_{2\frac{1}{2}}-x^2D^\circ_{2\frac{1}{2}}$	*Ti⁺*
4423.271(4)...	+ .05	0N	1d?	1.226	22601.38	$b^4P_{1\frac{1}{2}}-z^4D^\circ_{\frac{1}{2}}$	*Ti⁺?−Cr?*
4427.923(4)...	+ .03	−1N	−1	1.238	22577.63	$b^4P_{2\frac{1}{2}}-z^4D^\circ_{1\frac{1}{2}}$	*Ti⁺*
4441.721(4, 5).	− .01	3Nd?	5N	1.175	22507.50	$a^4P_{2\frac{1}{2}}-z^2D^\circ_{2\frac{1}{2}}$	*V−Ti⁺*
4482.441(4)...	+ .04	−3	.....	1.111	22303.03	$a^2G_{3\frac{1}{2}}-z^4F^\circ_{4\frac{1}{2}}$	*Ti⁺*
4495.428(4)...	− .03	0N	0	1.175	22238.60	$a^4P_{2\frac{1}{2}}-z^2D^\circ_{1\frac{1}{2}}$	*Fe−Zr⁺ Ti⁺*
4506.743(4)...	.00	−1	ob	1.126	22182.77	$a^2G_{4\frac{1}{2}}-z^4F^\circ_{4\frac{1}{2}}$	*Ti⁺*
4520.401(4)...	+ .03	−2	.....	1.111	21115.75	$a^2G_{3\frac{1}{2}}-z^4F^\circ_{3\frac{1}{2}}$	*Ti⁺*
4525.247.....	+ .04	−2	.....	1.079	22092.07	$a^2D_{2\frac{1}{2}}-z^4F^\circ_{1\frac{1}{2}}$	*Ti⁺?*
4552.291(4)...	+ .04	0	0	1.111	21960.83	$a^2G_{3\frac{1}{2}}-z^4F^\circ_{3\frac{1}{2}}$	*Ti⁺*
4609.273(4)...	+ .01	0	ob	1.175	21689.34	$a^4P_{2\frac{1}{2}}-z^2F^\circ_{2\frac{1}{2}}$	*Ti⁺−*
4662.759(4)...	+ .05	−1N	−1N	1.160	21440.55	$a^4P_{1\frac{1}{2}}-z^4F^\circ_{1\frac{1}{2}}$	*Ti⁺−*
4732.950.....	− .01	−3	.....	1.126	21122.58	$a^2G_{4\frac{1}{2}}-z^4G^\circ_{5\frac{1}{2}}$	*Ti⁺?*
4794.840.....	.00	−3	.....	1.126	20849.94	$a^2G_{4\frac{1}{2}}-z^4G^\circ_{4\frac{1}{2}}$	*Ti⁺?*
4806.340(4)...	+ .01	−2	−2	1.079	20800.06	$a^2D_{2\frac{1}{2}}-z^4G^\circ_{2\frac{1}{2}}$	*Ti⁺*
4821.008(4)...	.00	−2	.....	1.111	20736.77	$a^2G_{3\frac{1}{2}}-z^4G^\circ_{3\frac{1}{2}}$	*Ti⁺*
4849.174(4)...	− .01	0	−1	1.126	20616.33	$a^2G_{4\frac{1}{2}}-z^4G^\circ_{3\frac{1}{2}}$	*−Ti⁺*
4981.378(4)...	.00	−2	.....	1.559	20069.18	$b^2D_{1\frac{1}{2}}-z^4D^\circ_{2\frac{1}{2}}$	*Ti⁺*
5005.172(4)...	− .01	−1	od?	1.559	19973.78	$b^2D_{1\frac{1}{2}}-z^4D^\circ_{1\frac{1}{2}}$	*−Ti⁺*
5037.809.....	− .01	−2	.....	1.575	19844.38	$b^2D_{2\frac{1}{2}}-z^4D^\circ_{1\frac{1}{2}}$	*C₂? Ti⁺?*
5131.311(4)...	+ .03	−2	.....	1.885	19482.78	$b^2G_{3\frac{1}{2}}-z^2G^\circ_{4\frac{1}{2}}$	*Ti⁺*
5227.886.....	+ .02	−3	.....	2.586	19122.88	$b^2F_{2\frac{1}{2}}-y^2F^\circ_{3\frac{1}{2}}$	*Ti⁺*
6606.988(6)...	−0.03	−1N	ob	2.052	15131.32	$b^2P_{1\frac{1}{2}}-z^2D^\circ_{1\frac{1}{2}}$	*Ti⁺*
			V				
3820.305.....	0.00	0N	.....	1.059	26168.52	$a^4D_{2\frac{1}{2}}-w^4D^\circ_{3\frac{1}{2}}$	*V−*
3906.965.....	+ .02	1	1	1.190	25588.09	$a^4P_{1\frac{1}{2}}-v^4D^\circ_{2\frac{1}{2}}$	*V−*
3912.089.....	.00	0N	0N	1.213	25554.58	$a^4P_{2\frac{1}{2}}-v^4D^\circ_{3\frac{1}{2}}$	*−V*
3913.146.....	− .01	−2N	.....	1.178	25547.68	$a^4P_{\frac{1}{2}}-v^4D^\circ_{1\frac{1}{2}}$	*V?*
3925.354.....	+ .03	−2	.....	1.178	25468.22	$a^4P_{\frac{1}{2}}-v^4D^\circ_{\frac{1}{2}}$	*V?*
3927.346.....	− .02	−1	.....	1.190	25455.31	$a^4P_{1\frac{1}{2}}-v^4D^\circ_{1\frac{1}{2}}$	*V?*
3939.597.....	− .02	−1	.....	1.190	25376.15	$a^4P_{1\frac{1}{2}}-v^4D^\circ_{\frac{1}{2}}$	*Tb⁺?−V?*
4116.60.....	− .03	.....	0	0.261	24285.06	$a^6D_{\frac{1}{2}}-y^6D^\circ_{\frac{1}{2}}$	*V*
4158.379.....	+ .03	0	1d	0.285	24041.08	$a^6D_{3\frac{1}{2}}-y^4D^\circ_{2\frac{1}{2}}$	*CN V?*
4864.85.....	+ .03	.....	−1	1.178	20549.90	$a^4P_{\frac{1}{2}}-y^4P^\circ_{1\frac{1}{2}}$	*V*
5560.56.....	+ .01	.....	−2	0.040	17978.82	$a^4F_{3\frac{1}{2}}-z^6D^\circ_{3\frac{1}{2}}$	*V*
6090.515.....	−0.04	−3N	−2	1.059	16414.44	$a^4D_{2\frac{1}{2}}-y^6F^\circ_{3\frac{1}{2}}$	*V*

TABLE VI—*Continued*

Sun I.A.	Δλ O−C	Intensity		E.P.	Wave No. Vac.	Multiplet Designation	Suggested Solar Id.
		Disk	Spot				
			Pred V^+				
3126.768	0.00	1	.....	2.504	31972.67	$a^3H_5 - y^3H^\circ_6$	V^+—
3535.159	− .03	−3N	.....	1.067	28279.22	$a^3F_2 - z^3D^\circ_3$	V^+
3943.484	.00	1	1	1.470	25351.14	$a^3P_2 - z^5D^\circ_1$	V^+—
4051.056	+ .02	−1N	ob?	1.797	24677.97	$a^3G_4 - z^3G^\circ_3$	V^+
4150.102	− .01	−1N	.....	2.017	24089.02	$b^3G_3 - z^3F^\circ_4$	$-V^+$
4290.711	− .03	−2	.....	1.696	23299.63	$a^5P_3 - y^3D^\circ_2$	V^+
4310.706	− .03	2N	3d?	2.027	23191.56	$b^3G_4 - z^3G^\circ_5$	*CH* V^+?
4334.806	+ .01	0	1	2.017	23062.62	$b^3G_3 - z^3G^\circ_4$	V^+?—*Ti*
4382.319	+0.01	−2N	−2N	2.027	22812.58	$b^3G_4 - z^3G^\circ_3$	V^+?
			Cr				
3049.898	+0.01	−2N	.....	1.026	32778.48	$a^5D_4 - y^5F^\circ_3$	*Cr*
3071.436	.00	−1	.....	2.533	32548.64	$a^5G_3 - s^5F^\circ_3$	*Cr*?
3071.678	− .01	0	.....	2.534	32546.06	$a^5G_4 - s^5F^\circ_3$	*Cr*
3196.341	− .03	−2	.....	2.696	31276.76	$a^5P_3 - s^5F^\circ_4$	*Cr*
3201.263(7)	+ .02	−1	.....	2.696	31228.67	$a^5P_3 - s^5F^\circ_3$	*Cr*
3201.958	− .01	−2	.....	2.697	31221.89	$a^5P_2 - s^5F^\circ_3$	*Cr*
3204.574	− .01	−3	.....	2.696	31196.41	$a^5P_3 - s^5F^\circ_2$	*Cr*
3205.334	+ .03	−1	.....	2.697	31189.01	$a^5P_2 - s^5F^\circ_2$	*Cr*
3209.675	+ .02	−2	.....	3.001	31146.83	$b^5D_3 - w^3D^\circ_3$	*Cr*
3238.898	.00	−1N	.....	2.999	30865.82	$b^5D_1 - w^3D^\circ_2$	*Cr*?
3240.709	− .01	1	.....	3.001	30848.59	$b^5D_3 - w^3D^\circ_2$	Ti^+ *Cr*?
3259.600	− .03 + .01	0	.....	0.979 2.999	30669.79	$a^5D_2 - z^3D^\circ_1$ $b^5D_1 - w^3D^\circ_2$	*Cr*
3306.169	− .03	−3	.....	2.974	30237.81	$a^3P_2 - r^5F^\circ_3$	*Cr*
3320.493	+ .02	−3	.....	2.974	30107.38	$a^3P_2 - r^5F^\circ_1$	*Cr*?
3388.859	− .02 − .01	−1	.....	2.998 2.903	29500.02	$b^5D_4 - s^5D^\circ_4$ $a^3P_1 - s^5F^\circ_1$	*Cr*
3407.806	+ .03	0	.....	3.001	29336.00	$b^5D_3 - s^5D^\circ_3$	*Cr*
3411.569	− .02	−3	.....	3.000	29303.64	$b^5D_2 - s^5D^\circ_2$	*Cr*
3412.031	− .02	−3	.....	3.001	29299.68	$b^5D_3 - s^5D^\circ_2$	*Cr*?
3449.989	− .01	−2d?	.....	2.974	28977.32	$a^3P_2 - s^5F^\circ_3$	*Cr*
3453.849	− .03	−3N	.....	2.974	28944.93	$a^3P_2 - s^5F^\circ_2$	*Cr*
3470.741	+ .01	−1	.....	2.698	28804.08	$a^5P_1 - u^5D^\circ_0$	*Cr*
3475.320	− .04	−1	.....	3.001	28766.12	$b^5D_3 - s^5F^\circ_3$	$-Cr$
3541.546	.00	−2	.....	3.361	28228.21	$b^3P_2 - w^3D^\circ_3$	*Cr*
3598.613	.00	−3	.....	3.355	27780.58	$b^3P_1 - w^3D^\circ_1$	*Cr*
3604.934	− .02	−2	.....	2.698	27731.87	$a^5P_1 - t^5P^\circ_1$	*Cr*
3607.252	+ .01	−3	.....	2.999	27714.06	$b^5D_1 - t^5D^\circ_0$	*Cr*?
3608.590	+ .01	−1N	.....	3.000	27703.78	$b^5D_2 - t^5D^\circ_1$	*Cr*?—
3635.353	− .02	−1	.....	2.859	27499.83	$a^3P_0 - u^5D^\circ_1$	Ti^+ *Cr*?
3641.033	+ .04	1	.....	2.531	27456.93	$a^5G_2 - u^5F^\circ_3$	*Cr*—
3655.942	+ .02	−3N	.....	2.533	27344.97	$a^5G_3 - v^5D^\circ_4$	*Cr*
3662.365	− .03	−3	.....	2.531	27297.01	$a^5G_2 - v^5D^\circ_3$	*Cr*
3686.189	+ .02	−3	.....	2.534	27120.59	$a^5G_5 - v^5F^\circ_5$	*Cr*?
3833.704	− .01	0	.....	2.696	26077.06	$a^5P_3 - u^5F^\circ_2$	*Ti*—*Cr*
3847.434	− .03	−1	.....	2.998	25983.99	$b^5D_4 - x^3D^\circ_3$	*Cr*?
3876.312	0.00	0	.....	2.696	25790.43	$a^5P_3 - v^5F^\circ_2$	*Cr CN*

TABLE VI—*Continued*

Sun I.A.	Δλ O−C	Intensity		E.P.	Wave No. Vac.	Multiplet Designation	Suggested Solar Id.
		Disk	Spot				
			Cr—continued				
3877.346	−0.03	1	.....	2.697	25783.55	$a^5P_2 - v^5F^\circ_2$	*Cr CN*
3877.711	+ .01	−2	.....	2.697	25781.13	$a^5P_2 - v^5F^\circ_1$	*Cr*
3879.043	− .03	−1N	.....	2.698	25772.27	$a^5P_1 - v^5F^\circ_1$	*Cr?*
3886.942	.00	−1	.....	2.974	25719.89	$a^3P_2 - s^5P^\circ_2$	*Cr*
3914.956	+ .02	oN	oN	2.999	25535.86	$b^5D_1 - s^5P^\circ_2$	*Cr*
3975.959	− .02	−2	.....	2.532	25144.08	$a^5G_6 - z^5H^\circ_5$	*Cr*
4034.234	+ .02	1N	1	3.361	24780.87	$b^3P_2 - t^5D^\circ_1$	*Cr−*
4079.012	− .04	−1d?	−1	2.696	24508.85	$a^5P_3 - w^5D^\circ_2$	*Cr*
4086.134	− .02	o	o	2.859	24466.13	$a^3P_0 - v^5F^\circ_1$	*Ni Cr? Cr+?*
4088.852	− .01	−1	.....	2.697	24449.86	$a^5P_2 - w^5D^\circ_1$	*Cr?*
4118.430	− .02	−2	−1	2.903	24274.28	$a^3P_1 - v^5D^\circ_2$	*Cr?*
4129.962	.00	o	o	2.901	24206.50	$z^7P^\circ_4 - g^7D_4$	*Cr*
4130.454	− .01	o	o	2.901	24203.61	$z^7P^\circ_4 - g^7D_3$	*Cr*
4144.864	− .01	−1	.....	2.903	24119.46	$a^3P_1 - v^5F^\circ_2$	*Cr*
4163.123	− .03	−2d?	.....	2.533	24013.68	$a^5G_3 - y^5G^\circ_4$	*Cr?*
4240.202	+ .02	oN	o	3.000	23577.17	$b^5D_2 - u^5F^\circ_1$	*Cr−*
4246.420	+ .03	−2	.....	2.974	23542.66	$a^3P_2 - v^5F^\circ_3$	*Cr*
4247.122	.00	−1N	−1N	2.974	23538.76	$a^3P_2 - v^5F^\circ_2$	*Cr*
4251.336	− .03	od	1	2.859	23515.42	$a^3P_0 - w^5F^\circ_1$	*−Cr?*
4315.610	+ .04	−1N	−1	2.903	23165.20	$a^3P_1 - w^5F^\circ_2$	*Cr?−*
4362.955	+ .03	−1N	−1	2.859	22913.83	$a^3P_0 - y^3D^\circ_1$	*Cr*
4370.296	− .03	o	.....	2.974	22875.35	$a^3P_2 - u^5P^\circ_2$	*−Cr*
4406.045	+ .02	−1	−1	3.088	22689.74	$z^7F^\circ_1 - g^7D_2$	*Cr−*
4443.972	+ .03	−3	.....	3.112	22496.10	$z^7F^\circ_3 - g^7D_3$	*Cr?*
4459.363[8]	+ .01	1	2	2.696	22418.45	$a^5P_3 - w^5P^\circ_3$	*Cr*
4475.173	− .03	−3	−2	2.697	22339.27	$a^5P_2 - w^5P^\circ_2$	*Ti Cr*
4485.978	.00	o	−1	3.871	22285.45	$a^5F_2 - s^5D^\circ_3$	*Cr?−*
4493.381	− .02	−1	o	3.871	22248.74	$a^5F_2 - s^5D^\circ_2$	*−Cr*
4512.063	.00	−2	−2	3.154	22156.62	$z^7F^\circ_5 - g^7D_4$	*Cr?*
4518.589	− .01	o	od	2.534	22124.62	$a^5G_4 - x^5D^\circ_3$	*−Cr*
4530.110	− .01	−2N	.....	3.000	22068.36	$b^5D_2 - w^5D^\circ_3$	*Cr*
4536.509	− .03	−1	−1	3.307	22037.24	$z^5P^\circ_3 - e^5D_4$	*Cr*
4572.196	.00	−2	−1	3.308	21865.23	$z^5P^\circ_2 - e^5D_3$	*Cr*
4590.344	+ .03	−2	.....	3.875	21778.78	$a^5F_5 - s^5F^\circ_5$	*Cr?*
4593.830	+ .02	−1	−1	3.308	21762.26	$z^5P^\circ_2 - e^5D_2$	*Cr*
4595.054	+ .05	−2	−1	3.309	21756.46	$z^5P^\circ_1 - e^5D_2$	*Cr?−*
4804.650	+ .03	−2	−1	2.696	20807.37	$a^5P_3 - x^5D^\circ_3$	*Cr*
4828.718	+ .02	−3	−2	2.533	20703.66	$a^5G_3 - y^5F^\circ_4$	*Cr*
4832.550	+ .01	−3	.....	3.874	20687.25	$a^5F_4 - t^5D^\circ_4$	*Cr*
4838.829	+ .03	−3	.....	3.870	20660.41	$a^5F_1 - t^5D^\circ_2$	*Cr?*
4839.365	− .02	−3	.....	3.871	20658.12	$a^5F_2 - t^5D^\circ_2$	*Cr*
4841.499	− .02 − .01	−3	.....	3.872 3.871	20649.01	$a^5F_3 - t^5D^\circ_2$ $a^5F_2 - t^5D^\circ_1$	*Cr*
4841.675	+ .03	−2	−1?	3.870	20648.25	$a^5F_1 - t^5D^\circ_0$	*Cr Ni?*
4853.545	+ .02	−3	.....	2.696	20597.77	$a^5P_3 - x^5D^\circ_2$	*Cr*
4891.959	− .04	−3	.....	2.698	20436.02	$a^5P_1 - x^5D^\circ_1$	*Cr?*
4900.471	− .03	−3.	.....	3.370	20400.52	$z^7D^\circ_1 - g^7D_2$	*Cr*
4900.825	.00	−1	o	3.370	20399.05	$z^7D^\circ_1 - g^7D_1$	*−Cr*
4947.946	+0.03	−3	.....	3.395	20204.79	$z^7D^\circ_3 - g^7D_4$	*Cr*

TABLE VI—*Continued*

Sun I.A.	Δλ O−C	Intensity		E.P.	Wave No. Vac.	Multiplet Designation	Suggested Solar Id.
		Disk	Spot				
			Cr—continued				
4948.599	−0.04	−3N	.....	3.395	20202.12	$z^7D^\circ_3 - g^7D_3$	*Cr?*
4980.305	.00	−2	−2N	3.000	20073.51	$b^5D_2 - y^5G^\circ_3$	*Cr−*
4981.281	− .02	−3	.....	3.001	20069.58	$b^5D_3 - y^5G^\circ_3$	*Cr*
4983.605	− .02	−3	.....	3.413	20060.22	$z^7D^\circ_4 - g^7D_5$	*Cr*
5019.22	+ .02	.....	−1	0.964	19917.88	$a^5D_1 - y^7P^\circ_2$	*Cr*
5027.622	− .04	−3	.....	3.435	19884.59	$z^7D^\circ_5 - g^7D_5$	*Cr?*
5138.723	− .02	−2	0	0.979	19454.69	$a^5D_2 - z^7D^\circ_2$	*Cr?*
5182.353	.00	−3	.....	3.872	19290.90	$a^5F_3 - u^5D^\circ_2$	*Cr?*
5227.739	+ .02	−2	−1	2.697	19123.41	$a^5P_2 - y^5F^\circ_2$	*Cr?*
5292.809	+ .04	.....	−2	3.874	18888.32	$a^5F_4 - x^3D^\circ_3$	*Cr?*
5298.46	+ .02	.....	0	2.887	18868.19	$z^7P^\circ_3 - e^7D_2$	*Cr*
5460.885	− .03	−1	−1	2.998	18306.98	$b^5D_4 - z^5G^\circ_5$	*Cr*
5484.316	+ .01	−3	.....	2.999	18228.76	$b^5D_1 - z^5G^\circ_2$	*Cr?*
5488.346	+ .03	−3	.....	3.000	18215.38	$b^5D_2 - z^5G^\circ_2$	*Cr?*
5508.852	− .03	−3	.....	3.434	18147.58	$y^7P^\circ_3 - f^5S_2$	*Cr?*
5555.645	+ .02	−2	−1d	2.998	17994.73	$b^5D_4 - x^7P^\circ_4$	*C_2 Cr*
5562.285	− .02	−3	.....	3.001	17973.25	$b^5D_3 - x^7P^\circ_4$	*Cr*
5568.872	− .04	−1	0	3.000	17951.99	$b^5D_2 - x^7P^\circ_3$	*−Cr*
5569.326	.00	−3	.....	2.999	17950.52	$b^5D_1 - x^7P^\circ_2$	*Cr*
5580.456	− .03	−2	.....	3.423	17914.73	$y^7P^\circ_2 - f^7S_3$	*Cr*
5597.86	+ .02	.....	−1NBd?	3.823	17859.03	$z^5F^\circ_4 - e^5D_4$	*Cr V?*
5609.181	+ .04	−3	−2N?	3.434	17822.98	$y^7P^\circ_3 - f^7S_3$	*Cr*
5615.538	.00	0	0N?	3.809	17802.81	$z^5F^\circ_2 - e^5D_3$	*Cr−*
5792.100	− .03	−3	.....	0.957	17260.12	$a^5D_0 - z^7F^\circ_1$	*Atm? Cr?*
5797.55	+ .02	.....	−2	3.088	17243.89	$z^7F^\circ_1 - e^7D_2$	*Cr*
5798.009	+ .01	−2	.....	3.088	17242.53	$z^7F^\circ_1 - e^7D_1$	*Atm? Cr?*
5863.956	− .02	−2	.....	3.112	17048.63	$z^7F^\circ_3 - e^7D_2$	*Ni? Cr*
5916.028	+ .03	−2	−1	3.131	16898.56	$z^7F^\circ_4 - e^7D_4$	*Cr*
5916.772	+ .04	−2	−1	3.131	16896.44	$z^7F^\circ_4 - e^7D_3$	*Cr*
5920.334	.00	−3	.....	4.555	16886.27	$e^7S_3 - s^5D^\circ_4$	*Atm? Cr?*
5970.498	.00	−3	.....	4.555	16744.39	$e^7S_3 - s^5D^\circ_3$	*Cr?*
5981.869	− .03	−2	−1N?	3.154	16712.57	$z^7F^\circ_5 - e^7D_5$	*Cr*
5982.882	.00	−1	1	3.154	16709.73	$z^7F^\circ_5 - e^7D_4$	*Cr−*
6018.550	.00	−3	.....	3.872	16610.71	$a^5F_3 - u^5F^\circ_3$	*Cr?*
6025.216	− .03	−3	.....	3.875	16592.33	$a^5F_5 - u^5F^\circ_5$	*Cr*
6062.702	− .03	−2	1	3.181	16489.74	$z^7F^\circ_6 - e^7D_5$	*Cr*
6147.501	+ .01	−3	.....	3.874	16262.28	$a^5F_4 - v^5F^\circ_4$	*Cr?*
6449.445	− .02	−3N	.....	3.874	15500.94	$a^5F_4 - u^5P^\circ_3$	*Cr?*
6467.005	+0.04	−3	−1	0.979	15458.85	$a^5D_2 - z^7P^\circ_3$	*Cr*
			Cr^+				
3035.238	0.00	0	.....	3.091	32936.79	$b^4D_{1/2} - y^2P^\circ_{1\frac{1}{2}}$	*Cr^+*
3035.899	− .01	−1	.....	3.092	32929.62	$b^4D_{1\frac{1}{2}} - y^2P^\circ_{1\frac{1}{2}}$	*Cr^+*
3036.268	− .02 + .02	−1	.....	3.093 3.092	32925.61	$b^4D_{2\frac{1}{2}} - y^2P^\circ_{1\frac{1}{2}}$ $b^4D_{1\frac{1}{2}} - y^2P^\circ_{\frac{1}{2}}$	*Cr^+*
3138.407	+ .02	−2	.....	2.086	31854.10	$a^2P_{\frac{1}{2}} - z^4P^\circ_{\frac{1}{2}}$	*$Cr^+ - Sc^+$?*
3182.317	−0.03	0	.....	2.172	31414.59	$a^2P_{1\frac{1}{2}} - z^4P^\circ_{1\frac{1}{2}}$	*$-Cr^+$*

TABLE VI—*Continued*

Sun I.A.	Δλ O−C	Intensity		E.P.	Wave No. Vac.	Multiplet Designation	Suggested Solar Id.
		Disk	Spot				
			Cr⁺—continued				
3235.328.....	−0.03	0	.....	2.172	30899.88	$a^2P_{1\frac{1}{2}}-z^6P^\circ_{2\frac{1}{2}}$	$-Cr^+?$
3245.019.....	− .02	−1N	.....	2.172	30807.60	$a^2P_{1\frac{1}{2}}-z^6P^\circ_{1\frac{1}{2}}$	$Cr^+?$
3353.130[9]...	.00	2	.....	2.472	29814.34	$a^4D_{3\frac{1}{2}}-z^6D^\circ_{4\frac{1}{2}}$	$Cr^+?-$
3374.933[10]..	+ .02	0	.....	2.472	29621.74	$a^4D_{3\frac{1}{2}}-z^6D^\circ_{3\frac{1}{2}}$	$Cr\ Cr^+$
3467.136.....	+ .03	−2N	.....	2.444	28834.02	$a^4D_{2\frac{1}{2}}-z^6P^\circ_{3\frac{1}{2}}$	$\underline{Ni}\ Cr^+$
3568.313.....	− .01	−3	.....	3.698	28016.48	$a^4P_{\frac{1}{2}}-y^2P^\circ_{\frac{1}{2}}$	$Cr^+?$
3617.718.....	− .01	1	.....	2.424	27633.88	$a^4D_{1\frac{1}{2}}-z^2S^\circ_{\frac{1}{2}}$	Cr^+
3637.445.....	− .03	−3	.....	2.694	27484.02	$a'^4P_{2\frac{1}{2}}-z^2P^\circ_{1\frac{1}{2}}$	Cr^+
3664.212.....	+ .03	−2	.....	2.695	27283.26	$a'^4P_{1\frac{1}{2}}-z^2P^\circ_{\frac{1}{2}}$	Cr^+
3665.438.....	− .04	−3	.....	2.424	27274.13	$a^4D_{1\frac{1}{2}}-z^6F^\circ_{1\frac{1}{2}}$	$Cr^+?$
3687.987.....	− .04	−3	.....	2.444	27107.38	$a^4D_{2\frac{1}{2}}-z^6F^\circ_{1\frac{1}{2}}$	$Cr^+?$
3766.668.....	+ .02	3	.....	3.092	26541.15	$b^4D_{1\frac{1}{2}}-z^4F^\circ_{1\frac{1}{2}}$	$\underline{Fe}\ Cr^+$
3979.205.....	+ .03	−1	.....	4.055	25123.57	$b^4F_{1\frac{1}{2}}-y^2P^\circ_{\frac{1}{2}}$	$\underline{Sa}^+\ Cr^+?$
4030.350.....	− .02	0	0	3.090	24804.75	$b^4D_{3\frac{1}{2}}-z^6D^\circ_{4\frac{1}{2}}$	Cr^+
4064.054.....	+ .01	1	1	3.093	24599.05	$b^4D_{2\frac{1}{2}}-z^6D^\circ_{3\frac{1}{2}}$	Cr^+
4076.884.....	+ .01	1	1N	3.092	24521.64	$b^4D_{1\frac{1}{2}}-y^4P^\circ_{1\frac{1}{2}}$	$Fe\ Cr^+$
4087.801.....	+ .03	−1	−1N	3.090	24456.15	$b^4D_{3\frac{1}{2}}-z^6D^\circ_{2\frac{1}{2}}$	Cr^+
4089.965.....	+ .01	od?	0	3.093	24443.21	$b^4D_{2\frac{1}{2}}-z^6D^\circ_{2\frac{1}{2}}$	Cr^+
4146.500[11]..	+ .05	−1	−2	3.742	24109.95	$a^4P_{1\frac{1}{2}}-z^4D^\circ_{\frac{1}{2}}$	Cr^+
4154.290.....	− .01	0	0	3.092	24064.74	$b^4D_{1\frac{1}{2}}-z^2P^\circ_{\frac{1}{2}}$	$Cr^+?$
4170.639.....	− .01	−1	odBl	3.091	23970.41	$b^4D_{\frac{1}{2}}-z^4P^\circ_{1\frac{1}{2}}$	$CN?-Cr^+$
4497.266.....	− .02	−2	.....	3.091	22229.52	$b^4D_{\frac{1}{2}}-z^2S^\circ_{\frac{1}{2}}$	Cr^+
4507.232.....	+ .01	$\underline{-1}$	−1	3.093	22180.36	$b^4D_{2\frac{1}{2}}-z^6F^\circ_{3\frac{1}{2}}$	Cr^+
4572.871.....	+ .04	oN	−1?	3.092	21861.99	$b^4D_{1\frac{1}{2}}-z^6F^\circ_{1\frac{1}{2}}$	$Fe?\ Cr^+$
5232.517.....	+ .04	$\underline{-1}$	−2N	4.054	19105.96	$b^4F_{3\frac{1}{2}}-z^4F^\circ_{4\frac{1}{2}}$	Cr^+
5274.980.....	+ .03	$\underline{1}$	−1N	4.054	18952.16	$b^4F_{3\frac{1}{2}}-z^4F^\circ_{3\frac{1}{2}}$	Cr^+-Fe
5279.880.....	− .01	0	−1	4.056	18934.57	$b^4F_{4\frac{1}{2}}-z^4F^\circ_{3\frac{1}{2}}$	Cr^+
5368.122.....	+ .04	−3	.....	3.837	18623.32	$a^4F_{1\frac{1}{2}}-y^4P^\circ_{2\frac{1}{2}}$	Cr^+
5369.361.....	− .04	−2	.....	3.854	18619.03	$a^4F_{4\frac{1}{2}}-z^6D^\circ_{4\frac{1}{2}}$	$Cr^+?$
5430.368.....	.00	−1	−2	3.837	18409.85	$a^4F_{1\frac{1}{2}}-y^4P^\circ_{\frac{1}{2}}$	Cr^+
6076.913.....	+0.01	−1	−1NBd?	4.057	16451.18	$b^4F_{2\frac{1}{2}}-z^2P^\circ_{1\frac{1}{2}}$	$Cr^+?$
			Mn				
3639.133.....	−0.02	−3	.....	2.105	27471.27	$a^6D_{4\frac{1}{2}}-z^4F^\circ_{3\frac{1}{2}}$	Mn
3678.456.....	− .03	−3	.....	2.177	27177.61	$a^6D_{\frac{1}{2}}-z^4F^\circ_{1\frac{1}{2}}$	Mn
3749.367.....	+ .03	−1N	.....	2.928	26663.62	$a^4D_{1\frac{1}{2}}-y^4F^\circ_{1\frac{1}{2}}$	$Mn?$
3772.933.....	− .02	oNd?	.....	3.842	26497.08	$z^4P^\circ_{\frac{1}{2}}-e^4D_{1\frac{1}{2}}$	$CN-Mn?$
3890.570.....	− .01	1N	.....	3.368	25695.92	$a^4P_{\frac{1}{2}}-v^6P^\circ_{1\frac{1}{2}}$	$Nd^+\ Mn?$
3986.372.....	− .02	−2	.....	3.120	25078.40	$a^4G_{2\frac{1}{2}}-y^4F^\circ_{3\frac{1}{2}}$	Mn
4346.297.....	−0.03	1	1	2.272	23001.65	$z^8P^\circ_{2\frac{1}{2}}-e^6S_{2\frac{1}{2}}$	$-Mn?$
			Fe				
3097.491.....	−0.003	−1	.....	2.415	32274.86	$z^7D^\circ_4-4_3$	Fe
3113.667.....	+ .001	0	.....	2.458	32107.19	$z^7D^\circ_2-2_1$	Fe
3129.178[12]..	−0.003	0	.....	2.439	31948.04	$z^7D^\circ_3-6_2$	Zr^+-Fe

TABLE VI—*Continued*

Sun I.A.	Δλ O−C	Intensity		E.P.	Wave No. Vac.	Multiplet Designation	Suggested Solar Id.
		Disk	Spot				
			Fe—continued				
3136.086	0.000	−2	.....	2.389	31877.67	$z^7D^\circ_5 - 13_4$	*Fe*
3154.421(12)	+ .035	1	.....	2.167	31692.39	$a^5P_3 - 35^\circ_3$	*Fe−*
3155.131(12)	+ .014	1	.....	2.471	31685.26	$z^7D^\circ_1 - 6_2$	*Cr Fe*
3181.912(12)	− .001	1	.....	2.458	31418.59	$z^7D^\circ_2 - 11_2$	$\overline{\overline{Zr}}^+$ *Fe*
3240.122	+ .011	−1	.....	2.439	30854.16	$z^7D^\circ_3 - 31_3$	*Fe*
3256.497	− .024	1N	.....	2.458	30699.02	$z^7D^\circ_2 - 31_3$	*−Fe*
3269.433	+ .015	0	.....	2.188	30577.56	$a^5P_2 - 2^\circ_2$	*Fe*
3308.761	+ .017	2	.....	2.394	30214.13	$a^3H_6 - 31^\circ_5$	*Fe−Mn*
3314.868	+ .004	0	.....	2.839	30158.46	$z^7F^\circ_4 - 36_4$	*Fe−Mn*
3320.130	− .018	−3	.....	1.601	30110.67	$a^3F_2 - x^5P^\circ_1$	*V? Fe?*
3350.853(12)	− .022	−2	.....	2.927	29834.60	$z^7P^\circ_4 - 38_3$	*NH Fe*
3384.773	− .025	1	.....	0.986	29535.63	$a^5F_2 - y^3F^\circ_2$	*NH−Fe*
3404.449	+ .007	−3N	.....	2.985	29364.94	$z^7P^\circ_3 - 38_3$	*Fe*
3466.373	+ .026	−3N	.....	2.839	28840.37	$z^7F^\circ_4 - 4_3$	*Fe?*
3474.274	+ .008	−3	.....	2.870	28774.78	$z^7F^\circ_1 - 2_1$	*Fe*
3490.053	+ .009	−3	.....	2.863 2.863	28644.69	$z^7F^\circ_2 - 3_2$ $z^7F^\circ_2 - 4_3$	*Fe*
3512.812	+ .011	−1	.....	2.853	28459.11	$z^7F^\circ_3 - 7_2$	*Fe*
3513.605	+ .012	−2	.....	2.796	28452.69	$z^7F^\circ_6 - 18_5$	*Fe*
3542.572	+ .012	−1	.....	2.853	28220.04	$z^7F^\circ_3 - 11_2$	*Ti? Fe?*
3546.207(13)	+ .003	1	.....	2.422	28191.12	$a^3H_5 - 24^\circ_4$	*Fe Ce*$^+$
3547.221	− .003	3	.....	2.796	28183.06	$z^7F^\circ_6 - 25_5$	*Fe−*
3551.113	.00	1	.....	2.839	28152.17	$z^7F^\circ_4 - 17$	*Fe*
3554.453	+ .011	2	.....	2.927	28125.72	$z^7P^\circ_4 - 4_3$	*Fe Lu*$^+$ ·
3555.456	− .018	2	.....	2.853	28117.78	$z^7F^\circ_3 - 13_4$	*−Fe*
3559.465	+ .015	1	.....	2.870	28086.12	$z^7F^\circ_1 - 11_2$	*Fe*
3563.612	+ .004	−1	.....	2.796	28053.43	$z^7F^\circ_6 - 28_5$	*Fe*
3564.525	+ .012	3	.....	2.443	28046.25	$a^3H_4 - 26^\circ_4$	*Fe−*
3586.751(12)	+ .010	3	.....	2.796	27872.46	$z^7F^\circ_6 - 46_6$	*Fe*
3592.900(13)	+ .01 + .02	0	.....	2.188 2.796	27824.76	$a^5P_2 - x^3D^\circ_1$ $z^7F^\circ_6 - 58_5$	*Fe−Y*
3599.545	− .01	−3	.....	2.853	27773.40	$z^7F^\circ_3 - 21_2$	*Ni−Fe*
3609.473	+ .013	2	.....	2.853	27697.00	$z^7F^\circ_3 - 27_4$	*Fe−Cr Sa*$^+$
3616.157(12)	+ .009	2	.....	3.197	27645.81	$z^5D^\circ_4 - 38_3$	*Fe*
3619.115	+ .034	0	.....	2.927	27623.22	$z^7P^\circ_4 - 10_4$	*Fe?−*
3621.202	+ .01	2	.....	3.227	27607.30	$z^5D^\circ_3 - 55_3$	*Fe−Co*$^+$
3633.077(12)	+ .007	2	.....	2.927	27517.06	$z^7P^\circ_4 - 13_4$	*Fe*
3633.653	+ .009	−2	.....	3.025	27512.70	$z^7P^\circ_2 - 2_1$	*Fe*
3634.536	+ .018	−2	.....	2.863	27506.02	$z^7F^\circ_2 - 20_3$	*Fe*
3644.592	+ .008	0	.....	2.577	27430.12	$b^3F_3 - 2^\circ_2$	*Fe*
3646.098	− .001	−1	.....	2.863	27418.80	$z^7F^\circ_2 - 31_3$	*Fe*
3649.699	+ .002	−1	.....	2.927	27391.74	$z^7P^\circ_4 - 18_5$	*Fe*
3653.353	+ .004	1	.....	2.577	27364.35	$b^3F_3 - 4^\circ_2$	*Fe*
3673.774	+ .03	−3	.....	3.354	27212.24	$z^5F^\circ_4 - e^3G_3$	*Fe*
3675.450	+ .006	−1	.....	2.597	27199.84	$b^3F_2 - 4^\circ_2$	*Fe*
3685.663	+ .003	−3	.....	2.597	27124.47	$b^3F_2 - v^5P^\circ_2$	*Fe*
3685.776	+ .02	−3	.....	3.402	27123.64	$z^5F^\circ_2 - f^3D_3$	*Fe−Nd*$^+$?
3690.067	+0.002	−3	.....	2.577	27092.10	$b^3F_3 - v^5P^\circ_3$	*Fe*

TABLE VI—*Continued*

Sun I.A.	Δλ O−C	Intensity		E.P.	Wave No. Vac.	Multiplet Designation	Suggested Solar Id.
		Disk	Spot				
			Fe—continued				
3696.154.....	+0.032	−3N	.....	2.985	27047.48	$z^7P^\circ_3 - 13_4$	*Fe*
3711.941.....	+ .02	0	.....	2.443	26932.45	$a^3H_4 - 18^\circ_4$	*Fe*
3735.702.....	− .01	0Nd?	.....	2.414	26761.15	$a^3P_1 - w^5P^\circ_2$	*Ti?—Fe*
3742.569.....	+ .010	2	.....	3.025	26712.05	$z^7P^\circ_2 - 14_3$	*Fe—*
3747.006.....	+ .010	2	.....	2.985	26680.42	$z^7P^\circ_3 - 26_3$	*Fe—*
3763.573.....	+ .009	1	.....	2.474	26562.97	$a^3P_0 - 20^\circ_1$	*Fe*
3810.902.....	.00	0	.....	2.597	26233.09	$b^3F_2 - w^3D^\circ_1$	*Fe CN*
3811.043(12)..	.00 − .014	1	.....	2.716 2.577	26232.12	$a^3G_4 - 43^\circ_5$ $b^3F_3 - z^3H^\circ_4$	*Fe Co*
3811.809.....	+ .004	2	.....	3.354	26226.85	$z^5F^\circ_4 - 37_3$	*Fe—*
3824.752.....	+ .03	−1	.....	2.597	26138.10	$b^3F_2 - 10^\circ_1$	*CN Fe*
3826.627.....	− .01	1N	.....	2.443	26125.29	$a^3H_4 - x^5G^\circ_3$	*Fe*
3836.922.....	+ .008	1	.....	2.747	26055.19	$a^3G_3 - 2^\circ_2$	*Fe Gd+?*
3845.224.....	+ .010	1	.....	3.382	25998.94	$z^5F^\circ_3 - 37_3$	*CN,Fe*
3847.128(12)..	+ .030	−2N	.....	3.402	25986.07	$z^5F^\circ_2 - 38_3$	*Fe*
3848.299(14)..	+ .01	2	.....	2.597	25978.17	$b^3F_2 - w^3D^\circ_3$	*Fe—Ti*
3858.474.....	+ .02 .00	0	.....	3.638 3.227	25909.66	$z^5P^\circ_2 - f^3D_1$ $z^5D^\circ_3 - f^5D_2$	*CN Fe*
3887.374.....	+ .019	−2N	.....	2.747	25717.04	$a^3G_3 - v^5P^\circ_3$	*Fe Ti?*
3888.424(12)..	+ .01	2	.....	3.252	25710.10	$z^5D^\circ_2 - f^5D_2$	*Fe—*
3889.931(14)..	+ .01	1	.....	3.252	25700.14	$z^5D^\circ_2 - e^3D_1$	*Fe—Nd+ Ti*
3898.096.....	− .03	2	6Bl	3.671	25646.31	$z^5P^\circ_1 - f^3D_1$	*—Fe*
3905.191.....	+ .01	1	1	3.227	25599.72	$z^5D^\circ_3 - e^3D_2$	*Fe*
3910.536.....	+ .019	2	2	3.227	25564.73	$z^5D^\circ_3 - 6_2$	*Fe—*
3911.005(12)..	+ .031	3	3	2.597	25561.66	$b^3F_2 - 20^\circ_1$	*Fe?*
3922.086.....	.00 + .01	1	1d	3.278 2.471	25489.44	$z^5D^\circ_0 - e^3D_1$ $z^7D^\circ_1 - e^5D_1$	*Fe*
3922.676.....	+ .002	1	1	2.977	25485.61	$b^3G_4 - 31^\circ_5$	*Fe—Mn*
3936.772.....	− .02	0d?	0	3.197	25394.36	$z^5D^\circ_4 - e^3D_3$	*Mn?—Fe*
3948.476.....	− .005	−1N	.....	3.197	25319.09	$z^5D^\circ_4 - 14_3$	*Fe*
3949.235.....	.00	1	1	2.471	25314.22	$z^7D^\circ_1 - e^5D_2$	*Fe*
3962.400.....	− .021	0?	.....	3.227	25230.12	$z^5D^\circ_3 - 9_2$	*Fe*
3979.117.....	− .004	−1	.....	2.977	25124.12	$b^3G_4 - 35^\circ_3$	*Fe*
3986.298.....	− .001	0	0	3.227	25078.86	$z^5D^\circ_3 - 14_3$	*Fe*
3990.569.....	+ .016	0d?	1	3.227	25052.02	$z^5D^\circ_3 - 16_4$	*Fe—V*
4005.484.....	.00	1	1	2.577	24958.74	$b^3F_3 - x^5G^\circ_4$	*Fe*
4009.549.....	+ .007	1	1	3.197	24933.44	$z^5D^\circ_4 - 25_5$	*Fe*
4019.054(13)..	+ .01	1	2?	2.597	24874.47	$b^3F_2 - x^5G^\circ_3$	*Ce+ Ni Fe*
4020.024.....	− .023	0	0?	3.252	24868.47	$z^5D^\circ_2 - 43_1$	*Fe*
4042.763.....	+ .008	−1	−1	3.269	24728.60	$z^5D^\circ_1 - 43_1$	*Fe*
4043.993.....	+ .016	2	2	3.227	24721.08	$z^5D^\circ_3 - 26_3$	*Fe—*
4045.601.....	+ .008	2	2	3.197	24711.25	$z^5D^\circ_4 - 31_3$	*Fe—Zr+*
4046.083.....	+ .021	2	2	3.252	24708.31	$z^5D^\circ_2 - 19_2$	*Fe—*
4052.724(12)..	+ .006	1	1	3.227	24667.82	$z^5D^\circ_3 - 27_4$	*Fe*
4075.108.....	−0.04	2N	2	2.820	24532.32	$z^7F^\circ_5 - e^5F_4$	*Nd+—Fe*

TABLE VI—*Continued*

Sun I.A.	Δλ O−C	Intensity		E.P.	Wave No. Vac.	Multiplet Designation	Suggested Solar Id.
		Disk	Spot				
			Fe—continued				
4076.884(12)	+0.004	1	1N	3.252	24521.64	$z^5D^\circ_2 - 26_3$	*Fe Cr+*
4085.260	+ .013	1	5dBl	2.747	24471.36	$a^3G_3 - 18^\circ_4$	*Ce+ Fe*
4105.065	+ .007	−1	.....	3.415	24353.30	$z^5F^\circ_1 - 2_1$	*Fe*
4107.783	+ .029	−1	.....	3.587	24337.19	$z^5P^\circ_3 - 37_3$	*Fe−*
4116.962(12)	+ .010	1	1	3.227	24282.93	$z^5D^\circ_3 - 33_4$	*Fe*
4129.187(13, 14)	− .01	3	4	3.402	24211.04	$z^5F^\circ_2 - f^5D_3$	*Cr Fe*
4131.959	− .012	2	3	3.252	24194.79	$z^5D^\circ_2 - 32_3$	*Fe V*
4135.297	+ .030	od?	1N	3.382	24175.26	$z^5F^\circ_3 - 7_2$	*Fe?−Nd+*
4169.096	{.00 / + .03}	−1	o	{1.007 / 2.422}	23979.28	{$a^5F_1 - z^3F^\circ_2$ / $a^3H_5 - 54^\circ_5$}	*Fe*
4171.439	+ .016	−1	.....	3.005	23965.81	$b^3G_3 - 2^\circ_2$	*Fe*
4175.914	+ .019	1	1	3.382	23940.13	$z^5F^\circ_3 - 10_4$	*Fe*
4177.084(12)	+ .010	o	1	3.318	23933.42	$z^5F^\circ_5 - 27_4$	*Fe*
4178.631(12)	+ .019	−1	−1	3.638	23924.56	$z^5P^\circ_2 - 37_3$	*Fe*
4180.404(14)	− .01	1	1	2.716	23914.42	$a^3G_4 - x^5G^\circ_3$	*Fe*
4194.491(14)	.00	o	o	2.716	23834.10	$a^3G_4 - x^5G^\circ_4$	*Fe*
4197.102	+ .016	2	3	0.986	23819.28	$a^5F_2 - z^3F^\circ_3$	*Fe−*
4201.329	+ .006	−1	.....	3.415	23795.31	$z^5F^\circ_1 - 8_2$	*Fe*
4212.043	− .02	−1N	−1	3.402	23734.79	$z^5F^\circ_2 - e^3D_3$	*Gd+?−Fe*
4219.199(12)	.000	1	1	3.354	23694.53	$z^5F^\circ_4 - 26_3$	*Fe*
4228.722(12)	+ .007	1	1	3.354	23641.17	$z^5F^\circ_4 - 27_4$	*Fe*
4230.578(13)	+ .01	o	o	3.004	23630.80	$3M_2 - v^5P^\circ_3$	*Fe*
4237.084	+ .009	2	2	0.954	23594.52	$a^5F_3 - z^3D^\circ_3$	*Fe−*
4239.046	+ .04	−3	.....	2.747	23583.59	$a^3G_3 - x^5G^\circ_4$	*Fe?*
4246.572(12)	− .022	−2	.....	3.415	23541.80	$z^5F^\circ_1 - 43_1$	*Fe?*
4253.542	+ .025	−1	−1d?	3.318	23503.23	$z^5F^\circ_5 - 34_5$	*Fe−*
4269.862	− .009	2N	2	3.382	23413.39	$z^5F^\circ_3 - 27_4$	*−Fe*
4277.392(14)	.00	o	o	2.597	23372.18	$b^3F_2 - w^5D^\circ_1$	*Zr+? Fe*
4283.906	+ .038	−2N	−1	0.986	23336.64	$a^5F_2 - z^3D^\circ_3$	*Fe?*
4291.742	+ .006	−1N	.....	2.927	23294.03	$z^7P^\circ_4 - e^5F_5$	*Fe*
4306.601(12)	+ .024	o	oN	3.415	23213.66	$z^5F^\circ_1 - 22_1$	*CH Fe*
4307.058	− .019	−2d?	.....	3.354	23211.20	$z^5F^\circ_1 - 34_5$	*Fe*
4320.376(12)	+ .014	o	−1	3.382	23139.65	$z^5F^\circ_3 - 32_3$	*Co? Fe*
4323.372(14)	+ .01	o	o	2.443	23123.61	$a^3H_4 - y^5G^\circ_5$	*Fe*
4335.918	+ .002	−1	−1N	3.867	23056.70	$z^3D^\circ_3 - e^3G_3$	*Fe*
4336.616	+ .02	−1N	.....	3.867	23053.00	$z^3D^\circ_3 - 49_2$	*Fe Hf+?*
4336.876	+ .016	−1	.....	3.402	23051.61	$z^5F^\circ_2 - 31_3$	*Fe*
4338.835	+ .01	od	od	2.474	23041.21	$a^3P_0 - x^5P^\circ_1$	*Fe*
4341.252	+ .018	−1	−2	3.382	23028.38	$z^5F^\circ_3 - 33_4$	*Fe Gd+?*
4351.392	+ .022	−1	.....	3.402	22974.72	$z^5F^\circ_2 - 32_3$	*Fe?*
4392.589(13, 14)	+ .01	1	1	3.865	22759.24	$z^3F^\circ_4 - e^3G_4$	*Fe*
4406.163	+ .04	o	oBd?	3.912	22689.13	$z^3D^\circ_2 - 49_2$	*Fe?*
4414.050	+ .021	−2	.....	3.587	22648.59	$z^5P^\circ_3 - 6_2$	*Fe*
4428.551	− .02	1	1?	3.926	22574.43	$z^3F^\circ_3 - e^3G_3$	*Fe*
4450.764(14)	− .01	o	o	3.865	22461.77	$z^3F^\circ_4 - 40_3$	*Ce+?−Fe*
4455.452	+ .05	−2N	.....	3.943	22438.13	$z^3D^\circ_1 - 49_2$	*Fe?*
4471.810(13)	.00	−1	−1N	3.926	22356.06	$z^3F^\circ_3 - 50_2$	*Fe*
4480.278	+0.006	−1	−1N	3.587	22313.80	$z^5P^\circ_3 - 9_2$	*Fe Cr?*

TABLE VI—*Continued*

Sun I.A.	Δλ O−C	Intensity		E.P.	Wave No. Vac.	Multiplet Designation	Suggested Solar Id.
		Disk	Spot				
			Fe—continued				
4487.368.....	+0.010	−1	−1	3.587	22278.55	$z^5P^\circ_3 - 10_4$	*Fe*
4498.562.....	− .03	−1N	.....	2.853	22223.11	$z^7F^\circ_3 - e^5D_2$	*Fe*
4508.899.....	+ .016	−2	.....	3.587	22172.16	$z^5P^\circ_3 - 13_4$	*Fe*
4510.836.....	+ .013	0	0N	3.587	22162.64	$z^5P^\circ_3 - 14_3$	*Fe*
4513.722(14)..	.00	−1	0	2.577	22148.47	$b^3F_3 - y^5G^\circ_4$	*Fe? Ti*
4515.178(12, 14)	+ .01	0	0	2.863	22141.33	$z^7F^\circ_2 - e^5D_2$	*Fe*
4516.273.....	+ .001	−1	−1	3.587	22135.96	$z^5P^\circ_3 - 16_4$	*Fe*
4538.604.....	.00	−1N	−1d?	3.967	22027.05	$z^3F^\circ_2 - 50_2$	*Fe*
4545.695.....	− .006	−2	.....	3.638	21992.69	$z^5P^\circ_2 - 8_2$	*Fe*
4566.664.....	− .01	−3	.....	2.548	21891.71	$b^3F_4 - x^5P^\circ_3$	*Fe*
4571.448(14)..	+ .01	0	0	2.863	21868.80	$z^7F^\circ_2 - e^5D_3$	*Fe*
4572.871.....	+ .012	0N	−1?	3.638	21861.99	$z^5P^\circ_2 - 11_2$	*Fe? Cr+*
4578.050.....	+ .028	−1d?	−1N	3.671	21837.26	$z^5P^\circ_1 - 7_2$	*Fe*
4596.418.....	+ .004	1	1	3.638	21750.00	$z^5P^\circ_2 - 14_3$	*Fe*
4598.374.....	+ .05	−1	0	0.954	21740.74	$a^5F_3 - z^5P^\circ_2$	*Fe−*
4598.745.....	+ .001	0	0d	3.638	21738.99	$z^5P^\circ_2 - 43_1$	*Fe*
4611.194.....	+ .01	0	0	2.839	21680.30	$z^7F^\circ_4 - e^5D_4$	*Fe*
4626.802.....	+ .05	−1	−1	2.977	21607.17	$b^3G_4 - x^5G^\circ_5$	*Fe?*
4628.687.....	− .008	−1	.....	3.671	21598.37	$z^5P^\circ_1 - 11_2$	*Fe*
4631.039(14)..	.00	0N	0b	4.086	21587.39	$y^5D^\circ_4 - f^3D_3$	*Fe?*
4632.818.....	− .002	1	1	3.638	21579.11	$z^5P^\circ_2 - 19_2$	*Fe*
4635.630.....	+ .01	0	0	2.853	21566.02	$z^7F^\circ_3 - e^5D_4$	*Fe*
4655.247.....	+ .030	−1N	−1Bd?	3.671	21475.14	$z^5P^\circ_1 - 43_1$	*Fe?*
4673.280.....	+ .011	1	1	3.638	21392.28	$z^5P^\circ_2 - 26_3$	*Fe*
4684.220.....	+ .050	−1N	.....	2.414	21342.32	$a^3P_1 - z^5S^\circ_2$	*Fe?*
4720.579.....	+ .02	−2	.....	4.191	21177.94	$z^3P^\circ_2 - f^3D_2$	*Fe*
4739.658.....	+ .03	−3N	.....	2.474	21092.69	$a^3P_0 - x^5F^\circ_1$	*Fe*
4760.076.....	+ .007	−1	.....	3.025	21002.21	$z^7P^\circ_2 - e^5D_1$	*Fe*
4790.570.....	+ .01	−1	−1	4.136	20868.53	$y^5D^\circ_3 - 49_2$	*Fe*
4821.128.....	+ .034	0	−1	4.191	20736.26	$z^3P^\circ_2 - f^3D_3$	*Fe?−Ni*
4860.994(12, 14)	+ .01	0	1	3.382	20566.20	$z^5F^\circ_3 - e^3F_4$	*Fe−*
4862.604.....	.00	0	1	4.136	20559.39	$y^5D^\circ_3 - e^3G_4$	*Fe−V*
4911.541(14)..	+ .01	0	0	4.238	20354.54	$y^5F^\circ_3 - f^3D_3$	*Fe*
4957.705.....	+ .024	−2	.....	4.173	20165.01	$y^5D^\circ_2 - 61_3$	*Fe*
4987.857.....	+ .04	−3	.....	3.865	20043.11	$z^3F^\circ_4 - f^5D_4$	*Fe?*
4991.862(14)..	.00	−1	0	4.202	20027.03	$y^5F^\circ_4 - e^3G_4$	*Fe?−*
5012.160.....	.00	1	1?	4.173	19945.93	$y^5D^\circ_2 - 55_3$	*Fe*
5123.290(14)..	+ .01	−2N	0b	4.396	19513.29	$z^5G^\circ_3 - f^3D_2$	*Fe*
5164.687.....	− .01	−2	−2	2.577	19356.88	$b^3F_3 - x^5D^\circ_2$	*Fe*
5175.757.....	+ .046	−2d?	.....	0.087	19315.48	$a^5D_2 - z^7D^\circ_1$	*Fe−Ni?*
5184.199.....	+ .02	−2	.....	4.294	19284.03	$z^5G^\circ_5 - e^3G_4$	*Fe*
5222.398(12, 13)	+ .002	−1	0N	2.269	19142.98	$a^3P_2 - y^3F^\circ_2$	*Cr Fe*
5255.747.....	+ .016	−2	−2	4.265	19021.51	$y^5F^\circ_2 - 62$	*Fe*
5327.895.....	+ .04	−1	.....	4.396	18763.93	$z^5G^\circ_3 - 49_2$	*Fe?*
5464.112.....	+ .04	−3N	.....	4.454	18296.16	$z^3G^\circ_3 - 49_2$	*Fe?*
5493.248.....	− .001	−1	−1	4.416	18199.12	$z^3G^\circ_4 - 61_3$	*Fe*
5520.226.....	+0.032	−2N	.....	4.426	18110.18	$z^5G^\circ_2 - 61_3$	*Fe*

TABLE VI—*Continued*

Sun I.A.	Δλ O−C	Intensity		E.P.	Wave No. Vac.	Multiplet Designation	Suggested Solar Id.
		Disk	Spot				
			Fe—continued				
5536.599.....	+0.02	−1	0	2.819	18056.63	$b^3P_2 - z^5S^\circ_2$	*Fe*
5563.700.....	+ .01	0	2	2.414	17968.67	$a^3P_1 - y^3F^\circ_2$	*Fe*—
5567.285.....	+ .017	−2	−1	4.396	17957.10	$z^5G^\circ_3 - 62$	*Fe*?—
5579.357.....	+ .02	−1	0	4.212	17918.25	$y^5D^\circ_0 - e^3D_1$	*Fe*
5589.011.....	+ .003	−2	−1N	4.454	17887.30	$z^3G^\circ_3 - 61_3$	*Fe*?
5607.673.....	+ .006	0	0	4.136	17827.77	$y^5D^\circ_3 - 10_4$	*Fe*
5608.982.....	+ .008	−1	−1	4.191	17823.61	$z^3P^\circ_2 - f^5D_3$	*Fe*
5658.672.....	+ .01	0	0	4.265	17667.10	$y^5F^\circ_2 - f^5D_1$	*Fe*
5666.787(13)..	− .02	−2	−2?	4.136	17641.80	$y^5D^\circ_3 - 17_3$	*Ni*—*Fe*?
5678.407.....	+ .03	−2	0b?	3.867	17605.70	$z^3D^\circ_3 - e^3F_2$	*Fe*?
5730.864.....	+ .008	0N	−1d?	4.199	17444.55	$y^5D^\circ_1 - 8_2$	*Fe*
5753.983.....	+ .016	−2N	−1Bd?	2.443	17374.46	$a^3H_4 - y^3F^\circ_3$	*Atm? Fe*?
5762.847.....	+ .01	0	1	4.283	17347.74	$y^5F^\circ_1 - e^3D_1$	*Fe*?—
5807.804.....	+ .02	−1	−1?	3.278	17213.45	$z^5D^\circ_0 - e^7D_1$	*Fe*
5835.589.....	+ .02	−1	−2	2.819	17131.49	$b^3P_2 - x^5D^\circ_3$	*Fe*?
5912.706.....	+ .01	−1N	−1	1.551	16908.06	$a^3F_3 - z^5P^\circ_2$	*Fe? Atm.ww*?
5943.602.....	+ .02	0	1N	4.238 2.188	16820.16	$y^5F^\circ_3 - 17_3$ $a^5P_2 - y^5F^\circ_2$	*Fe*
5958.246(13)..	+ .016	1	1N	0.954	16778.82	$a^5F_3 - z^7P^\circ_2$	*Atm. ww Fe*?
5986.134.....	+ .04	−2	−2Bd?	4.775	16700.65	$y^3D^\circ_2 - f^3D_1$	*Fe*?
6015.264.....	+ .02	−2	.....	2.213	16619.78	$a^5P_1 - y^5F^\circ_2$	*Fe*
6097.106.....	+ .02	−3	−1	2.167	16396.70	$a^5P_3 - z^3P^\circ_2$	*Fe*?
6137.509.....	+ .01	−2	−1	3.318	16288.76	$z^5F^\circ_5 - e^7D_4$	*Fe*?
6141.064(13)..	+ .04	−2	.....	4.266	16279.33	$z^3P^\circ_0 - 24_1$	*Fe*?
6171.010.....	.00	−3	.....	4.713	16200.33	$y^3D^\circ_3 - 49_2$	*Fe*
6199.515(13)..	+ .008	−2	−1	2.548	16125.84	$b^3F_4 - y^5P^\circ_3$	*Fe*
6209.760.....	+ .043	−3N	.....	3.943	16099.24	$z^3D^\circ_1 - e^5F_2$	*Fe*
6253.847.....	+ .02	−1	od	4.713	15985.74	$y^3D^\circ_3 - 50_2$	*Fe*—
6271.289(13)..	+ .02	0	1	3.318	15941.28	$z^5F^\circ_5 - e^7D_5$	*Fe*?
6293.952.....	+ .03	−1d?	−1N	4.814	15883.88	$y^3D^\circ_1 - e^3P_2$	*Fe*
6351.305.....	+ .033	−3	−2N	4.294	15740.45	$z^5G^\circ_5 - 46_6$	*Fe*?
6376.180.....	− .017	−3	.....	4.302	15679.05	$z^5G^\circ_6 - 46_6$	*Fe*
6385.744.....	+ .031	0	0	4.713	15655.56	$y^3D^\circ_3 - 63$	*Fe*—
6483.954.....	+ .01	−1N	0	1.478	15418.44	$a^3F_4 - z^5F^\circ_3$	*Fe*
6603.374.....	+ .04	−3N	.....	2.414	15139.60	$a^3P_1 - y^5F^\circ_1$	*Fe*
6634.132.....	+ .03 + .03	0	0	4.454 4.775	15069.41	$z^3G^\circ_3 - 17_3$ $y^3D^\circ_2 - 55_3$	*Fe*
6648.130.....	+ .05	−2	−1	1.007	15037.68	$a^5F_1 - z^7F^\circ_2$	*Fe*
7091.957(12)..	+ .039	−2	−2N	4.934	14096.60	$x^5D^\circ_3 - e^3G_4$	*Fe*?
7256.132.....	−0.01	−2	.....	4.934	13777.66	$x^5D^\circ_3 - 55_3$	*Fe*
			Fe+				
3142.225.....	0.00	0	.....	1.663	31815.40	$a^4P_{2½} - z^4F^\circ_{1½}$	*Fe*+
3161.953(15)..	− .02	3	.....	1.688	31616.90	$a^4P_{1½} - z^4F^\circ_{1½}$	*Fe Fe*+
3163.096.....	−0.01	1	.....	1.663	31605.48	$a^4P_{2½} - z^4F^\circ_{2½}$	*Fe*+

TABLE VI—*Continued*

Sun I.A.	Δλ O−C	Intensity		E.P.	Wave No. Vac.	Multiplet Designation	Suggested Solar Id.
		Disk	Spot				
			Fe⁺—continued				
3234.933.....	−0.01	0	.....	0.982	30903.65	$a^4D_{3\frac{1}{2}}-z^6D^\circ_{2\frac{1}{2}}$	Fe^+
3264.785.....	.00	2	.....	1.036	30621.09	$a^4D_{2\frac{1}{2}}-z^6D^\circ_{1\frac{1}{2}}$	Fe^+-Zr^+
3285.422(16)..	.00	2	.....	1.072	30428.75	$a^4D_{1\frac{1}{2}}-z^6D^\circ_{\frac{1}{2}}$	Fe^+
3313.997.....	− .01	1	.....	1.092	30166.39	$a^4D_{\frac{1}{2}}-z^6D^\circ_{1\frac{1}{2}}$	Fe^+
3974.172.....	.00	1	1	2.693	25155.38	$b^4P_{1\frac{1}{2}}-z^4P^\circ_{2\frac{1}{2}}$?	Fe^+
4064.765.....	− .01	−2	.....	2.843	24594.75	$b^4F_{1\frac{1}{2}}-z^4P^\circ_{\frac{1}{2}}$	Fe^+
4087.277.....	+ .01	−1	−1	2.572	24459.29	$b^4P_{2\frac{1}{2}}-z^4F^\circ_{1\frac{1}{2}}$	Fe^+
4088.729.....	− .03	−1	.....	2.832	24450.60	$b^4F_{2\frac{1}{2}}-z^4P^\circ_{1\frac{1}{2}}$	Fe^+
4122.667.....	.00	1	oN	2.572	24249.33	$b^4P_{2\frac{1}{2}}-z^4F^\circ_{2\frac{1}{2}}$	Fe^+
4128.744.....	+ .01	2	0	2.572	24213.64	$b^4P_{2\frac{1}{2}}-z^4D^\circ_{1\frac{1}{2}}$	Fe^+
4138.365.....	− .06	oN	.....	2.816	24157.34	$b^4F_{3\frac{1}{2}}-z^4P^\circ_{2\frac{1}{2}}$	$-Fe^+$?
4258.168.....	+ .03	1N	oN	2.693	23477.69	$b^4P_{1\frac{1}{2}}-z^4F^\circ_{1\frac{1}{2}}$	Fe^+
4369.408.....	+ .01	1	−1	2.766	22879.99	$b^4P_{\frac{1}{2}}-z^4F^\circ_{1\frac{1}{2}}$	Fe^+
4472.934.....	+ .02	1	0	2.832	22350.44	$b^4F_{2\frac{1}{2}}-z^4F^\circ_{1\frac{1}{2}}$	Fe^+
4534.173.....	− .01	1	0	2.843	22048.58	$b^4F_{1\frac{1}{2}}-z^4F^\circ_{2\frac{1}{2}}$	Fe^+
4541.525.....	.00	2	1	2.843	22012.88	$b^4F_{1\frac{1}{2}}-z^4D^\circ_{1\frac{1}{2}}$	Fe^+
4582.835.....	+ .01	1	−1	2.832	21824.46	$b^4F_{2\frac{1}{2}}-z^4F^\circ_{3\frac{1}{2}}$	Fe^+
4595.692.....	− .01	−2	.....	2.843	21753.43	$b^4F_{1\frac{1}{2}}-z^4D^\circ_{2\frac{1}{2}}$	Fe^+
4601.384.....	.00	−1	ob	2.879	21726.52	$a^6S_{2\frac{1}{2}}-z^4D^\circ_{1\frac{1}{2}}$	Fe^+
4620.522.....	.00	2	0	2.816	21636.54	$b^4F_{3\frac{1}{2}}-z^4D^\circ_{3\frac{1}{2}}$	Fe^+
4656.983.....	− .03	1	0	2.879	21467.14	$a^6S_{2\frac{1}{2}}-z^4D^\circ_{2\frac{1}{2}}$	Fe^+
4663.711.....	− .01	0	ob	2.879	21436.17	$a^6S_{2\frac{1}{2}}-z^4F^\circ_{3\frac{1}{2}}$	Fe^+
4666.756.....	+ .01	1	0	2.816	21422.18	$b^4F_{3\frac{1}{2}}-z^4F^\circ_{4\frac{1}{2}}$	Fe^+
5256.934.....	− .06	−1	−3	2.879	19017.23	$a^6S_{2\frac{1}{2}}-z^6F^\circ_{2\frac{1}{2}}$	Fe^+
5284.114.....	.00	2	0	2.879	18919.40	$a^6S_{2\frac{1}{2}}-z^6F^\circ_{1\frac{1}{2}}$	Fe^+
5316.783.....	− .01	3	2	3.207	18803.15	$a^4G_{3\frac{1}{2}}-z^4D^\circ_{2\frac{1}{2}}$	Fe^+
5337.729.....	− .03	0	−1Bl	3.217	18729.36	$a^4G_{2\frac{1}{2}}-z^4D^\circ_{2\frac{1}{2}}$	Fe^+
5346.549(17)..	− .03	od	0	3.217	18698.47	$a^4G_{2\frac{1}{2}}-z^4F^\circ_{3\frac{1}{2}}$	Fe^+
5362.871.....	+ .01	3	2	3.186	18641.56	$a^4G_{4\frac{1}{2}}-z^4D^\circ_{3\frac{1}{2}}$	Fe^+
5414.077.....	+ .01	0	−1	3.207	18465.25	$a^4G_{3\frac{1}{2}}-z^4D^\circ_{3\frac{1}{2}}$	Fe^+
5425.261.....	+ .04	1	oN	3.186	18427.18	$a^4G_{4\frac{1}{2}}-z^4F^\circ_{4\frac{1}{2}}$	Fe^+
5435.702.....	− .10	−3	.....	3.217	18391.79	$a^4G_{2\frac{1}{2}}-z^4D^\circ_{3\frac{1}{2}}$	Fe^+?
6239.962.....	.00	−1	ob	3.873	16021.32	$b^4D_{\frac{1}{2}}-z^4P^\circ_{1\frac{1}{2}}$	Fe^+
6369.479.....	− .05	0	ob	2.879	15695.54	$a^6S_{2\frac{1}{2}}-z^6D^\circ_{1\frac{1}{2}}$	Fe^+
6407.310.....	+ .05	oN	ob	3.872	15602.87	$b^4D_{1\frac{1}{2}}-z^4P^\circ_{2\frac{1}{2}}$	Fe^+
6432.690.....	− .03	1	−2	2.879	15541.31	$a^6S_{2\frac{1}{2}}-z^6D^\circ_{2\frac{1}{2}}$	Fe^+
7222.400.....	+ .04	−2N	.....	3.872	13842.00	$b^4D_{1\frac{1}{2}}-z^4D^\circ_{\frac{1}{2}}$	Fe^+
7224.500.....	+ .05	−2N	.....	3.873	13837.98	$b^4D_{\frac{1}{2}}-z^4D^\circ_{\frac{1}{2}}$	Fe^+
7301.503.....	− .05	−3	.....	3.875	13692.05	$b^4D_{2\frac{1}{2}}-z^4F^\circ_{2\frac{1}{2}}$	Fe^+
7308.094(18)..	+ .08	−2	.....	3.872	13679.70	$b^4D_{1\frac{1}{2}}-z^4D^\circ_{1\frac{1}{2}}$	Fe^+
7310.208.....	+ .06	−1	.....	3.873	13675.74	$b^4D_{\frac{1}{2}}-z^4D^\circ_{1\frac{1}{2}}$	$Atm\ Fe^+$
7449.365(18)..	+ .02	−1	.....	3.872	13420.27	$b^4D_{1\frac{1}{2}}-z^4D^\circ_{2\frac{1}{2}}$	Fe^+
7462.342.....	− .07	2	5	3.875	13396.93	$b^4D_{2\frac{1}{2}}-z^4D^\circ_{2\frac{1}{2}}$	$Cr\ Fe^+$?
7515.887(18)..	+ .02	−1	.....	3.887	13301.49	$b^4D_{3\frac{1}{2}}-z^4D^\circ_{2\frac{1}{2}}$	Fe^+
7533.418(18)..	+ .05	−1	.....	3.887	13270.54	$b^4D_{3\frac{1}{2}}-z^4F^\circ_{3\frac{1}{2}}$	Fe^+
7655.474(18)..	+ .02	−1N	.....	3.875	13058.96	$b^4D_{2\frac{1}{2}}-z^4D^\circ_{3\frac{1}{2}}$	Fe^+
7711.737.....	+0.02	1	−2	3.887	12963.68	$b^4D_{3\frac{1}{2}}-z^4D^\circ_{3\frac{1}{2}}$	Fe^+

TABLE VI—*Continued*

Sun I.A.	Δλ O−C	Intensity		E.P.	Wave No. Vac.	Multiplet Designation	Suggested Solar Id.
		Disk	Spot				
				Co			
3261.640	+0.01	4	.....	0.430	30650.61	$b^4F_{4\frac{1}{2}}-y^2G^\circ_{3\frac{1}{2}}$	*Co*−
3386.879	+ .02	−2	.....	2.945	29517.26	$z^6F^\circ_{4\frac{1}{2}}-29$	*Co?*
3413.520	.00	2	.....	0.101	29286.90	$a^4F_{3\frac{1}{2}}-z^4G^\circ_{2\frac{1}{2}}$	*Co*−
3520.392	.00 − .04	−3	.....	1.733 1.778	28397.84	$a^4P_{1\frac{1}{2}}-x^4F^\circ_{2\frac{1}{2}}$ $a^4P_{\frac{1}{2}}-x^4F^\circ_{1\frac{1}{2}}$	*Co*
3554.798	− .03	0N	.....	1.703	28122.99	$a^4P_{2\frac{1}{2}}-x^4F^\circ_{3\frac{1}{2}}$	−*Co*
3607.005	− .02	−3	.....	1.999	27715.95	$b^4P_{\frac{1}{2}}-x^2D^\circ_{1\frac{1}{2}}$	*Co*
3723.611	+ .02	1	.....	1.733	26848.04	$a^4P_{1\frac{1}{2}}-4^\circ_{\frac{1}{2}}$	*Co?*−*Ti*+
3992.021	+ .03	−2	.....	0.174	25042.91	$a^4F_{2\frac{1}{2}}-z^6G^\circ_{2\frac{1}{2}}$	*Co*
4006.477	− .01	−1	.....	2.706	24952.56	$b^2D_{2\frac{1}{2}}-w^4D^\circ_{3\frac{1}{2}}$	*Co?*
4254.083	+ .01	−2	.....	3.607	23500.24	$z^4F^\circ_{3\frac{1}{2}}-e^4H_{3\frac{1}{2}}$	*Co*
4282.581	+ .03	−2	.....	3.553	23343.86	$z^4F^\circ_{3\frac{1}{2}}-e^4H_{4\frac{1}{2}}$	*Co*
4487.946	+ .03	−2	.....	3.553	22275.68	$z^4F^\circ_{3\frac{1}{2}}-4_{3\frac{1}{2}}$	*Co?*−
4734.185	+ .03	−3	.....	3.758	21117.07	$z^4D^\circ_{1\frac{1}{2}}-10$	*Co?*
4834.357	.00	−3	.....	1.999	20679.52	$b^4P_{\frac{1}{2}}-y^2D^\circ_{1\frac{1}{2}}$	*Co?*
5017.387	− .01	−3	.....	3.265	19925.15	$z^6G^\circ_{2\frac{1}{2}}-e^4F_{1\frac{1}{2}}$	*Co?*
5085.685	− .02	−2	−2	0.627	19657.57	$b^4F_{1\frac{1}{2}}-z^6F^\circ_{2\frac{1}{2}}$	*Co?*
5085.907	− .03	−3N	.....	4.008	19656.71	$y^4G^\circ_{4\frac{1}{2}}-e^4H_{4\frac{1}{2}}$	*Co?*
5333.153	.00	−2	.....	1.733	18745.43	$a^4P_{1\frac{1}{2}}-z^2F^\circ_{2\frac{1}{2}}$	*Co?*
5334.966	+ .02	−3	.....	4.008	18739.06	$y^4G^\circ_{4\frac{1}{2}}-8$	*Co*
5389.309	− .03	−3	.....	3.238	18550.11	$z^6G^\circ_{3\frac{1}{2}}-e^4F_{4\frac{1}{2}}$	*Co?*
5991.022	+0.03	−3N	.....	1.874	16687.03	$b^4P_{2\frac{1}{2}}-z^2F^\circ_{3\frac{1}{2}}$	*Co*
				Ni			
3118.558	−0.01	−1	.....	3.179	32056.84	$z^5D^\circ_4-f^5F_4$	*Ni*
3131.709	.00	0	.....	3.292	31922.22	$z^5D^\circ_3-f^5F_3$	*Ni*
3193.735	− .01	−1N	.....	3.292	31302.28	$z^5D^\circ_3-i^3F_3$	*Ni*
3194.765	+ .01	−2	.....	3.405	31292.19	$z^5G^\circ_5-e^5G_4$	*Ni*
3231.078	− .01	−3	.....	3.405	30940.52	$z^5G^\circ_5-e^5H_5$	*Ni*
3275.593	− .01	−2	.....	3.465	30520.06	$z^5G^\circ_4-f^5F_3$	*Ni*
3298.014	− .01	−3	.....	3.483	30312.58	$z^5D^\circ_0-e^5P_1$	*Ni*
3308.938	+ .03	−3N	.....	3.582	30212.51	$z^5G^\circ_2-f^5F_1$	*Ni*
3309.325	+ .01	−3N	.....	3.405	30208.98	$z^5G^\circ_5-g^3G_4$	*Ni*
3331.255	− .01	−1N	.....	3.528	30010.11	$z^5G^\circ_3-f^5F_3$	*Ni*
3337.341	− .01	−3	.....	3.590	29955.39	$z^5F^\circ_4-e^5H_4$	*Ni*
3351.069	+ .01	−1	.....	0.000	29832.68	$a^3F_4-z^5F^\circ_3$	*Ni*
3367.300	+ .01	−1	.....	3.384	29688.88	$z^5D^\circ_2-i^3D_3$	*Ni*
3396.508	+ .01	−2	.....	3.590	29433.59	$z^5F^\circ_4-e^3H_4$	*Ni*
3405.505	+ .01	−3	.....	3.683	29355.83	$z^5F^\circ_3-e^5H_3$	*Ni*
3412.464	− .01	−3	.....	3.384	29295.96	$z^5D^\circ_2-f^3P_2$	*Ni*
3415.684	+ .01	0	.....	3.524	29268.35	$z^5F^\circ_5-f^5F_4$	*Ni*
3428.428	+ .01	1	.....	3.683	29159.56	$z^5F^\circ_3-f^5F_2$	*Ni*
3471.615	− .01	−2	.....	3.683	28796.82	$z^5F^\circ_3-e^5G_3$	*Ni*
3483.631	+ .01	−2	.....	3.683	28697.50	$z^5F^\circ_3-g^3G_3$	*Ni*
3517.034	+ .01	−3	.....	3.724	28424.95	$z^5F^\circ_2-f^5F_3$	*Ni*
3564.684	+ .01	−2	.....	1.927	28045.00	$a^3P_2-x^3F^\circ_3$	*Ni*
3573.279	+0.01	−3	.....	3.683	27977.54	$z^5F^\circ_3-f^5F_4$	*Ni*

TABLE VI—*Continued*

Sun I.A.	Δλ O−C	Intensity		E.P.	Wave No. Vac.	Multiplet Designation	Suggested Solar Id.
		Disk	Spot				
			Ni—continued				
3611.559	+0.02	−1	.....	0.164	27681.01	$a^3F_3 - z^5G^\circ_2$	*Ni*
3630.235	− .02	0	.....	3.824	27538.60	$z^3G^\circ_4 - e^3H_4$	*Ni*
3651.655	− .01	1	.....	3.639	27377.07	$z^3F^\circ_4 - e^5D_4$	*Ni Cr*$^+$
3696.297	.00	0	.....	1.927	27046.43	$a^3P_2 - y^3P^\circ_1$	*Ni*
3696.664	+ .01	0	.....	1.927	27043.75	$a^3P_2 - y^3P^\circ_2$	*Ni*
3701.613	− .02	−2	.....	3.527	27007.59	$z^3P^\circ_2 - f^1F_3$	*Ni?*
3705.114	− .01	−2	.....	0.421	26982.07	$a^1D_2 - z^5F^\circ_1$	*Ni*
3721.032	+ .04	−3	.....	3.817	26866.65	$z^3G^\circ_5 - g^3G_4$	*Ni?*
3723.394	+ .01	−1	.....	3.824	26849.61	$z^3G^\circ_4 - e^5G_5$	*Ni*
3724.260	.00	−2	.....	3.924	26843.36	$z^3G^\circ_3 - e^5G_3$	*Ni*
3885.867	.00	0	.....	0.274	25727.02	$a^3F_2 - z^5D^\circ_1$	*Ni*
3904.632	− .01	1	1	0.421	25603.38	$a^1D_2 - z^5G^\circ_2$	*Ni*
3924.176	.00	1	1	4.088	25475.87	$y^3F^\circ_3 - f^5F_3$	*Ni*
3938.736	− .02	−1	.....	4.149	25381.70	$y^3F^\circ_2 - f^5F_2$	*Ni*
3946.202	+ .02	0	0	0.164	25333.68	$a^3F_3 - z^5D^\circ_3$	*Ni*−
3958.642	+ .04	−1	.....	3.780	25254.07	$z^3F^\circ_2 - g^3F_2$	*Pd Ni?*
3995.864	+ .02	−1	.....	4.149	25018.83	$y^3F^\circ_2 - i^3F_2$	*Ni*
4029.298	− .02	−2	.....	3.690	24811.23	$z^3D^\circ_2 - h^3D_3$	*Ni*
4035.986	+ .03	−1	−1	3.639	24770.12	$z^3F^\circ_4 - g^3F_3$	*Ni*
4038.279	+ .01	−1	−1N	3.639	24756.05	$z^3F^\circ_4 - g^3F_4$	*Ni*
4049.734	+ .02	1N	1	3.690	24686.03	$z^3D^\circ_2 - f^3S_1$	*Ni*−
4051.188	+ .01	0N	0	4.088	24677.17	$y^3F^\circ_3 - g^3G_4$	*Ni Nd*$^+$
4093.652	+ .04	−1	.....	0.164	24421.20	$a^3F_3 - z^5D^\circ_4$	*Ni*
4102.763	+ .03	−1N	−1	4.217	24366.96	$y^3D^\circ_2 - g^3G_3$	*Ni*
4148.722	− .03	−1	−1?	3.450	24097.04	$z^5D^\circ_1 - f^3F_2$	*Ni*
4161.312	− .03	−2	.....	3.179	24024.13	$z^5D^\circ_4 - e^5F_3$	*Ni*
4225.048	+ .01	−2	.....	3.816	23661.73	$z^3D^\circ_1 - f^3S_1$	*Ni*
4230.404	+ .01	−2	−2	3.780	23631.77	$z^3F^\circ_2 - g^3F_3$	*Ni*
4235.523	− .02	−2	.....	4.136	23603.21	$y^3D^\circ_3 - i^3D_3$	*Ni*
4285.205	+ .02	−1	−1N	3.384	23329.56	$z^5D^\circ_2 - e^5F_1$	*Ni*
4302.082	− .04	−1	−1	3.465	23238.04	$z^5G^\circ_4 - f^3F_3$	*W? Ni*
4414.234	+ .02	−1	−1	3.292	22647.65	$z^5D^\circ_3 - e^3F_3$	*Ni*
4513.914	+ .01	−2	.....	3.527	22147.53	$z^3P^\circ_2 - f^3D_1$	*Ni*
4523.746	+ .01	−2N	.....	3.528	22099.40	$z^5G^\circ_3 - e^3G_3$	*Ni*
4565.126	− .04	−1N	.....	3.384	21899.08	$z^5D^\circ_2 - e^3F_3$	−*Ni*
4565.427	− .02	−1	−1	3.365	21897.64	$z^5G^\circ_6 - e^3G_5$	*Ni?*
4629.952	− .03	−2d?	.....	4.072	21592.47	$z^1P^\circ_1 - f^3S_1$	*Ni*
4646.972	+ .04	−2N	.....	3.620	21513.38	$z^3F^\circ_3 - e^3F_2$	*Ni*
4664.326	.00	−1N	.....	3.620	21433.34	$z^3F^\circ_3 - f^1D_2$	*Ni*
4681.051	.00	−2	.....	3.620	21356.77	$z^3F^\circ_3 - e^3G_3$	*Ni*
4713.814	− .03	−1	−1N	3.527	21208.33	$z^3P^\circ_2 - e^5F_3$	*Ni?*
4723.349	− .02	−2	.....	3.663	21165.52	$z^3D^\circ_3 - e^3F_2$	*Ni*
4741.357	+ .02	−3	.....	3.663	21085.13	$z^3D^\circ_3 - f^1D_2$	*Ni*
4760.220	− .01	−3	.....	3.683	21001.58	$z^5F^\circ_3 - e^3F_2$	*Mo?*−*Ni*
4834.817	− .01	−2	.....	3.663	20677.55	$z^3D^\circ_3 - e^5F_2$	*Ni*
4837.668	+ .02	−3	.....	2.729	20665.36	$a^1G_4 - w^3D^\circ_3$	*Ni?*
4841.675	0.00	−2	−1?	3.690	20648.26	$z^3D^\circ_2 - e^1P_1$	*Cr Ni?*

TABLE VI—*Continued*

Sun I.A.	Δλ O−C	Intensity		E.P.	Wave No. Vac.	Multiplet Designation	Suggested Solar Id.
		Disk	Spot				
			Ni—continued				
4843.506.....	−0.02	−1	−1	4.149	20640.45	$y^3F^\circ_2 - g^3F_3$	*Co−Ni*
4849.078.....	− .04	−3	.....	3.524	20616.74	$z^5F^\circ_5 - e^3G_5$	*Ni?*
4853.286.....	− .01	−1	−2	3.881	20598.86	$z^1D^\circ_2 - f^3F_2$	*Ni*
4873.258.....	− .02	0	−1	3.724	20514.44	$z^5F^\circ_2 - e^3G_3$	*Ni*
4886.719.....	.00	−2	.....	3.690	20457.93	$z^3D^\circ_2 - e^5F_2$	*Ni*
4890.440.....	.00	−3	−2	3.752	20442.36	$z^5F^\circ_1 - e^3F_2$	*Ni?*
4921.170.....	− .01	−3	.....	3.582	20314.72	$z^5G^\circ_2 - f^3D_2$	*Ni*
4941.911.....	− .03	−3	.....	3.590	20229.46	$z^5F^\circ_4 - e^3F_3$	*Ni*
4976.695.....	− .02	−2	.....	4.217	20088.07	$y^3D^\circ_2 - g^3F_3$	*Ni*
4995.660.....	+ .01	−1	−2	3.620	20011.81	$z^3F^\circ_3 - e^3F_4$	*Ni*
5162.906.....	− .02	−2	.....	3.816	19363.56	$z^3D^\circ_1 - e^3P_0$	*Ni C_2*
5175.757.....	− .03	−2d?	.....	3.831	19315.48	$z^1F^\circ_3 - e^5F_2$	*Fe−Ni?*
5288.220.....	+ .01	−2	.....	3.881	18904.71	$z^1D^\circ_2 - e^5F_2$	*Ni*
5328.739.....	+ .04	−3	.....	3.727	18760.96	$z^3P^\circ_0 - e^3S_1$	*Ni*
5351.840.....	− .01	−2	.....	3.924	18679.98	$z^3G^\circ_3 - f^3F_4$	*Ni*
5666.787.....	.00	−2	−2?	4.088	17641.80	$y^3F^\circ_3 - f^1D_2$	*Ni-Fe?*
5925.835.....	+ .04	−3	.....	1.669	16870.59	$b^1D_2 - z^5F^\circ_1$	*Ni*
6165.174.....	− .01	−3	.....	4.088	16215.66	$y^3F^\circ_3 - f^3D_2$	*Ni*
6576.906.....	−0.05	−3	.....	5.280	15200.53	$w^3D^\circ_3 - i^3F_3$	*Ni*
			Zr^+				
3027.613.....	0.00	0	.....	0.357	33019.73	$b^4F_{2\frac{1}{2}} - z^2P^\circ_{1\frac{1}{2}}$	Zr^+?−
3120.733(19)..	+ .02	0	.....	0.710	32034.49	$a^2F_{2\frac{1}{2}} - y^2F^\circ_{3\frac{1}{2}}$	*Zr* Zr^+?
3180.992(19)..	+ .03	−2	.....	0.464	31427.67	$b^4F_{4\frac{1}{2}} - z^2G^\circ_{4\frac{1}{2}}$	Zr^+
3205.654(19)..	− .01	−2	.....	0.407	31185.90	$b^4F_{3\frac{1}{2}} - z^2G^\circ_{3\frac{1}{2}}$	$Ti^+ - Zr^+$
3240.874(19)..	+ .03	−3	.....	0.318	30847.00	$b^4F_{1\frac{1}{2}} - y^2D^\circ_{2\frac{1}{2}}$	Zr^+
3255.983.....	− .03	−3	.....	0.798	30703.87	$a^2F_{3\frac{1}{2}} - y^4D^\circ_{2\frac{1}{2}}$	Zr^+
3297.068.....	+ .02	0N	.....	1.819	30321.28	$c^2D_{2\frac{1}{2}} - w^2D^\circ_{1\frac{1}{2}}$	*NH?* Zr^+?
3354.891(19)..	− .04	−1N	.....	0.094	29798.69	$a^4F_{3\frac{1}{2}} - z^2F^\circ_{3\frac{1}{2}}$	Zr^+?
3508.899.....	− .03	−1	.....	1.765	28490.85	$c^2D_{1\frac{1}{2}} - y^4P^\circ_{\frac{1}{2}}$	$-Zr^+$
3550.107.....	.00	−3	.....	1.819	28160.15	$c^2D_{2\frac{1}{2}} - y^4P^\circ_{1\frac{1}{2}}$	Zr^+
3604.806.....	+ .01	−3	.....	0.524	27732.86	$a^2D_{1\frac{1}{2}} - z^4D^\circ_{\frac{1}{2}}$	Zr^+
3720.262.....	− .02	−2N	.....	0.754	26872.21	$a^2P_{1\frac{1}{2}} - y^2D^\circ_{1\frac{1}{2}}$	Zr^+
3955.833.....	+ .02	−2	.....	0.556	25272.00	$a^2D_{2\frac{1}{2}} - z^4F^\circ_{1\frac{1}{2}}$	Zr^+
4267.285.....	− .01	−2	.....	2.399	23427.53	$b^2F_{3\frac{1}{2}} - x^2F^\circ_{2\frac{1}{2}}$	Zr^+
4348.640.....	.00	−1N	−1	2.409	22989.25	$b^2F_{2\frac{1}{2}} - x^2F^\circ_{3\frac{1}{2}}$	Zr^+
4697.810(19)..	+ .01	−2	.....	1.231	21280.58	$b^4P_{2\frac{1}{2}} - z^4F^\circ_{3\frac{1}{2}}$	Zr^+
4794.666(19)..	+ .04	−3	.....	0.995	20850.70	$a^4P_{2\frac{1}{2}} - z^4G^\circ_{3\frac{1}{2}}$	Zr^+?
4857.101(19)..	+ .04	−2	.....	1.231	20582.68	$b^4P_{2\frac{1}{2}} - z^4F^\circ_{2\frac{1}{2}}$	Zr^+?
4989.973(19)..	+ .05	−2	.....	1.203	20034.61	$b^4P_{1\frac{1}{2}} - z^4F^\circ_{1\frac{1}{2}}$	Zr^+?−
5549.332(19)..	−0.01	−3	.....	1.231	18015.20	$b^4P_{2\frac{1}{2}} - z^4G^\circ_{2\frac{1}{2}}$	Zr^+?

NOTES TO TABLE VI

1. Solar identification based on observed laboratory wave-length; multiplet designation not previously assigned.
2. A. S. King has kindly examined one of his plates at Mount Wilson and measured a Ti^+ line at λ 3679.690, the *Ti* arc line previously listed at λ 3679.690 being at λ 3679.749.
3. Observed Ti^+ at λ 4174.11 (2 V) not previously assigned to a multiplet.
4. Present in the spectrum of α Persei.
5. Spot intensity due to *V*.
6. Present in the spectrum of γ Cygni, intensity 2.
7. Line measured in spark by Exner and Haschek at λ 3201.27.
8. Observed *Cr* at λ 4459.41 (4n III).
9. Observed in spark by Exner and Haschek; measures in arc discordant with predicted position.
10. Line measured in spark by Exner and Haschek at λ 3374.96; observed as an arc line by King (2 III).
11. *Cr* arc line observed at λ 4146.49 (2 IV).
12. Intensity listed by Burns and Walters; measured laboratory wave-length unpublished (*Publications of the Allegheny Observatory*, **6**, 159 [No. 11] 1929).
13. Measured to one decimal place by Kayser, *Handbuch der Spectroscopie*, **6**, 896, 1912.
14. Line measured on plate of *Fe* arc taken at Mount Wilson by A. S. King.
15. Observed Fe^+ to red of *Fe*.
16. Observed Fe^+ not included in published list of Fe^+ lines of known multiplet designation.
17. In the spot spectrum a band line is to the red; Fe^+ is to the violet and obliterated.
18. Wave-length by Meggers, *Publications of the Allegheny Observatory*, **6**, 13 (No. 3), 1919.
19. Identified as predicted Zr^+ by C. C. Kiess and H. K. Kiess, *Bureau of Standards Journal of Research*, **5**, 1240 (Reprint No. 255), 1930.

high even levels, which they call 2W, 3W, etc., the prefixes 2, 3, etc., alone are used here. Similarly for the unclassified odd levels, denoted by them as 1R, 2R, etc., the notation 1°, 2°, etc., has been adopted. In a few instances the inner-quantum numbers given here differ from the published values. In cases of difference the value indicated by the combinations has been assigned unless the published value is based on observed Zeeman patterns; but final decision cannot be made until more has been done on the analysis of the spectrum.

For elements other than *Fe*, numerical designations have been assigned by the writer, the numbers being in the order of increasing distance of the level above the zero or lowest level. A large number of miscellaneous levels for *Co* have been labeled in this manner.

The origin of 21 spot lines has been determined by prediction; 13 of these have been attributed to *Ti*, 3 to *V*, and 5 to *Cr*. These lines, which are included in both Tables IV and VI, belong to ele-

ments whose lines are decidedly strengthened in the spot spectrum relative to the disk spectrum.

The appearance of several of the predicted Ti^+ lines in the spectra of α Persei (indicated by reference (4) in Table VI) and of γ Cygni lends additional confirmation to the suggested solar identifications.

TABLE VII

STRONGEST UNIDENTIFIED LINES

SUN I.A.	INTENSITY		SUN I.A.	INTENSITY	
	Disk	Spot		Disk	Spot
3903.856.....	2	5Bl	4699.342.....	$\underline{3}$	2
4001.171.....	3	3N	4748.143.....	4	3
4015.613.....	3	3	4771.474.....	3	2
4052.502.....	3	3?	5298.499.....	0	3
4112.916.....	1	4Bl	5731.226.....	−1	5dBl
4132.540.....	3	3	5914.218.....	$\underline{4}$	5
4159.188.....	$\underline{4}$	3	5929.686.....	2	3
4184.000.....	4	3	6155.148*.....	$\underline{5}$N	2N
4672.336.....	3N	2			
4678.176.....	3N	2			

* Identified as *Si* by C. C. Kiess, unpublished material.

The strongest unidentified lines, with solar wave-lengths and disk and spot intensities taken directly from the main table, are listed separately in Table VII. Only those lines having intensity 3 or greater in the disk or spot spectrum are included. A longer list is available for those interested.

[*To be continued*]

REVIEWS

Revision of Rowland's Preliminary Table of Solar Spectrum Wave-Lengths with an Extension to the Present Limit of the Infra-Red. By C. E. St. John, C. E. Moore, L. M. Ware, E. F. Adams, H. D. Babcock. Washington: Carnegie Institution, 1928. Pp. xxi+238.

This volume, which is the standard authority for absorption lines in the solar spectrum, is far more than a mere revision of Rowland's classic work. Observations at Mount Wilson extending over more than a decade are represented by the wave-lengths, in international Angstroms, of the Fraunhofer lines from λ 2975 to λ 10,219, based upon the standards of wave-length established by the International Union for Co-operation in Solar Research. In addition to the wave-lengths to three decimal places, the catalogue contains identifications, intensities in the spectra of the disk and of spots, temperature classifications from furnace spectra, classifications according to behavior under pressure, and excitation potentials, for as many of the lines as possible. A supplementary table lists those lines found normally in the chromosphere only. Fifty-seven elements in all are identified as present in the sun, leaving thirty-five not known to occur there.

In the preparation of the tables St. John and his collaborators have worked with characteristic thoroughness, and the result belongs among those compilations of fundamental data which form the indispensable but not always fully appreciated basis for the spectacular advances in theoretical and observational astrophysics.

P. C. Keenan

Photo-electric Cells and Their Applications. Edited by John S. Anderson. London: Physical and Optical Societies, 1930. Pp. xii+236. 12*s.* 6*d.*

This book is a collection of the papers presented at the meeting on June 4 and 5, 1930, of the Physical and the Optical Societies of London for a discussion of photo-electric cells and their applications. Thirty-one papers are given which occupy 218 pages of the book, the remaining 18 pages being devoted to the discussions of the papers.

The introductory lecture gives the early history of photo-electric and selenium cells. Following this are several papers on the manufacture and the characteristics of cells. One paper gives a complete electrostatic method for the measurement of photo-electric currents, and several papers, both theoretical and practical, deal with the amplification of photo-electric currents by thermionic valves. Several papers deal with the applications of the photo-electric cells to specific problems, such as the measurement of small angles, as precision instruments in general and spectral photometry, as the sensitive elements in recording microphotometers, for the measurement of the amount of ozone in the upper atmosphere, and their uses in biology. The concluding papers discuss other types of light-sensitive cells such as the selenium and the "Thalofide" cells.

The authors of the papers have given valuable suggestions for the future development and use of photo-electric cells.

C. T. ELVEY

Johannes Kepler Festschrift, Teil I. By DR. KARL STÖCKL. Regensburg, Germany, 1930. 8vo. Pp. 355. Pls. 28, Figs. 37. RM. 15, unbound; 18, bound.

The tercentenary of Kepler's death was made the occasion of a celebration in his honor at Regensburg on September 24 and 25, 1930, which is fully reported in this volume. It does not appear that Regensburg itself played an important part among the places which hard circumstances brought this great philosopher to dwell in, during his troubled but brilliant career. Born in Weil-der-Stadt, in Württemberg in the Black Forest, his early education was received in Catholic schools, but he entered the Protestant Seminary for Theology at Tübingen where he received his degree of Magister at the age of twenty. In 1594 he became professor of mathematics and theology in Graz. Religious conflicts soon developed in Austria and made it necessary for him to leave and accept a position as assistant to Tycho at Prague, to be engaged in the reduction of the new planetary tables by Tycho. Upon the death of the irascible old man, a year later, Kepler became mathematician to the Emperor Rudolph. While there, he published the first two of his laws, but he found it difficult to live on the unpaid bounty of the ruler. In 1612 he wearied of the struggle for existence and took a position at Linz in the Gymnasium. His third law was published in his work *Harmonices mundi libri V* in 1619. Meanwhile the Thirty Years' War was raging and he and his family were driven

about, taking refuge for considerable periods in Regensburg. Then he devoted much energy in the attempt to collect his unpaid salary of 12,000 gulden. He died at Regensburg on November 15, 1630, from exposure on a long ride to that city where he hoped to secure justice from an imperial diet meeting there.

The celebration was attended by a number of astronomers and philosophers, who made appropriate addresses. We may mention among them Professor E. Anding, who spoke on "The Lifework of Kepler"; Professor M. Caspar, on "Kepler the Man"; Professor M. von Rohr, in two papers on "The Process of Vision" and on "Binocular Vision"; Dr. K. Stöckl on "Magnetism"; Professor A. Wilkins on the topic "From Kepler to the Modern Theory of Planetary Motions"; Professor M. Wolf, who offered for christening the two minor planets Kepler and Ratisbona; and Professor E. Zinner on "The Portraits of Kepler." Professor J. Bauschinger was also a speaker at the principal banquet.

The volume contains facsimiles of important documents concerning Kepler and his family and several of his portraits, together with pictures of the various places in Regensburg with which he was connected.

A second part of this work is promised to contain a complete bibliography of Kepler's writings.

F.